NBSIR 82-2488

Fire Endurance Tests of Selected Residential Floor Construction

U.S. DEPARTMENT OF COMMERCE
National Bureau of Standards
National Engineering Laboratory
Center for Fire Research
Washington, DC 20234

April 1982

NBSIR 82-2488

FIRE ENDURANCE TESTS OF SELECTED RESIDENTIAL FLOOR CONSTRUCTIONS

J. B. Fang

U.S. DEPARTMENT OF COMMERCE
National Bureau of Standards
National Engineering Laboratory
Center for Fire Research
Washington, DC 20234

April 1982

U.S. DEPARTMENT OF COMMERCE, Malcolm Baldrige, *Secretary*

NATIONAL BUREAU OF STANDARDS, Ernest Ambler, *Director*

TABLE OF CONTENTS

LIST OF TABLES

LIST OF FIGURES

LIST OF FIGURES (continued)

Fire Endurance Tests of Selected Residential Floor Constructions

J. B. Fang

National Bureau of Standards
Washington, D.C. 20234

A series of ten load-bearing, wood- and steel-framed residential floors was evaluated for structural fire resistance in a fire endurance furnace. Nine wood-frame and one light guage steel-frame, protected and unprotected floor-ceiling assemblies, each measuring 3.05 x 2.44 m in size, were exposed from the underside to either the newly developed high-intensity, short-duration fire exposure or the standard ASTM E119 temperature-time curve. The fire endurance time based on the passage of flames to the unexposed face of the floor with unprotected wood joists varied from 6 to 9 minutes under the newly developed fire exposure and 16 to 18 minutes when subjected to the standard ASTM fire exposure. Under the identical fire exposure, the exposed steel-framed floor failed in approximately 4.5 minutes compared to 9 minutes for the unprotected wood-frame floor. The wood floors evaluated in the test furnace had a shorter fire resistance period in comparison with those tested previously under room fire conditions, probably due to faster charring rates and additional heat contribution from the burning of combustible materials in the structure with the excess air present in the furnace. The heat contributed by the burning floor assemblies was measured by the oxygen consumption technique.

Key words: fire endurance, fire tests, flame through, floors, furnace tests, joists, steel, wood.

1. INTRODUCTION

In order to minimize the spread of fire beyond the room of origin, building codes may specify fire endurance requirements for floors, walls, and ceilings so that they act as barriers to withstand fire exposure without loss of design function. This provides time to permit building occupants to evacuate safely and fire fighters to bring the fire under control prior to collapse of the building. However, there are no fire endurance requirements in the codes for single family residences. The standard ASTM E119 test method [1] developed more than a half century ago, is commonly used for evaluating the fire endurance of building components for use in public buildings, institutions, apartment buildings, etc., which require ratings of one hour or more. This test would have several shortcomings if it were used to establish ratings of less than one hour for residential floor assemblies if they should be required by the codes for single family residences in the future. The unrealistically slow buildup of the furnace temperature and the customary use of negative pressures and high levels of excess air which are not present in a room fire, as well as the slow time response of the furnace thermocouples used for temperature control, make the E119 test unsuitable for the above purpose. This report describes the last stage of a research project to establish a new fire endurance test for residential floor assemblies. The gas temperature versus time curve, the gas pressure below the ceiling, and the oxygen concentration required were established by a series of basement recreation room fire tests using modern furnishings [2,3]. A series of selected floor/ceiling assemblies were then tested in this room under the above set of conditions [4]. In the last phase of the project, reported here, some of the assemblies were tested in a furnace modified to produce the above conditions of temperature, pressure, and excess air. The fire endurance times of these selected assemblies were compared between the room fire, the furnace test with the new exposure, and the furnace test with the E119 exposure. The heat contributed by the burning floor assemblies was measured by the oxygen consumption technique.

2

2. EXPERIMENTAL DETAILS

2.1 Test Furnace

The entire series of fire endurance tests were conducted with a pilot furnace having internal dimensions of 2.95 m long x 2.44 m wide and a height of 2.85 m. The furnace can be used for testing 2.44 x 3.05-m (8 x 10-ft) floor assemblies in a horizontal position, or 3.05 x 2.44-m (10 x 8-ft) high wall panels in a vertical orientation. The basic construction of the furnace consists of a fire brick floor 0.18 m in total depth and 0.34-m thick composite walls, each consisting of a 6.4-mm thick steel plate shell, 76 mm of block insulation, 203 mm of castable refractory brick, and 51 mm thick ceramic fiber block lining.

The furnace is fired with natural gas. Originally eight nozzle-mixing gas burners were distributed evenly into 2 rows of 4 burners each over the floor area, and mounted on the bottom of the furnace in an upright position. Each burner supplied combustion air through a center tube and fuel gas through a grid over an annular space around the tube. This construction is designated Furnace Modification I. The heat output rates from a single burner ranged between 70 and 350 kW. The heat output rate from each burner was controlled by regulating the fuel flow rate while the air supply was maintained at a constant rate. Due to the presence of unstable flames, these upward firing burners were replaced by two new gas burners which were installed horizontally from the west furnace wall and used for tests 6 and 7. This construction is designated Furnace Modification Ia. These new medium-velocity, nozzle-mixing gas burners fed gaseous fuel through the center tube of the concentric nozzle and supplied air through the annular space around the tube. Each burner had a wide operating range, from 18 to 440 kW. Also, these burners used a stoichiometric fuel air mixture and were capable of operating without flame instability under a reducing atmosphere. For tests 8 to 10, an additional six new gas burners were

3

put in the east and west furnace walls. This construction is designated Furnace Modification Ib.

The fire endurance test furnace was situated within a large, air conditioned building to minimize the effect of variable outdoor weather conditions. It was fitted with one observation window in each of three sidewalls of the furnace. Combustion products were vented through four dampered flues, one in each corner of the furnace, that were connected to a common exterior stack. A variable speed blower was used in the stack for the last five tests to provide better control of the pressure.

2.2. Test Assemblies

Each floor-ceiling assembly measuring 2.44 m wide by 3.05 m long (8 x 10 ft) was laid atop the specimen support frame installed around the edges of the top opening of the furnace. This produced an exposure area of 2.18 x 2.79 m (7.17 x 9.17 ft). The assembly was subjected to an approximately uniform distributed load, applied by means of steel blocks.

The following types of floor assemblies were tested and a descriptive summary of the main structural elements, applied loading, and fire exposure conditions for individual tests are presented in table 1.

Assemblies 1, 2, and 8

The floor framing consisted of nominal 51 x 203-mm (2 x 8-in) wood joists spaced 0.61 m (24 in) on center, with the exception of two end joists positioned 0.59 m (23 1/4 in) from the adjacent joists to accommodate the 2.44-m (8-ft) furnace width. The construction details and instrumentation layout of the floor assembly are shown in figure 1. Each joist was kiln-dried, construction grade no. 2, southern pine. Each joist was 2.97 m long and both ends were secured to nominal

4

51 x 203-mm wood rim joists with two 90 mm (3 1/2 in) long 16d common nails. The rim joists were toenailed using 16d common nails spaced 0.41 m on center to wood sill plates resting on top of a layer of 64 mm (2 1/2 in) thick fire brick that covered the specimen support frame. The sill plates were pressure treated southern pine lumber. Cross-section dimensions were 38 x 127 mm (1 1/2 x 5 in) for assembly 1, and 38 x 114 mm (1 1/2 x 4 1/2 in) for assembly 2. The latter size placed the edges of sill plates flush with those of the specimen support frame. Solid wood bridging was installed along the mid-span of the floor joists.

A single layer of 18-mm (23/32-in) thick underlayment grade, Douglas fir plywood subfloor was laid with the long dimension perpendicular to the joists and the end joints staggered 1.22 m (48 in) between the adjacent rows. The plywood was supplied in 1.22 x 2.44-m (4 x 8-ft) sheets with tongue and groove edges on the long sides and marked APA Group 1, interior with exterior glue. The subfloor was secured to each joist with 64-mm (2 1/2-in) long 8d coated common nails spaced 0.15 m (6 in) on center along edges and 0.25 m (10 in) on center along intermediate members. The pockets formed by the plywood subfloor, the rim joists, and the sill plates were filled with 89-mm (3 1/2 in) thick, R11 glass fiber insulation blankets with aluminum foil faced vapor barrier. An olefin carpet with foam rubber backing was fastened to the plywood deck at its perimeter with 16-mm (5/8-in) long carpet tacks placed 0.2 m (8 in) apart.

The ceiling was a layer of 16-mm (5/8-in) thick, type X, gypsum wallboard positioned with long edges at right angles to the floor joists. Wood pieces, which were cut from nominal 51 x 102-mm southern pine lumber, were installed along the outer boundary of fire exposed surface of the assembly. The gypsum board was secured to the joists and boundary with 45-mm (1 3/4-in) long coated drywall nails spaced at 0.15 m (6 in) on center along the edges of the board and 0.3 m (12 in) on center in the field. All exposed nail heads and joints were taped and covered with joint compound, and the ceiling-wall seams were

finished with wood trim. The exposed face of the gypsum board ceiling
was painted with two coats of white interior flat latex paint.

Assemblies 3 to 7 and 9

Each test assembly was similar to assembly 1, except there was no
gypsum board ceiling. The floor system was supported by nominal
51 x 203-mm (2 x 8-in) kiln dried, construction grade no. 2, southern
pine joists spaced 0.61 m (24 in) on center, with the exception of a
0.59-m (23 1/4-in) spacing for the two end joists aside from their
adjacent ones. Figure 2 shows the construction details of the unpro-
tected floor-ceiling assembly and the arrangement of instrumentation.
The sill plates, each measuring 38 x 114 mm (1 1/2 x 4 1/2 in) in
cross-section, were made from the sections of nominal 51 x 152-mm
(2 x 6-in) pressure-treated southern pine lumber. The subfloor was
18 mm (23/32 in) thick, underlayment grade, Douglas fir plywood with
tongue and groove edges on the long sides. An olefin carpet with foam
rubber backing was installed on top of the plywood deck.

Assembly 10

The structural members used to support the floor-ceiling assembly
were C-shaped galvanized steel joists, 184 mm (7 1/4 in) deep with a
45-mm (1 3/4-in) flange, a 14-mm (9/16-in) stiffening lip, and a
1.26-mm (18 gauge) thickness. The joists were spaced 0.81 m (32 in) on
center beginning with one joist placed along the horizontal centerline
of the furnace width and each joist was strengthened at both ends
through short web reinforcement, i.e., attachment of a short piece of
the steel joist, 152 mm (6 in) in length, to the web of the floor joist.
Figure 3 shows the details of the test floor and the layout of
instrumentation. Each joist was cut 2.97 m (117 in) long and fastened
to nominal 51 x 203-mm (2 x 8-in) wood rim joists with two 64-mm
(2 1/2-in) long, 8d common nails driven through steel end clips. The
rim joists were toenailed to 38 x 114-mm (1 1/2 x 4 1/2-in) wood sill

6

plates resting on the top of a single layer of fire bricks over the support frame for the test specimen, with 90-mm (3 1/2-in) long 16d common nails spaced 0.41 m on center.

The subfloor was 18-mm (23/32-in) thick, underlayment grade, Douglas fir plywood with tongue and groove edges on the long sides and marked APA group 1, interior with exterior glue. The plywood was laid with the long dimension perpendicular to the joists and secured to the steel framing using 48-mm (1 7/8-in) long type 512 screws spaced 0.15 m on center at the panel edges and 0.30 m on center at the intermediate supports. The 2.44 m by 3.05 m olefin carpet with a foam rubber backing was fastened to the plywood deck with 16-mm (5/8-in) long carpet tacks spaced approximately 0.2 m on center along its perimeter.

Prior to the fire test, the moisture content of wood-base materials used in the assemblies was determined with an electric moisture meter by measuring the electric resistance between two pin-type electrodes driven into the wood. The moisture content was found to range from 7 to 9 percent with an average of 7.9 percent for wood joists, and from 7 to 8.5 percent with a mean value of 7.3 percent for the plywood subfloor. The initial weights and the estimated total available heat of combustible materials for each test assembly are listed in Table 2. The calorific values used for the potential heat calculations were 18.6 MJ/kg (8000 Btu/lb) for the wood and 46.5 MJ/kg (19900 Btu/lb) for the olefin carpet with foam rubber backing.

2.3 Structural Loading

Prior to fire exposure the test assembly was subjected to an approximately uniform load, which was achieved by evenly distributing steel blocks over the top face of the assembly. Each steel block measured 140 x 203 x 152 mm (5 1/2 x 8 x 6 in) and weighed 22.7 kg (50 lbs). For tests 1 and 2 the applied load was calculated to stress the floor joists to the maximum total deflection and the bending moment

permitted by design specifications. In order to compare the fire
performance results of the floor assemblies evaluated in the test
furnace with those obtained under the room burnout conditions [4], the
structural loadings for tests 3 to 5 and 8 to 10 were selected to
develop the same magnitude of bending stresses in the floor joists as
those produced in assemblies 3, 7 and 4 in the previous test series.
A live load of 265 kg/m^2 (54 psf), which corresponded to approximately
93 percent of the respective maximum design load based on the maximum
allowable bending stresses for wood joists, was applied to each assembly
used in tests 3 through 9 as shown in Table 1. Detailed calculation of
the required load for assembly 3 is given in Appendix A and the layout
of steel blocks over the carpeted floor of the test assembly is shown
in Figure 4.

3. TEST MEASUREMENTS

3.1 Temperature

The temperatures of the combustion gases in the upper part of the
furnace chamber were monitored through nine commercial metallic-
sheathed, mineral-insulated, fast response thermocouples and nine ASTM
E119-standard protected furnace thermocouples. The average temperature
derived from either these fast response, or from the ASTM furnace
thermocouples was used to control the fuel input to the test furnace so
that the newly developed temperature-time curve [3] or the ASTM E119
temperature-time curve, respectively, was followed. The equation used
to describe the newly developed temperature-time curve is the following:

$$T = \frac{A_o + A_1 t + A_2 t^2 + A_3 t^3}{B_o + B_1 t + B_2 t^2 + B_3 t^3} \qquad (1)$$

where $A_o = 0$ $B_o = 1$

$A_1 = 3.83 \times 10^1$ $B_1 = 4.49 \times 10^{-2}$

8

$$A_2 = -1.58 \times 10^{-2} \qquad B_2 = -4.56 \times 10^{-5}$$
$$A_3 = 9.05 \times 10^{-6} \qquad B_3 = 3.36 \times 10^{-8}$$

and where T is in °C and t in seconds. The measuring junctions of the thermocouples were located 0.31 m (12 in) below the supporting frame for the test specimen or 0.38 m (15 in) below the bottoms of the floor joists at the midpoint and quarter points of the lengthwise span as shown in Figure 5. All fast response thermocouples were commercially made from 1.02 mm (0.04 in), diameter chromel-alumel wires, enclosed within 6.4 mm (0.25 in) outside diameter stainless steel tubes having a 0.9-mm (0.036-in) wall thickness and insulated with magnesium oxide. The ASTM furnace thermocouples were of 1.02-mm (0.04-in) chromel and alumel wires, insulated with porcelain tubes, and protected by capped nominal 13 mm (0.5 in) diameter black wrought-iron pipes. The furnace gas temperatures were also measured with five bare-junction 0.51-mm (0.02-in) diameter (no. 24B&S gauge), double-cable chromel-alumel thermocouples. These thermocouples were positioned along the vertical centerline of the furnace chamber at 0.31, 0.61, 1.42, 3.11 and 2.79 m below the supporting frame for the test structure. The junctions were formed by welding the chromel wire from one cable to the alumel wire from the other cable in order to eliminate the current leakage through the insulation materials within the individual thermocouple cables at temperatures above 800°C. The surface temperatures of the furnace walls at selected locations were measured with the thermocouple beads attached to the exposed and unexposed surfaces of ceramic fiber blocks installed as the hot face veneer linings over the existing refractory linings. This low thermal inertia block lining was necessary to achieve the very rapid temperature rise in the furnace required by the proposed high intensity short duration fire exposure.

The temperatures of the unexposed surface of the test assembly were determined with 15 bare-beaded, 0.51-mm (20 mil) wire diameter, chromel-alumel thermocouples placed underneath ceramic fiber pads, 152 mm (6 in) square by 13 mm (0.5 m) thick, and attached to the top

9

surface of the carpeted flooring as shown in Figures 1 to 3. The temperatures of the top and bottom surfaces of the floor joists and the unexposed surface temperatures of the plywood subfloor were also measured with the bare-beaded, double-cable thermocouples.

3.2 Floor Deflection

The deflection of the test assembly during the test was measured at the mid points and selected quarter points of three centrally located floor joists as shown in Figures 1 to 3. Nickel steel cables and linear-displacement potentiometers mounted on a panel along with small pulleys were employed to provide indications of the relative movements of the floor surface.

3.3 Furnace Pressure

The static pressures at various heights inside the test furnace were monitored continuously through four nominal 64-mm (1/4-in) diameter steel pipes extending through the east and west walls into the furnace with their open ends flush with the wall surfaces. The four locations used for pressure measurements included one each at the east and west walls along the vertical centerline of the interior wall 0.10 m (4 in) down from the supporting frame for the test specimen, one at the west wall 1.19 m (47 in) below the supporting frame, and the remaining one near the bottom of the east wall 2.72 m (107 in) away from the supporting frame as shown in Figure 5. The exterior ends of the pipes were connected by copper tubing to variable reluctance pressure transducers.

3.4 Heat Flux and Flow Rate

The total heat fluxes incident at selected locations were measured with three Gardon-foil type, water-cooled heat flux gauges. Two of these gauges were mounted flush with the internal surface of the south wall 0.76 m (30 in) away from its vertical centerline and 1.19 m (47 in)

10

below the supporting frame for the test assembly, and one in the east wall 0.31 m (12 in) away from its vertical centerline and 1.19 m (47 in) down from the supporting frame.

The axial velocity of the primary combustion air inside a 0.25 m (10 in) outside diameter, light-gage metal pipe was monitored continuously with a pitot tube in conjunction with a variable reluctance differential transducer. The pitot tube was placed at the center of the circular pipe facing upstream. The delivery rate of gaseous fuel to the furnace burners was metered throughout the test with an orifice plate flowmeter.

3.5 Gas Concentrations and Data Acquisition

Continuous gas samples were withdrawn from the flue gas stream with steel tubing and analyzed for O_2, CO_2, and CO after passing through a series of cold traps and filtering tubes. The concentrations of CO_2 and CO were measured with non-dispersive infrared gas analyzers and O_2 with a polarographic-type oxygen cell.

The output signals from the thermocouples and various transducers were automatically recorded by a high speed digital data acquisition system. The test data were logged every 8 seconds and then transferred to the computer for processing, tabulating, and plotting.

4. TEST PROCEDURE

4.1 Fire Test

Each test assembly was built and installed in the test frame of the furnace. A few days prior to fire exposure, the assembly was loaded uniformly with steel blocks to the prescribed load density. The fire test was initiated by igniting the aerated fuel gas from the burners with spark-ignited gas bypass pilots. The readings from nine protected

11

fast response or ASTM furnace thermocouples were averaged to provide the mean furnace gas temperature, which was made to follow the proposed or the standard ASTM E119 time-temperature curve by manual control of the gas flow to the burners. Visual observations and photographic and video tape records were made of the burning characteristics of the test assembly including floor deflection, time for burn-through, and time for structural failure.

4.2 Fire Endurance Criteria

The fire endurance of a floor construction is characterized by the time of failure defined as one of the following:

1. Structural failure is considered to have occurred when the test assembly cannot withstand the applied load and collapses. The collapse of the test assembly can be anticipated to occur when the total deflection has equaled or exceeded $L^2/800d$, and the rate of deflection has attained or surpassed $L^2/150d$ per hour, where L is the span between supports of a structural element, in meters, and d is the distance between the upper and lower extreme fibers of a structural component or assembly, in meters [7]. For the assemblies tested, the critical values for the deflection and the rate of deflection were equal to 48mm and 0.071mm/s, respectively.

2. Integrity failure is considered to have occurred when flames or hot gases have passed through the test assembly to its unexposed side.

3. Thermal insulation failure is considered to have occurred when the average temperature on the unexposed surface of the test assembly increased more than 139°C (250°F) above its initial temperature or by more than 181°C (325°F) at any one point.

12

5. TEST RESULTS

A log of visual observations and records from video tape recordings taken from above the test assembly during a typical test run (test 1) is given in Appendix B. The following are general observations of the performance of each test floor subjected to the prescribed fire conditions.

Assembly 1

Failure of gypsum board ceiling with falling of small fragments away from the assembly was observed at 16 min:25 sec. Penetration of flames through the plywood deck/olefin carpet floor to the unexposed side occurred at 20 min:6 sec. The burn-through region was located 0.71m from the east furnace wall between the center joist and its adjacent joist to the north. The deflection of the test structure measured at the center point showed an appreciable increase after 18 min:16 sec and attained a downward movement rate of 0.56mm/s at time of test termination. The maximum values of the average and an individual temperature attained on the unexposed surface during the test were 56 and 106°C, respectively, since the thermocouple locations were away from the burn-through region.

Assembly 2

The protective layer of gypsum board used as the ceiling finish began to disintegrate and fall from the test assembly at 30 min:20 sec. Failure of the floor assembly was observed at 34 min:0 sec by the passage of flames through to the carpeted surface in a region 0.9m west and 0.8m south of the center of the test floor. The floor was found to sag more rapidly at 35 min:4 sec with a maximum deflection rate of 0.35mm/s, which eventually led to the collapse of the center joist. The average temperature of the surface thermocouples located away from the burn-through region on the unexposed side, increased quickly to

13

241°C at 35 min:8 sec and an individual temperature rise exceeded 181°C at the same time.

Assembly 3

Flame penetration of plywood subfloor/carpet flooring was observed at 6 min:4 sec in the region centered at 1.07m west and 0.25m north of the middle of the assembly. Floor deflection showed a significant increase at 5 min:10 sec, at which time the center joist was deforming at a rate of 0.6mm/s. A total distance of 57mm occurred at 7 min after the start of the test. The entire test structure collapsed and fell into the furnace 2 min:8 sec later than the structural failure time calculated based on the deflection limits proposed by Ryan and Robertson [7]. An individual temperature rise on the unexposed surface near the center of the test floor exceeded 181°C at 6 min:34 sec, but the average temperature was less than 49°C at time of test termination.

Assembly 4

Passage of flames and hot gases through the assembly to the unexposed side occurred at 6 min:7 sec. The burn-through region was situated between the west quarterpoint of the center joist and that of its adjacent joist to the south and on the west side of the tongue and groove joint between two sheets of plywood underlayment. Additional penetrations of flames to the unexposed surface were observed at 6 min:40 sec at several locations near the center of the test floor. Structural collapse of the center joist based on floor deflection measurements occurred at 7 min:52 sec. One thermocouple positioned on the carpet in the vicinity of the center of the assembly indicated a steep temperature rise to 247°C at 6 min:56 sec and the average surface temperature rise of the unexposed face exceeded 139°C at 7 min:13 sec.

14

Assembly 5

The flame penetration of the carpeted plywood subfloor occurred at
7 min: 0 sec in the region centered at the east one-third point along
the joist located north of the center joist. The record of floor
deflection measured at the center of the test floor showed a consider-
able deflection rate at 8 min:48 sec and the maximum downward flexure
rate of 3.4mm/s occurred at 10 min:32 sec. One surface thermocouple
located on the carpet surface in the neighborhood of the burn-through
region registered 223°C at 10 min:8 sec and the maximum average
temperature of the unexposed surface was 177°C at the end of the test.

Assembly 6

Penetration of flames to the unexposed surface was observed at
16 min:8 sec in the middle of the area surrounded by the east furnace
wall, the center joist, the east tongue and groove joint between the
two sheets of plywood subfloor, and the floor joist south of the center
joist. The floor deflection measured at the center of the test assembly
increased rapidly at 14 min:50 sec and the total deflection was 175mm
when the test was terminated at 16 min:50 sec. A single thermocouple
on the carpeted floor near the center of the assembly indicated 209°C
at 16 min and the average value of the readings of surface thermocouples
on the unexposed side at test termination was 202°C above its initial
value.

Assembly 7

Flames penetrated the carpeted plywood deck near the east one-third
point along the floor joist located north of the center joist at
17 min:35 sec. The region where the fire broke out was centered at
1.22m from the east furnace wall and 0.76m away from the north wall.
The downward deflection of the test floor increased steadily at a rate
of 2.7mm/s to a total distance of 303mm at 17 min:40 sec. An individual

temperature, measured at the point 430mm northeast of the center of the test floor on the unexposed face, showed a rapid increase to 217°C at 17 min:10 sec and the average surface temperature increased to 106°C after 18 minutes of test duration.

Assembly 8

The gypsum board ceiling near the center of the test structure started to break up and fall at 15 min:40 sec. Penetration of flames to the unexposed surface took place at 24 min:22 sec in the space between the center joist and its adjacent joist to the south near the west tongue and groove joint of two sheets of plywood underlayment. The center of the flame-through region was situated 0.91m from the south edge and 0.69m from the west edge of the test assembly. A significant increase in the floor deflection was noticed at 24 min:10 sec, and the floor deflected downward at a rate of 6.3mm/s to a total distance of 150mm at 26 min:30 sec. An individual temperature rise on the unexposed surface located near the center of test floor exceeded 181°C at 25 min:23 sec, but the average surface temperature was less than 102°C throughout the duration of the test.

Assembly 9

Failure of the test assembly due to flames passing through to the unexposed surface in the area located between the center and the south joists and near the west tongue and groove joint formed by two sheets of plywood subfloor was observed at 9 min:09 sec. The burn-through region was centered at 0.66m from the west edge and 0.94m from the south edge of the test floor. The floor deflection measured at the center of the test assembly attained a significant rate at 8 min:30 sec and a peak deflection rate of 0.88mm/s occurred at 10 min:00 sec. The temperature rise of one thermocouple positioned on the carpeted surface near the center of the test floor surpassed 181°C at 9 min:38 sec but the average temperature of the unexposed surface was 74°C at time of test termination.

16

Assembly 10

The fire burned through the region situated above the intersection
of the centrally located floor joist and the west tongue and groove
joint between two sheets of plywood underlayment at 4 min:38 sec.
Deflection measurements at the center point of the test assembly indi-
cated a rapid increase at 2 min:45 sec and the maximum downward flexure
at a rate of 5.5mm/s occurred at 5 min:47 sec. One individual thermo-
couple in contact with the carpeted surface near the center of the test
structure exceeded 181°C above its initial temperature at 4 min:24 sec
and the averaged temperature rise of the unexposed surface surpassed
131°C at 5 min:48 sec.

6. DISCUSSION

The newly developed temperature-time curve in Figure 6(a) was
derived by approximating the upper layer gas-temperature history
obtained by fast response thermocouples from a typical test run in a
series of basement recreation room burnout tests [3] with a smooth curve
and setting zero time as the beginning of the rapid temperature rise
period. The development of this new temperature-time curve, which
represents a high intensity, short duration fire exposure and is
regarded as a more realistic description of the severity of room fires
likely found in residential occupancies, was discussed elsewhere [3,4].
The gas temperatures plotted in the Figures 6(b) to 6(d) and 7 were
derived by averaging the readings of nine equally spaced thermocouples
located on a plane 0.38m below the underside of the test assembly.
Figures 6(b) and 6(d) illustrate the ability of the furnace to follow
the newly developed temperature time curve. Figure 6(c) illustrates
the departure of the furnace temperature from the newly developed
temperature-time curve when it is constrained to follow the E119 curve.
The temperature in Figure 6(c) is measured with fast response
thermocouples, even though the furnace is controlled with the ASTM
thermocouples. The newly developed fire exposure has a steeper

17

temperature rise during the initial stage and a shorter period of time at higher temperatures than the standard ASTM E119 curve. Figure 7 shows that temperatures as measured with the ASTM thermocouples for the tests covered in Figure 6(d) follow the E119 fairly well from 5 minutes onward. (The E119 curve is not defined between 0 and 5 minutes.) Tests 1 and 2, which were of protected wood joist floors with a high level of excess air in the furnace, showed rapid increases in their peak levels toward the end of test period. This was due to increased rates of heat released by combustion of the volatile products from the pyrolyzing wood in the test structure with the excess air.

The performance of the floor-ceiling assemblies subjected to various fire environments in the test furnace are summarized in terms of fire endurance (periods) in Table 3. The fire endurance of a test assembly is expressed as the duration of a specified fire exposure prior to failure as defined by any one of the following events: (1) passage of flames through openings or cracks developed in the assembly, (2) structural collapse, and (3) attainment of an average temperature of 139°C or an individual temperature of 181°C above the initial temperature on the unexposed surface, whichever takes place earliest. The structural failure time shown in the table was based on the instant when the floor deformation exceeded both the total deflection of 48mm and the deflection rate of 0.071mm/s in accordance with the load failure criteria proposed by Ryan and Robertson [7]. For most of the assemblies tested, the rate of deflection surpassed its specified limit earlier than the total deflection. Also, listed in the table are the maximum values of total deflection measured at the center of the individual floor-ceiling assemblies.

As shown in Table 3, the failure times of the unprotected wood joist floors due to flame-through varied from approximately 6 to 9 minutes for the newly developed temperature time curve (tests 3, 4, 5, and 9) depending on the amount of excess air available to burn the exposed wood-base materials in the furnace and to deteriorate the

18

structural integrity of the floor. For conditions of the test refer back to Table 1. A protective layer of 16mm thick, type X gypsum board as the ceiling finish provided an additional fire endurance of approximately 15 minutes for exposure to the new time-temperature curve (test 1) and 18 minutes to the ASTM E119 standard fire exposure (test 2). Under a similar rate of air supply to the furnace, the ASTM E119 fire exposure appears to be less severe and results in a delayed failure time for the floor assembly compared to the newly developed fire exposure (test 2 versus test 1 and test 6 versus test 9). The structural failure times listed in Table 3, as calculated from the failure criteria developed by Ryan and Robertson [7], were shorter than the times to actual collapse of the floor joists, which were observed generally to occur soon after the termination of the test. These deflection limits may be a useful alternate criterion for defining the failure of load-carrying capacity of the building members. However, the structural deflection may be affected by many factors which need to be understood in order to establish the validity of the relationship between the limits and actual test results. The times for the average temperature of the nine uniformly-distributed thermocouples on the unexposed floor surface to reach 139°C and for a single thermocouple to reach 181°C above the initial temperature usually occurred somewhat after the flames passed through the test structure. Also shown in Table 3, the maximum deflection at the center of each test assembly varied widely from about 50 to 330mm depending upon the degree of charring and burning of floor joists, the type of fire exposure employed, and the time from the flame-through to test termination.

Table 4 presents the flame penetration times of the assemblies evaluated in the fire endurance furnace compared with the failure times on the same constructions under room fire environments along with the measured oxygen content in the flue gas stream. The protected and unprotected wood-frame floors under the newly developed fire exposure with small amounts of excess air exhibited passage of flames in approximately 24 and 9 minutes, respectively, compared to 35 and 12

minutes under the fire conditions produced from the burning of typical furniture and interior finish materials in a room [4]. The earlier failure of the floors in the furnace was attributed to rapid reduction in the thickness of the subfloor and in the cross-sectional area of the floor joists caused by the more intense burning and faster charring rates of the wood-base materials caused by the greater amount of excess air present in the test furnace. The passage of flames to the unexposed side of the assembly in the furnace tests was purely burn-through of the plywood subfloor, while in the room fire tests, the increased deflection of floor joists with elevated temperatures promoted joint separation and developed openings for flames passing through. The flame-through time of the exposed light gauge steel-framed floor assembly was comparable with that for the counterpart room fire test as both tests were run in fire environments with reduced oxygen levels. Also illustrated in the table, the wood floors with and without the gypsum board ceiling exposed to the ASTM E119 standard fire exposure (tests 2 and 6) were penetrated by flames in 34 and 17 minutes, respectively. In the first case, the excess air in the furnace was high and, in the second case, it was low.

Summary data on the average flow rates of the air and fuel gas supply to the furnace, the concentration of oxygen in the flue gas, average heat flux measured at furnace walls, and the average char rate for the tests performed are tabulated in Table 5. The table also lists the flow rate of excess air, which was equal to the difference between the flow rates of air supplied and stoichiometric air required for complete combustion of fuel gas. The average char rate for each individual assembly was calculated from on the thickness of the plywood subfloor and the total duration of fire exposure up to time of burn-through. The char rate of the plywood deck was lowest for tests 6 and 7 which had the lowest amount of excess air. The char rates were highest in tests 1 and 2. This may have been because the average furnace temperature was higher during the exposure period which did not start until the fire penetrated the gypsum board ceiling.

Figures 8 and 9 show the time variation of the volumetric flow rates of air and fuel supplied to the test furnace for all of the tests.

The concentrations of CO_2, CO, and O_2 in the flue gas prior to discharge to the chimney, are shown in Figures 10(a) to 10(j) as a function of time for the individual tests. As expected for a given air supply rate, the oxygen level in the furnace gases decreased with increasing inflow rates of the gaseous fuel and the volatile components from the thermally decomposing cellulosic materials in the test assembly. The gaseous fuel and combustible volatiles eventually burned to deplete the available oxygen inside the furnace chamber. Figures 11(a) and 11(b) display the average static pressure in the upper part of the furnace chamber as a function of time. These furnace pressures were obtained by averaging the readings of two pressure probes, one each positioned in the east and west furnace walls and 0.17 m beneath the test assembly. Except for brief excursions, a furnace pressure of 15 $\pm$ 5 Pa (0.06 $\pm$ 0.02 in water column) was maintained throughout each test after 2 min or less from the start except for test 5. In that test the pressure within the furnace became less than atmospheric when it was necessary to reduce the rate of fuel and combustion air starting about 4 minutes before the termination of the test. These negative pressures caused cool air to be drawn into the furnace through various cracks and openings developed in the test structure, increasing the concentration of oxygen in the flue gas as illustrated in Figure 10(e). This inward movement of cold air may have induced a greater heat loss by convection from the exposed surfaces and resulted in a small increase in the time to failure of test assembly 5 over that of 3 and 4 as shown in Table 3.

The total rates of heat release in the fire endurance furnace as a function of time for the individual tests are shown in Figures 12(a) to 12(c). The heat release rates were calculated from the experimental data on the concentrations of O_2, CO_2, and CO, and the flow rate of flue gas using a heating value of 19210 kJ/m^3 of oxygen consumed for the fuel

gas and the pyrolysis products from the assembly. The detailed derivations of the equations utilized for the energy production calculations are given in Appendix C. The heat release rates for tests 1 to 7, which were run prior to installation of a pitot tube for flue gas velocity measurement, were computed by assuming the mass flow rate of the flue gas equal to the sum of the flow rates of the air and fuel gas supplied to the furnace. In order to lower the furnace gas temperature in test 8, to follow the descending portion of the newly developed temperature-time curve, cooling water supplied at a rate of 139 g/s, which corresponds to a heat extraction of 3/4 kW for water vaporization, was injected into the furnace from 20 min after the start of the test until its termination. No correction due to mass addition of cooling water was made on the latter portion of the heat release rate curve for test 8. As shown in the figures, the rates of heat production in the furnace tests during the high-intensity, short-duration fire exposure were significantly greater than those under the ASTM standard fire exposure. For a given air supply rate, the unprotected floor assemblies had higher heat release rates than the protected floors due to earlier occurrence of ignition and heat production from the wood joists and the plywood subfloor.

The heat release rates calculated by the oxygen consumption method are compared to those derived from the fuel gas input rate multiplied by its heating value for tests 1, 2, and 8 in Figures 13(a) and 13(b). As shown, the rates of heat release computed from the measured flue gas flow rates and oxygen concentrations were found to be in reasonably good agreement (within approximately 3 percent) with the heat output rates derived from fuel combustion. This approximation holds for the period between ignition of the gas burners and disintegration of the gypsum board ceiling. The continuous increase in the total heat release rate toward the end of this period is attributed to the heat production from the burning of the combustible materials of the test assembly in the presence of excess air inside the furnace. The total amount of heat produced in the test furnace and the heat output from the gas

22

burners due to fuel combustion for the time interval between the start of the test and the occurrence of flame-through at the floor for each test are given in Table 6. Total heat production and fuel-contributed heat production were obtained from integrations of respective heat release rate vs. time curves mentioned previously. The low values in total heat release for tests 6 and 7, as shown in the table, are questionable. There were some difficulties in the flue gas sampling system at the beginning of the test for test 6 and in the air inflow measurement for test 7. Table 6 also presents the amount of heat given off by the individual assemblies, calculated from the difference between the total heat production and the fuel contributed heat release. The temporal variation of the total heat release and the amount of heat produced by fuel combustion for each test are shown in Figures 14(a) to 14(j). Note that the total heat release rate curve on each figure should be multiplied by a factor to make it coincide with the gaseous fuel prior to the time at which the assemblies begin to contribute fuel. This is necessary because of the inaccuracies in measuring the volume flow rate in the furnace exhaust duct. At any given time, the difference between these two curves provides a measure of the heat released by the combustible assembly up to that time.

Figure 15 is a graph of the gas temperature for test 8 as measured by three types of thermocouples positioned 0.38 m below the test structure at the center of the furnace. The temperature readings of the sheathed fast-response thermocouples fell between the readings of the regular 0.5 mm double-cable thermocouples and the ASTM thermocouples in response to the rapid increase in furnace gas temperature during the early stages of the test. As the test progressed, the temperature differences gradually decreased with decreasing rate of gas temperature change.

The change of the average incident heat flux with time measured at the furnace walls for the various tests are shown in Figures 16(a) through 16(d). These heat fluxes for tests 1 to 7 were obtained by

23

averaging the readings of three total-heat-flux gauges installed with
the sensing elements flush with the interior surfaces of the south and
east furnace walls. For tests 8 to 10, the average value was derived
from two heat flux gauges situated in the south wall. The levels of
heat flux incident at the furnace walls during the high-intensity
short-duration fire exposure were generally higher than those observed
under the ASTM E119 standard fire exposure because of the fact that the
former exposure had higher furnace gas and wall surface temperatures.

In order to estimate the rate of heat loss to the furnace walls
and assess the accuracy and reliability of the direct measurements with
the heat flux gauges, calculations were made of the heat flux incident
at selected locations during the fire endurance test. These heat fluxes
at the exposed surfaces were computed using the measured surface
temperature data and the assumption that the furnace walls are thermally
semi-infinite solids. The equations and procedures used for the heat
flux calculations are described fully in a previous report [3]. For
these calculations the density, surface emissivity, thermal diffusivity,
and thermal conductivity of the ceramic fiber blocks utilized as
interior wall linings were, respectively: 133 kg/m^3, 0.95, 1.43 x
10^5 m^2/s, and 5.61 x 10^5 kW/m-K for the surface temperatures below 260°C,
and 3.01 x 10^7 T$_s$ - 2.21 x 10^5 kW/m·K, for the surface temperatures (T$_s$)
above 260°C. Figures 17(a) to 17(e) illustrate a comparison of the
calculated and measured surface heat fluxes, acting near the centers of
the south and east furnace walls, as a function of time for tests 1, 2,
and 8. As shown, there is reasonably good agreement between the
calculated heat fluxes and those determined with the heat flux gauges.
However, the measured heat fluxes should be greater than the calculated
values due to the higher rate of convective heat exchange with a water
cooled heat flux gauge. The difference between these curves may be
partially attributed to the uncertainty of the numerical values used
for the material thermal properties in the calculations. The rate of
heat loss to the furnace walls averaged over the period from the start
of the test to the failure of the gypsum board ceiling was estimated

24

from the surface temperature data and found to be approximately 195kW or 10.6 percent of the rate of heat produced from fuel combustion for test 1, 110kW or 8 percent for test 2, and 270kW or 14.9 percent of total energy released in the furnace for test 8.

7. SUMMARY

This is the final report of a long-term project to develop a fire endurance test for residential floor construction. The ASTM E119 test is not applicable here, where ratings of less than one hour are required, because (1) its slow rate of temperature rise is not characteristic of the burning of the combustible contents in modern dwellings, (2) the slow response time thermocouples do not provide adequate control during the critical, short duration of the test, and (3) the test is conducted under negative or neutral furnace pressure which is not representative of room fires. This project started with a residential fire load survey [8] which led to the adoption of a standard recreation-room configuration as the basis for a new test. The movable contents fire load of 23 kg/m^2 (4.7 lbs/ft^2) included a polyurethane couch and chair as well as other items of furnishing. A parametric study of the effect of ventilation, interior finish, fire load, and room size on the temperature-time curve developed during room fire tests of this configuration was then conducted [3]. Next a series of room fire tests were conducted on seven selected residential floor constructions using this basic configuration [4]. In the last phase of this project, which is reported here, three of these assemblies were tested in a fire endurance furnace using both the ASTM E119 and the newly constructed temperature-time curve so that a comparison could be made between the two types of exposure in the furnace and between the furnace and the room fire test. Tests were also run with low and high percentages of excess air in order to examine the effect of oxygen concentration in the furnace on the failure time of combustible construction. The extensive research conducted on this project has culminated in the recommendation of a new fire endurance test for

25

residential floor constructions. The following observations were made as a result of the present tests:

1. The wood joist floors exposed to the newly developed fire conditions in the gas-fired furnace had a shorter time to failure compared with the earlier residential room fire tests on the same floor constructions. This was due primarily to the increased burning rates of the combustible materials in the test structure with the excess air present inside the test furnace.

2. Individual test assemblies resisted flame penetration in the furnace fire tests for a time approximately 40 percent shorter when tested under the newly developed time-temperature curve as compared with the ASTM fire exposure.

3. A protective layer of 16mm thick, type X gypsum board on the ceiling acted as a thermal barrier on the fire-exposed side of the assembly and increased the time-to-failure by approximately 15 minutes for the high-intensity, short-duration fire exposure and by about 18 minutes for the standard ASTM E119 fire exposure.

4. The rates of heat release calculated by the oxygen consumption method were generally consistent with the heat output rates of the gas burners, up to the time of fuel contribution by the assemblies. The difference between the heat release rate calculated by the oxygen consumption method and the heat output of the burner at later times provides a good measure of the heat released by the assemblies.

5. In the case of the protected assemblies (tests 1 and 2) a steep rise in the furnace gas temperature was observed immediately after the combustible floor was involved in the fire. This was the result of the rapid heat production from the combustion of the flammable volatiles from the pyrolyzing wood-base materials

in the excess air atmosphere. This effect was reduced (test 8) when the percentage of air supplied to the furnace was reduced. It is important that the oxygen concentration in the furnace exhaust duct be specified during the tests.

6. Under the new fire exposure condition, the unprotected wood-frame floor suffered the passage of flames in 9 minutes compared with 4.5 minutes for the exposed light gauge steel-framed floor. There was an opening up of seams due to the sag of the steel joists in the latter case.

7. The fast response thermocouple has a shorter time lag and provides a better indication of the true furnace gas temperature compared with the ASTM E119 furnace thermocouple, especially during the early stage of the test.

8. RECOMMENDATIONS

The following recommendations are made:

1. A new fire endurance test should be submitted to ASTM for the purpose of rating residential floor constructions which require endurance times of less than one hour. The new test should have the following features:

   (a) The temperature-time curve shown in figure 6a and given by equation 1 should be used to control the furnace temperature. It is based on a series of residential recreation room fire tests reported in NBSIR 80-2120. The proposed temperature-time curve is shifted by 85 seconds from the one developed in that report so that zero time corresponds to the beginning of the rapid temperature rise period and coincides with the time at which the gas is turned on in the fire endurance furnace. It may be necessary to insulate the

walls of the furnace with ceramic fiber in order to achieve the rapid rise portion of the prescribed temperature-time curve.

(b) The furnace temperature should be measured and controlled by metallic-sheathed mineral insulated fast response thermocouples described in this report.

(c) The pressure measured at the top of the furnace should be at least +10 Pascals.

(d) The oxygen concentration of the flue gas should be as low as possible to correspond to the ventilation limited condition in the room. Very low levels may be difficult to achieve in some furnaces. A level of 5 percent may be a practical limit based on these experiments. The actual value measured during the test should be reported.

2. The oxygen concentration in the exhaust flue during standard ASTM E119 tests should be reported because of its impact on the failure time of combustible constructions.

3. Oxygen consumption measuring equipment may be added to existing ASTM E119 furnaces in order to obtain the heat release rate of assemblies, whenever that information is requested.

9. ACKNOWLEDGEMENTS

28

in the planning of the tests and for his valuable assistance in the
preparation of this report.

9. REFERENCES

[1] "Standard Methods of Fire Tests of Building Construction and
     Materials," ANSI/ASTM E119, 1981 Annual Book of ASTM Standards,
     Part 18, pp. 879-904 (American Society for Testing and Materials,
     Philadelphia, Pa., 1981).

[2] Fang, J. B., Static Pressures Produced by Room Fires, Nat. Bur.
     Stand. (U.S.), NBSIR 80-1984 (February 1980).

[3] Fang, J. B. and Breese, J. N., Fire Development in Residential
     Basement Rooms, Nat. Bur. Stand. (U.S.), NBSIR 80-2120
     (October 1980).

[4] Fang, J. B., Fire Performance of Selected Residential Floor
     Constructions Under Room Burnout Conditions, Nat. Bur. Stand.
     (U.S.), NBSIR 80-2134 (December 1980).

[5] "National Design Specification for Stress-Grade Lumber and Its
     Fastenings," National Forest Products Association, 1973.

[6] "Design Values for Wood Construction," A Supplement to the 1977
     Edition of National Design Specification for Wood Construction,
     National Forest Products Association (June 1978).

[7] Ryan, J. V. and Robertson, A. F., Proposed Criteria for Defining
     Load Failure of Beams, Floors and Roof Constructions During Fire
     Tests, J. of Res., Nat. Bur. Stand. (U.S.) 63C, 121-124 (1959).

[8] Issen, L. A., Single-Family Residential Fire and Live Loads
     Summary, Nat. Bur. Stand. (U.S.), NBSIR 80-2155 (December 1980).

Appendix A

Calculation of the Load to be Applied During the Fire Test

The design value for the nominal 51 x 203-mm (2 x 8-in) construction grade no. 2, southern pine joists used in test 3 is given in references 5 and 6 as follows:

allowable extreme fiber stress in bending, F_b = 8.27 x 10^6 Pa (1200 psi)

modulus of elasticity, E = 1.1 x 10^{10} Pa (1.6 x 10^6 psi)

moment of inertia, I = 1.983 x 10^{-5} m^4 (47.64 in^4)

section modulus, S = 2.153 x 10^{-4} m^3 (13.14 in^3)

All floor joists were simply supported with a span length of 2.79 m (110 in) and spaced 0.61 m (24 in) on center.

Dead load for Assembly 3:

Plywood subfloor (18 mm thick)	10.9 kg/m^2
Wood joists and bridging	9.8 kg/m^2
Carpet flooring	1.8 kg/m^2
Total dead load	22.5 kg/m^2 (4.6 psf)

(1) Deflection

The maximum deflection allowable for a floor joist is limited to 1/360 of the span length and is equal to

$$D = \frac{L}{360} = \frac{2.79}{360} = 0.00775 \text{ m} \ (0.305 \text{ in})$$

The uniform load corresponding to this maximum total deflection at mid-span can be calculated as

30

$$w = \frac{384}{5} \frac{EID}{L^4} = \frac{(384)(1.1 \times 10^{10})(1.983 \times 10^{-5})(0.00775)}{(5)(2.79)^4}$$

$$= 2143 \ (N/m) = 218.5 \ kg/m \ (147 \ lb/ft)$$

and the maximum load distributed evenly on the floor joists with a 0.61m joist spacing is

$$\text{total allowable load} = 218.5 \times \frac{1}{0.61} = 358 \ kg/m^2 \ (73.4 \ psf)$$

The applied load permitted to meet the maximum allowable deflection is

$$\text{live load} = \text{total load} - \text{dead load}$$

$$= 358 - 23 = 335 \ kg/m^2 \ (68.6 \ psf)$$

(2) Bending Moment

The maximum bending moment occurs at the center of the span and can be calculated as

$$M = F_b S = (8.27 \times 10^6)(2.153 \times 10^{-4}) = 1781 \ N\text{-}m \ (15770 \ in\text{-}lb)$$

The total load per unit length on a joist, which induces this maximum bending moment is

$$w = \frac{8M}{L^2} = \frac{(8)(1781)}{(2.79)^2} = 1830 \ (N/m) = 186.6 \ kg/m \ (125 \ lb/ft)$$

and can also be expressed in terms of unit area as

$$\text{total allowable load} = 186.6 \times \frac{1}{0.61} = 306 \ kg/m^2 \ (62.7 \ psf)$$

The live load permitted to develop the maximum allowable bending stresses in the joists is

31

live load = 306 - 23 = 283 kg/m^2 (58 psf)

Therefore, the applied load capable of being carried by the floor joists, which are fully stressed to maximum allowed by design specification, is 283 kg/m^2 (58 psf).

Total loads to Assembly 4 in the previous test series [4]:

Live load	195 kg/m^2
Plywood Subfloor	9.5 kg/m^2
Wood joists	8.1 kg/m^2
Carpet flooring	1.8 kg/m^2
Total loads	214.4 kg/m^2 (43.9 psf)

The load on one floor joist with a joist spacing of 0.61m (24 in) on center is

$$w = 214.4 \times 0.61 = 131 \text{ kg/m (87.9 lb/ft)} = 1280 \text{ N/m}$$

and the maximum bending moment for this loading is equal to

$$M = \frac{wL^2}{8} = \frac{(1280)(3.25)^2}{8} = 1690 \text{ N-m (14960 in-lb)}$$

The uniform load on a joist producing this bending moment at the middle of span can be calculated as

$$w = \frac{(8)(1690)}{(2.79)^2} = 1736 \text{ (N/m)} = 176 \text{ kg/m (118 lb/ft)}$$

and the total load can also be expressed as

$$\text{total load} = 176 \times \frac{1}{0.61} = 288 \text{ kg/m}^2 \text{ (59 psf)}$$

32

The permissible live load, to develop the same magnitude of bending stresses in the joists as those in assembly 4 in the previous test series, can be obtained readily as

$$\text{live load} = 288 - 23 = 265 \text{ kg/m}^2 \text{ (54 psf)}$$

Appendix B
Log of General Observations During Test 1

Time (min:sec)	Events
1:20	Light glowing appearing on gypsum board ceiling in center area.
1:40	Smoking occurring along the edges of plywood deck, particularly on the front side.
2:08	Gypsum board paper face charring and flaking off.
2:30	Smoke escaping from the perimeter of the carpeted flooring on the unexposed side.
3:20	Small flames appear on wood sill plate along the front edge.
4:45	Flames from sill plates around the edges of the floor are flickering.
6:00	Smoke rising from the right rear corner on the unexposed side is increasing.
10:50	Fire-exposed gypsum board surfaces show dull red.
12:00	Inside of the cavity formed by the supporting frame for loading mechanism above test assembly filled with dense smoke.

34

16:10	Gypsum board cracks have developed in the area centered at the quarter-point toward the east side between the center and the north floor joists.
16:25	Gypsum board falling from the cracked area.
16:50	One piece of gypsum board in the south-east corner falling off.
18:16	Appreciable floor deflection occurring at the central check point.
18:25	Gypsum board falling away at several additional areas.
18:35	Whole fire-exposed surface of the floor involved in flaming.
19:40	Heavy smoke coming from the east edge on unexposed side.
20:06	Burn-through in the region near the quarter-point toward the east furnace wall between the center and the north joists.
20:48	Gas off and test stopped.

Appendix C

Derivation of the Equations Used for Calculating Rate of Heat Produced

in Test Furnace

Consider a rectangular parallelpiped-shaped test furnace in which the
heat is liberated from combustion of the fuel gas with air, both being
metered separately prior to admittance to the furnace. The combustible
test specimen, installed in the ceiling-position of the furnace, and
exposed to hot furnace gas on the lower side, thermally degrades into
volatile decomposition products and char. Additional heat is released
from the gas-phase combustion of the pyrolyzates and from the solid-
phase oxidation of the char on the specimen surface. All products of
combustion are vented through an exhaust duct to a chimney.

In order to derive the pertinent equations for heat production rate
calculations, the following simplifying assumptions are made:

1. The furnace gases are perfectly mixed with no variations in their
    composition and temperature.

2. The fuel gas introduced into the furnace and the combustible
    pyrolyzates from the decomposing sample react instantaneously
    with the oxygen in the air supply.

The continuity equations describing the conservation of the total mass
and the gas species around the furnace chamber may be written in the
following form:

$$\frac{d(V\rho_g)}{dt} = \sum_i F_i W_i - F_g W_g \tag{C-1}$$

$$\frac{d(V\rho_g X_{jg}/W_g)}{dt} = \sum F_i X_{ji} - F_g X_{jg} - V \sum_j \nu_j r \tag{C-2}$$

36

where $\sum_i F_i W_i = F_a W_a + F_f W_f + F_p W_p + F_w W_w$;

$$\sum_j \nu_j r = \nu_j' r_f + \nu_j'' r_p;$$

V is the volume of the furnace chamber; ρ_g is the density of combustion gases; t is time; F_k and W_k are the molar flow rate and the average molecular weight, respectively, of the gas mixture in stream k; the subscripts a, f, p, w and g denote the air, fuel, pyrolyzate, water and combustion gas streams, respectively; the water stream is provided for injecting the metered cooling water into the furnace to lower the gas temperature when it exceed the prescribed temperature level; X_{jk} is the concentration of the gas species j in the stream k, expressed in mole fraction; the gas species include oxygen, fuel, pyrolyzate, nitrogen, CO_2, CO, and H_2O; ν_j' and ν_j'' are the ratios of the stoichiometric coefficient of the gas species j to that of the fuel, and to that of the pyrolyzate, respectively; r_f and r_p are the rates of disappearance of the fuel and the pyrolyzate, respectively, expressed in moles per unit time per unit volume of the combustion gas.

In general, the rate of change of total mass of the gases in the furnace can be neglected when compared with the inlet and exit mass flow rates. With this approximation, an expression for the rate of oxygen consumption due to combustion of the fuel and the pyrolyzate can be obtained from equation (C-2) as

$$V \sum \nu_{O_2} r = (F_a X_{O_2 a}/F_g - X_{O_2 g}) F_g \tag{C-3}$$

Using this relationship, the rate of heat release within the furnace can be expressed by

$$\dot{Q} = (r_f \, \Delta H_f + r_p \, \Delta H_p) \, V$$

$$= K \phi (F_a X_{O_2 a}/F_g - X_{O_2 g}) F_g \nu \tag{C-4}$$

where $\phi = (r_f + r_p \Delta H_p / \Delta H_f)/(r_f + r_p \nu''_{O_2}/\nu'_{O_2})$ and $K = \Delta H_f/(\nu'_{O_2} \nu)$, the heat of combustion of the fuel per unit volume of oxygen consumed at the reference state of 25°C and 1 atm; ΔH_f and ΔH_p are the heats of combustion of the fuel and that of the pyrolyzate, respectively, in kJ/g-mole, and ν is the molar volume of oxygen at 25°C and 1 atm, e.g., ν is equal to $22.414 \times 10^3 \times (298.15/273.15)$ or 0.02446 m^3/g-mole for an ideal gas.

Assuming that both the air and the combustion gas behave as ideal gases, one obtains the following expression for the rate of heat release:

$$\dot{Q} = K\phi \left[X_{O_2a} \dot{V}_a T_g/(\dot{V}_g T_a) - X_{O_2g} \right] (298.15/T_g) \dot{V}_g \qquad (C-5)$$

where V_i and T_i are the volume flow rate and the absolute temperature of the gas mixture in stream i.

With the assumption of perfect gases for both the fuel gas and the pyrolyzates, the volumetric flow rate of the combustion gases in the effluent stream can be expressed by

$$\dot{V}_g = [\dot{V}_a + \dot{V}_f T_a W_f/(T_f W_a) + \dot{V}_p T_a W_p/(T_p W_a) + \dot{m}_w T_a \nu/(298.15\ W_a)]$$

$$[T_g W_a/(T_a W_g)] \qquad (C-6)$$

where $\dot{m}_w = F_w W_w$, the mass flow rate of cooling water injected into the furnace.

The combustion gases exhausting from the test furnace were analyzed after the removal of water vapor from the sample. The moisture-free flue gas produced under fuel limited combustion in the furnace consisted of CO_2, CO, O_2, and N_2. The concentrations of these gases, as measured with gas analyzers, can be expressed by

$$x^A_{CO_2} = F_g X_{CO_2g}/P$$

$$x^A_{CO} = F_g X_{COg}/P \quad\quad\quad (C-7)$$

$$x^A_{O_2} = F_g X_{O_2g}/P$$

$$x^A_{N_2} = 1 - x^A_{CO_2} - x^A_{CO} - x^A_{O_2}$$

where $P = F_g (X_{CO_2g} + X_{COg} + X_{O_2g}) + F_a X_{N_2a}$

The concentrations of CO_2, CO, and O_2 in the combustion gas stream can be obtained by solving these simultaneous equations, and the water content can be estimated based on the ratio of the moles of H_2O produced to the moles of CO_2 and CO formed from combustion of the fuel gas and the pyrolyzates and on the mass flow rate of cooling water injected into the furnace. Thus,

$$X_{CO_2g} = (F_a X_{N_2a}/F_g)(x^A_{CO_2}/x^A_{N_2})$$

$$X_{COg} = (F_a X_{N_2a}/F_g)(x^A_{CO}/x^A_{N_2})$$

$$X_{O_2g} = (F_a X_{N_2a}/F_g)(x^A_{O_2}/x^A_{N_2}) \quad\quad\quad (C-8)$$

$$X_{H_2Og} = (\nu_{H_2O}/(\nu_{CO_2} + \nu_{CO})](x^A_{CO_2} + x^A_{CO})$$

$$[F_a X_{N_2a}/(F_g x^A_{N_2})] + \dot{m}_w/(F_g W_w)$$

Where ν_{H_2O}, ν_{CO_2}, and ν_{CO} are the stoichiometric coefficients of H_2O, CO_2, and CO, respectively, and can be determined from the general combustion equation for the fuel gas and the pyrolyzates with air.

Since the sum of the mole fractions of O_2, CO_2, CO, H_2O, and N_2 gases in the flue gas stream must be equal to unity, this results in

$$F_a X_{N_2 a} / (F_g X_{N_2}^A) = Z/(1 + Y) \qquad \text{(C-9)}$$

where

$$Y = \nu_{H_2O} \, (X_{CO_2}^A + X_{CO}^A)/(\nu_{CO_2} + \nu_{CO})$$

$$Z = 1 - \dot{m}_w/(F_g W_w), \text{ and } G_g = 298.15 \, \dot{V}_g/(v T_g)$$

Substituting this relation into equation (C-8) gives

$$X_{CO_2 g} = Z X_{CO_2}/(1 + Y)$$

$$X_{COg} = Z X_{CO}^A/(1 + Y)$$

$$X_{O_2 g} = Z X_{O_2}^A/(1 + Y) \qquad \text{(C-10)}$$

$$X_{N_2 g} = Z X_{N_2}^A/(1 + Y)$$

$$X_{H_2 Og} = (Y + 1 - Z)/(1 + Y)$$

The average molecular weight of the combustion gases can be estimated from the equation below:

$$W_g = 32 X_{O_2 g} + 44 X_{CO_2 g} + 28 X_{COg} + 18 X_{H_2 Og} + 28 X_{N_2 g} \qquad \text{(C-11)}$$

The total rate of heat production in the test furnace can be calculated from equations (C-5) and (C-10).

The quantity ϕ can be expressed as

$$\phi = \left(\frac{\nu'_{O_2}}{\nu''_{O_2}} + \frac{r_p}{r_f} \left(\frac{\Delta H_p}{\nu''_{O_2}} \right) \left(\frac{\nu'_{O_2}}{\Delta H_f} \right) \right) \Bigg/ \left(\frac{\nu'_{O_2}}{\nu''_{O_2}} + \frac{r_p}{r_f} \right)$$

where $\dfrac{\Delta H_f}{\nu'_{O_2}}$ and $\dfrac{\Delta H_p}{\nu''_{O_2}}$ are the quanties of heat produced per mole of O_2 for

the fuel and pyrolysis products respectively. To an engineering approximation the heat produced per mole of O_2 consumed is equal to 420 kJ/mole (13.1 MJ/kg) for most materials. Thus ϕ can be taken to be unity in equations (C-5) and (C-10).

Table 1. Descriptions of Test Assemblies, Applied Load,
and Fire Exposure Conditions

Test No.	Furnace ⌖ Modification	Structural Elements			Joist Spacing		Applied Load		Percentage of Maximum Allowable Stress	Fire Exposure	Level of Excess Air
		Floor Joist*	Plywood Subfloor** Thickness	Gypsum Board Ceiling Thickness							
			mm in	mm in	m	in	kg/m²	lb/ft²			
1	I	Wood Joist	18 23/32	16 5/8 (Type X)	0.61	24	265	54	100	Newly Developed	High
2	I	Wood Joist	18 23/32	16 5/8 (Type X)	0.61	24	265	54	100	ASTM E 119	High
3	I	Wood Joist	18 23/32	none	0.61	24	265	54	94	Newly Developed	High
4	I	Wood Joist	18 23/32	none	0.61	24	265	54	93	Newly Developed	High
5	I	Wood Joist	18 23/32	none	0.61	24	265	54	93	Newly Developed	High
6	Ia	Wood Joist	18 23/32	none	0.61	24	265	54	93	ASTM E 119	Low
7	Ia	Wood Joist	18 23/32	none	0.61	24	265	54	93	ASTM E 119	Low
8	Ib	Wood Joist	18 23/32	16 5/8 (Type X)	0.61	24	265	54	93	Newly Developed	Low
9	Ib	Wood Joist	18 23/32	none	0.61	24	265	54	93	Newly Developed	Low
10	Ib	Steel Joist	18 23/32	none	0.81	32	270	55	68	Newly Developed	Low

*Wood joists, southern pine, nominal 51 x 203 mm (2 x 8 in)
 Steel joists, Super-C, 44.5 mm wide x 184.2 mm deep x 1.3 mm thick (1-3/4 in x 7-1/4 in x 18 ga)
 Span length of all floor joists was 2.79 m (9.17 ft)
**An olefin carpet with foam rubber backing was installed over the plywood subfloor
⌖I refers to the original NBS Combination furnace. Ia and Ib refer to the two successive
 modifications as described in Section 2.1.

Table 2. Initial Weights and Total Available
Heat of Combustible Materials in Test Assemblies

Test Assembly	Initial Weights of the Combustibles, kg								Total Available Heat, MJ
	Floor Joists	Solid Bridging	Plywood Subfloor	Olefin Carpet	Wood Trim	Wood Framing	Rim Joists	Sill Plates	
1	33.9	8.6	72.6	13.6	0.9	13.6	45.1	30.8	4450
2	33.6	8.2	68.5	13.6	0.9	14.1	44.9	27.7	4310
3	34.9	10.0	80.3	13.2	0	0	44.4	26.3	4270
4	32.7	5.5	70.3	13.2	0	0	41.7	23.6	3860
5	34.8	8.1	66.2	13.2	0	0	42.8	24.5	3910
6	36.2	8.2	64.4	13.2	0	0	37.3	26.3	3920
7	32.9	8.2	67.6	12.2	0	0	39.7	27.0	3850
8	34.5	10.4	68.9	16.3	0.9	12.7	46.3	30.4	4550
9	30.5	10.4	67.1	15.9	0	0	39.5	32.2	4080
10	0	0	71.7	13.6	0	0	45.8	29.0	3360

Table 3. Summary of the Fire Endurance Times of
Floor/Ceiling Assemblies Under Furnace Fire Conditions

Assembly No.	Time to		Time for the Unexposed Surface to Increase		Maximum Deflection	
	Flame Through min:sec	Structural Failure* min:sec	Avg. Temp. 139 deg C min:sec	1-point Temp. 181 deg C min:sec	Time min:sec	Center Point mm
1	20:06	N. R.	N. R.	N. R.	20:48	47
2	34:00	35:20	35:08	34:50	35:28	331
3	6:04	6:53	N. R.	6:39	7:00	57
4	6:07	7:52	7:13	6:53	8:00	274
5	7:00	7:36	10:39	10:06	10:48	271
6	16:08	14:42	16:46	16:00	16:50	175
7	17:35	13:10	N. R.	17:08	18:10	310
8	24:22	24:59	N. R.	25:23	26:30	150
9	9:09	8:48	N. R.	9:38	10:00	95
10	4:38	2:48	5:48	4:24	5:50	231

*No collapse of the joist, time refers to excessive deflection rate and downward bending [7].
N.R. -- not reached.

44

Table 4. A Comparison of Failure Times Due to Flame Penetration (in minutes) of Floor Assemblies Evaluated in the Test Room and in the Fire Endurance Furance

Floor Assemblies	Room Fire Test	Furnace Tests			
		Newly Developed Fire Exposure		ASTM E 119 Curve	
		Low Air	High Air	Low Air	High Air
Protected Wood Frame	35:08 (0.7%)*	24:22 (6.4%) Test 8	20:06 (9.8%) Test 1	--	34:00 (12.8%) Test 2
Unprotected Wood Frame	12:02 (0%)	9:09 (3.5%) Test 9	6:04, 6:07 7:0** (8.7, 9.6, 12.9%) Tests 3, 4, 5	16:08, 17:35 (4.4, 3.8%) Tests 6, 7	--
Unprotected Steel Frame	3:58 (0.9%)	4:38 (5.8%) Test 10	--	--	--

*The value in the parentheses was the average concentration of oxygen in the flue gas stream for the furnace tests and the average concentration at the top of the doorway for the room fire tests.
**A portion of this test was run at negative pressure.

45

Table 5. Flow Rates of Air and Fuel Supply, Oxygen Content in Flue Gas, Incident Heat Flux, and Char Rate

Test No.	Furnace Modification	Type of Exposure	Protected with Gypsum Board	Average Flow Rate m³/s			% Excess Air	O_2 Concentration in Flue Gas Vol %		Maximum Incident Heat Flux kW/m²	Char* Rate mm/s
				Air	Fuel	Excess Air		Average	Minimum		
1	I	New	Yes	0.829	0.0423	0.426	51.4	9.8	3.6	275	0.0815
2	I	ASTM	Yes	0.834	0.0320	0.529	63.4	12.8	4.8	213	0.0818
3	I	New	No	0.782	0.0227	0.566	72.4	8.7	5.3	147	0.0495
4	I	New	No	0.797	0.0166	0.639	80.2	9.6	6.5	116	0.0491
5	I	New	No	0.88***	0.0038	0.598	94.3	12.9	9.8	97	0.0429
6	Ia	ASTM	No	0.286	0.0289	0.011	3.85	4.4	2.4	77	0.0186
7	Ia	ASTM	No	0.282	0.0281	0.014	4.96	3.8	2.4	98	0.0171
8	Ib	New	Yes	0.656	0.0382	0.292	44.5	6.4	3.3	208	0.0345
9	Ib	New	No	0.650	0.0392	0.277	42.6	3.5	1.2	224	0.0328
10	Ib	New	No	0.464	0.0260	0.216	46.6	5.8	1.7	132	**

*Char rate is taken to be the thickness of the subfloor divided by its fire exposure time prior to flamethrough.
**Flamethrough was due to the opening of seams rather than burnthrough of the plywood in this test.
***Dropped to 0.28 m³/s after 4 minutes.

Table 6. A Summary of Heat Release During Fire Endurance Testing

Test No.	Time Duration s	Total Heat Release MJ	Average Heat Release Rate MW**	Contributed Heat Release MJ	
				Fuel	Structure
1	1206	2225	1.85	1954	271
2	2040	2850	1.40	2497	353
3	364	690	1.90	317	373
4	367	677	1.85	234	443
5	420	421	1.00	61	360
6	968	913*	*** 0.94	1078	--
7	1055	980*	*** 0.93	1142	--
8	1462	2683	1.84	2133	550
9	549	1192	2.17	820	372
10	278	365	1.31	272	93

*Low values were due to problems with the flue gas sampling system for test 6 and the air
  inflow measurement for test 7.
 **Including both the gas and the structure
***Questionable data, see page 21.

47

Figure 1. Construction details and instrumentation layouts for test assembly no. 1

48

R11 INSULATION

SECTION B-B

SECTION A-A

PLYWOOD
SUBFLOOR

CARPET

WOOD
JOIST

A

660   560   305   915

495   725   725   495

610   610   610   610

127

610   597

699

610   928

699

305

305

699   928

1220

826

597

B   B

A

All dimensions in mm.

Figure 2.   Construction details and instrumen-
            tation layouts for test assembly
            no. 3

49

Figure 3. Construction details and instrumentation layouts for test assembly no. 10

50

Figure 4. Layout of steel blocks distributed uniformly over the top of the test assembly
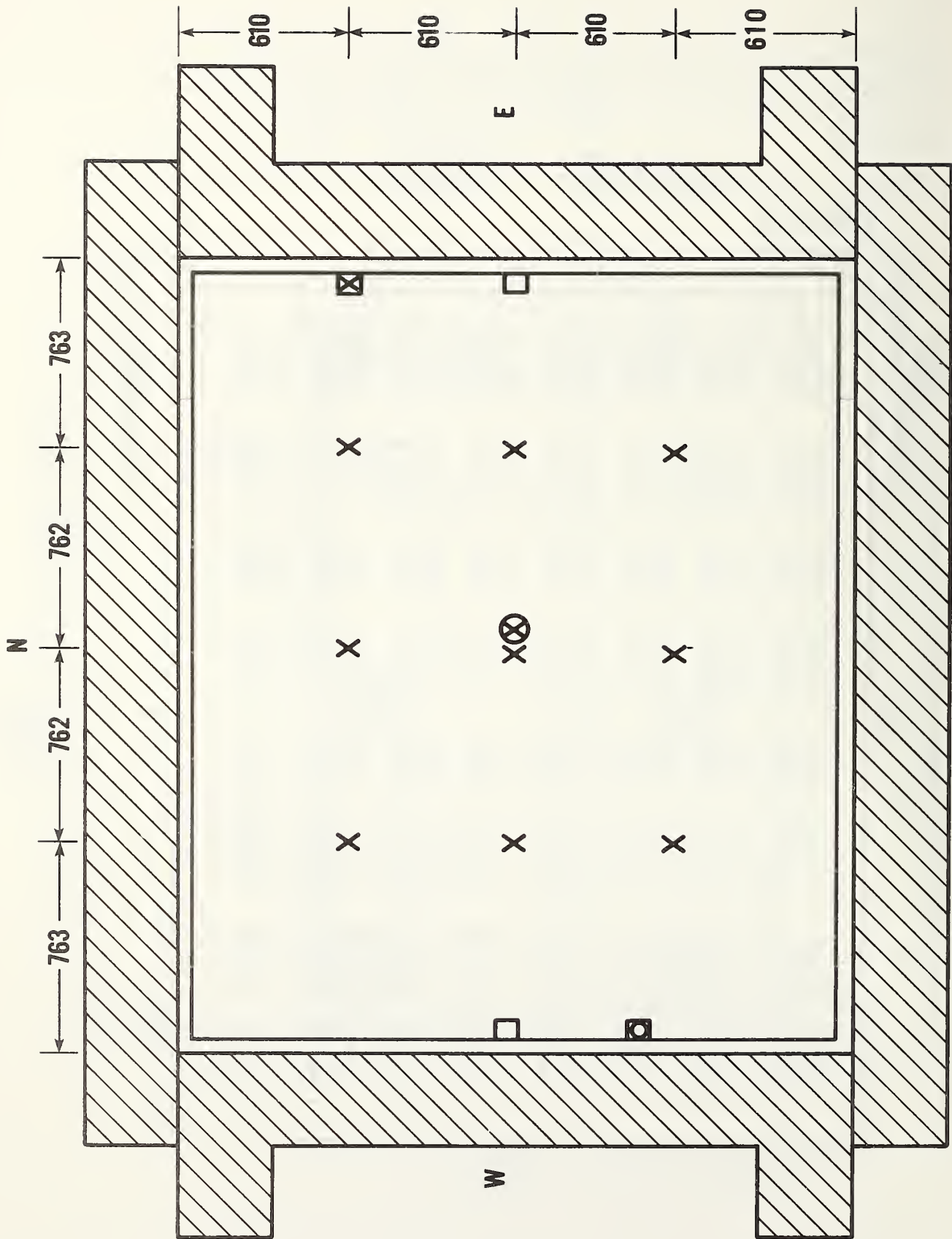
Figure 5. Floor plan of test furnace showing locations of thermocouples and pressure probes
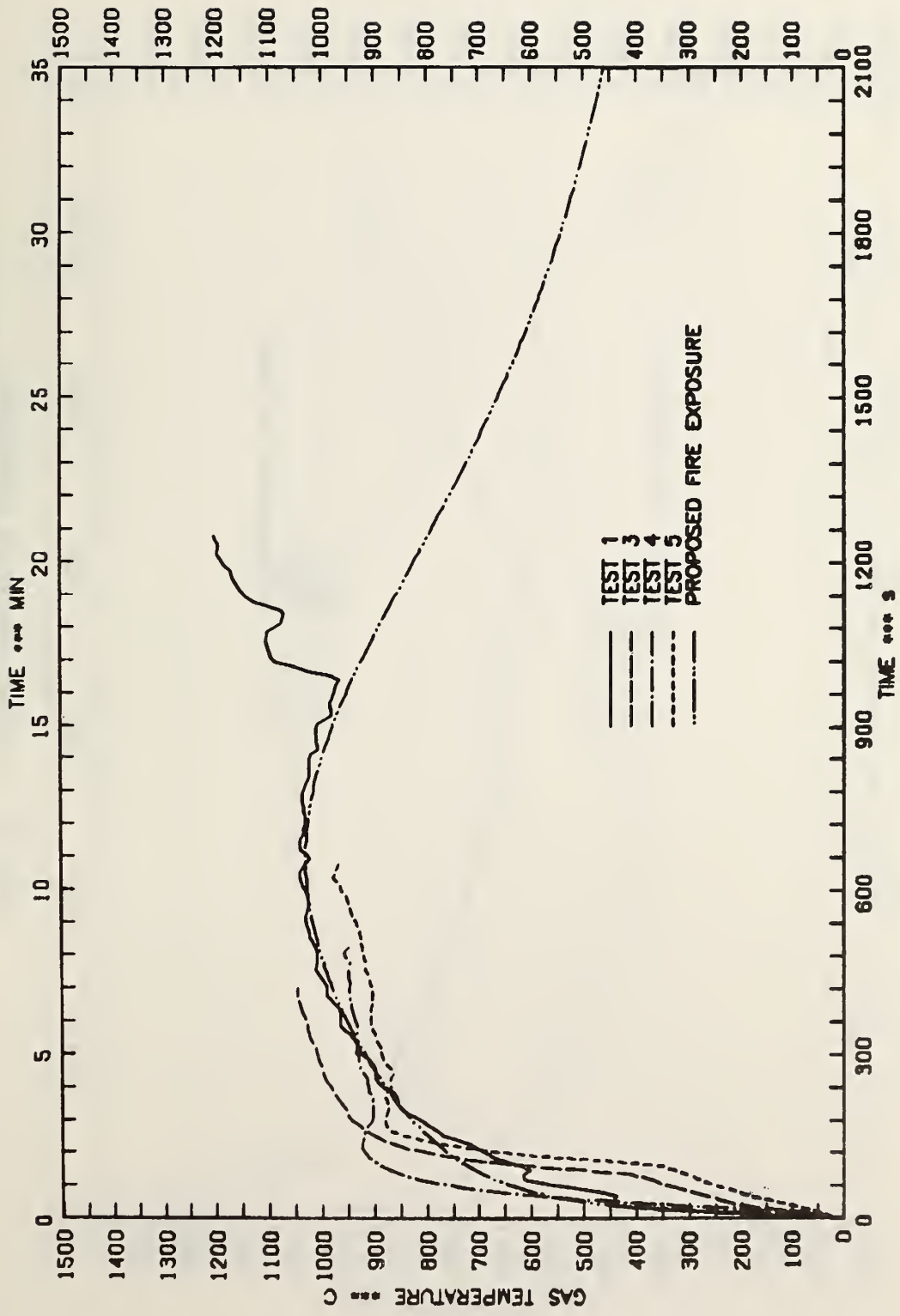
All dimensions in mm.

52

FIGURE 5A — AVERAGE FURNACE GAS TEMPERATURE
MEASURED WITH FAST RESPONSE THERMOCOUPLES

53
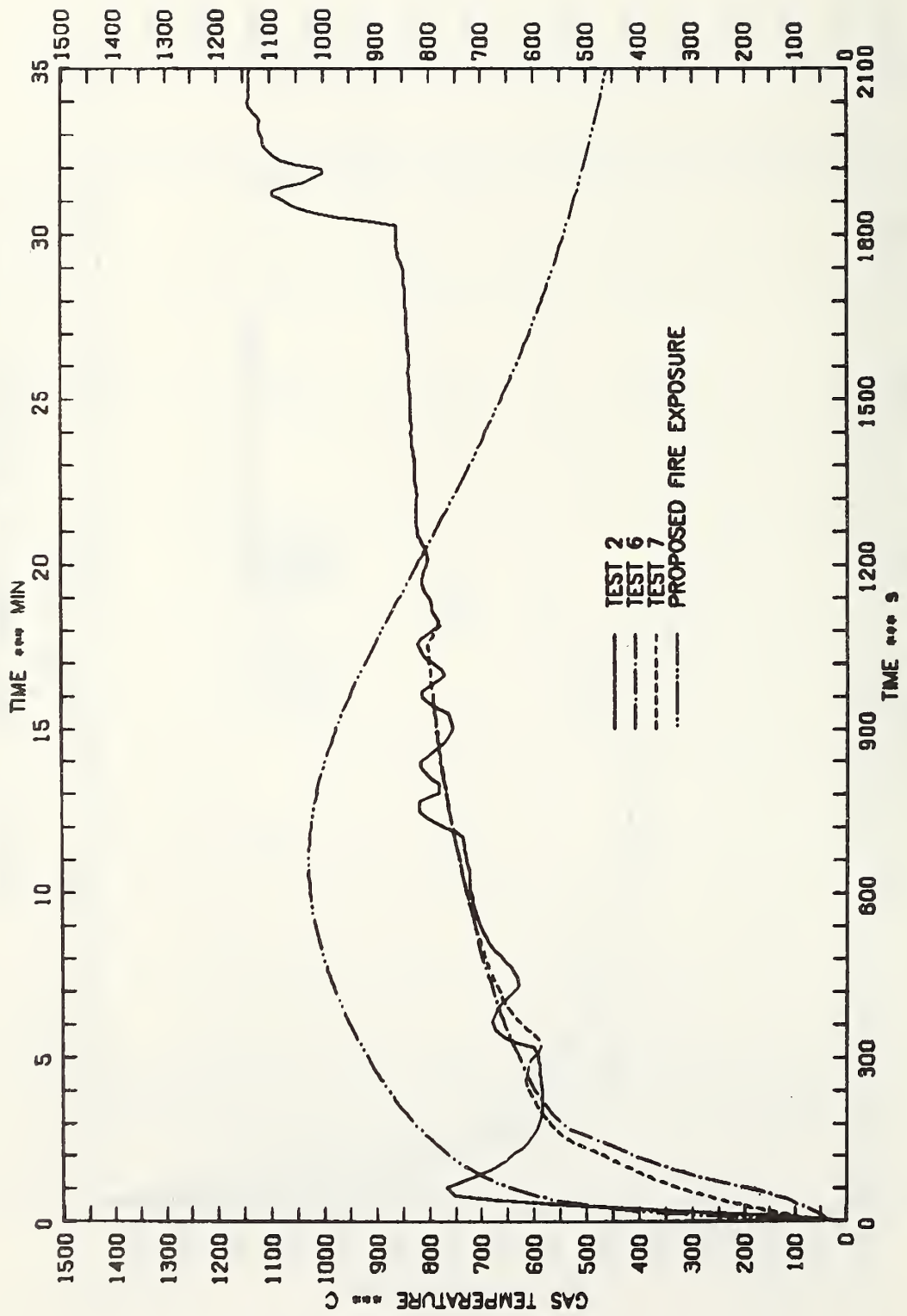
FIGURE 6.B – AVERAGE FURNACE GAS TEMPERATURE
MEASURED WITH FAST RESPONSE THERMOCOUPLES

54
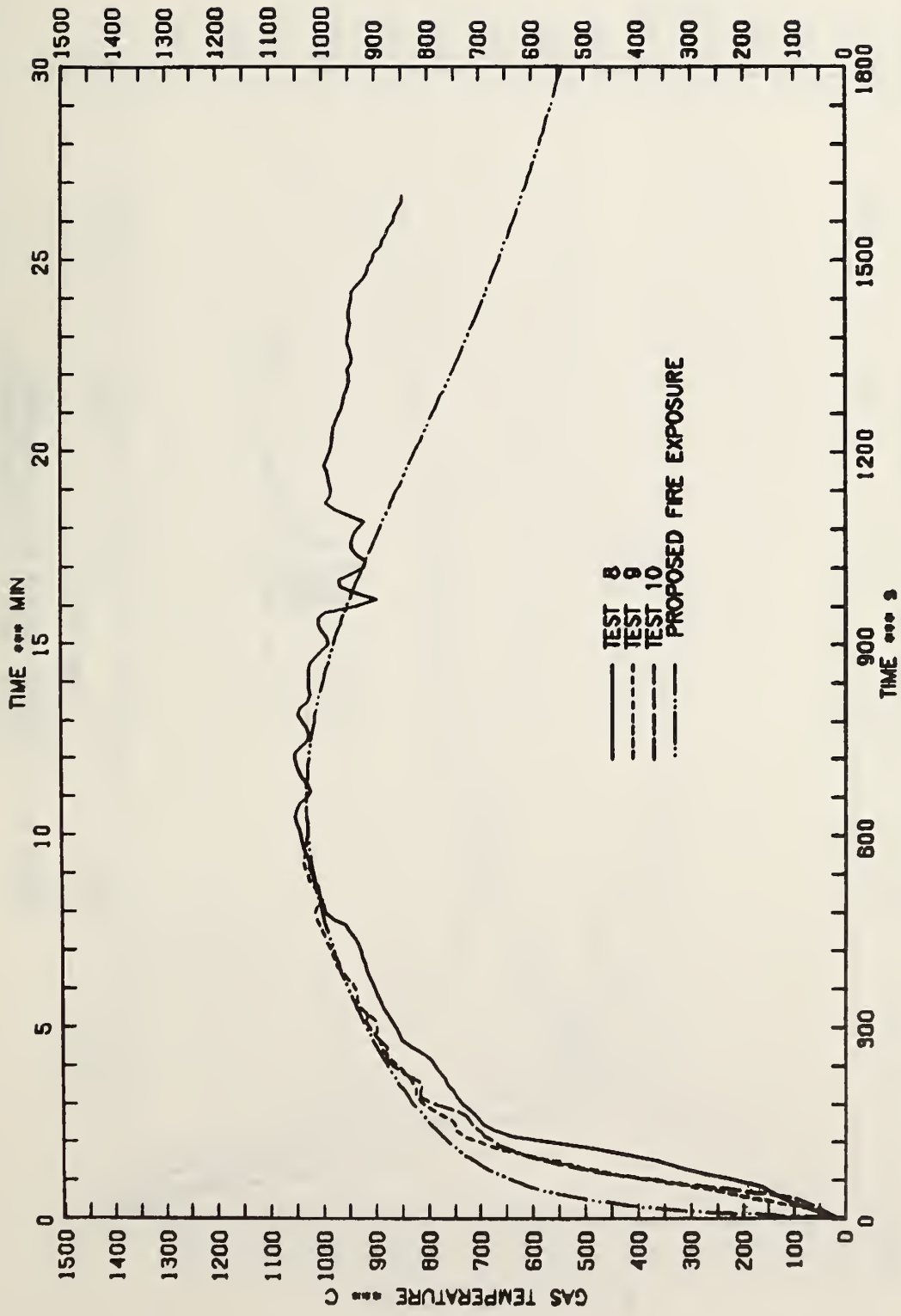
FIGURE 6.C - AVERAGE FURNACE GAS TEMPERATURE
MEASURED WITH FAST RESPONSE THERMOCOUPLES

55
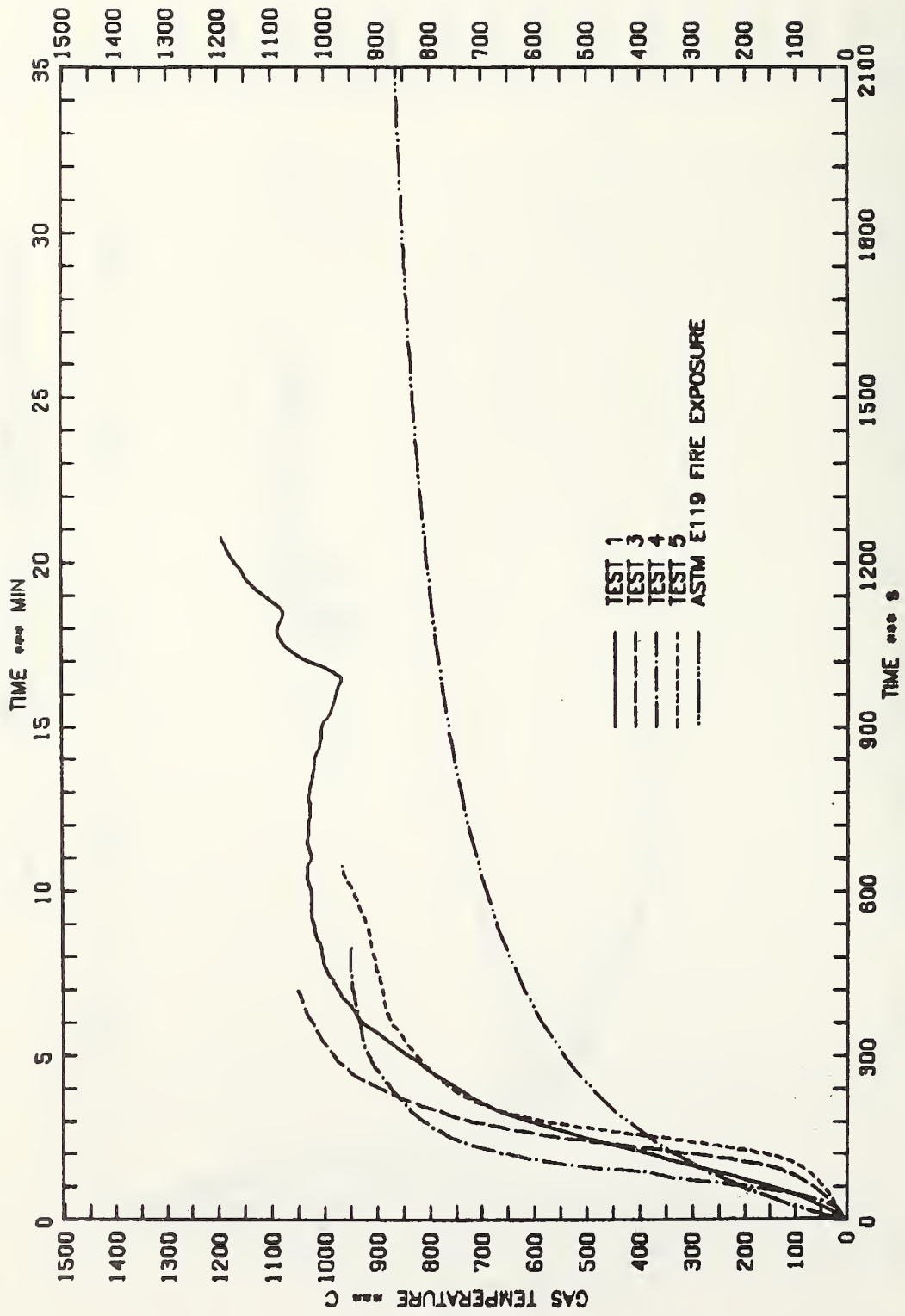
FIGURE 7A — AVERAGE FURNACE GAS TEMPERATURE
MEASURED WITH ASTM THERMOCOUPLES
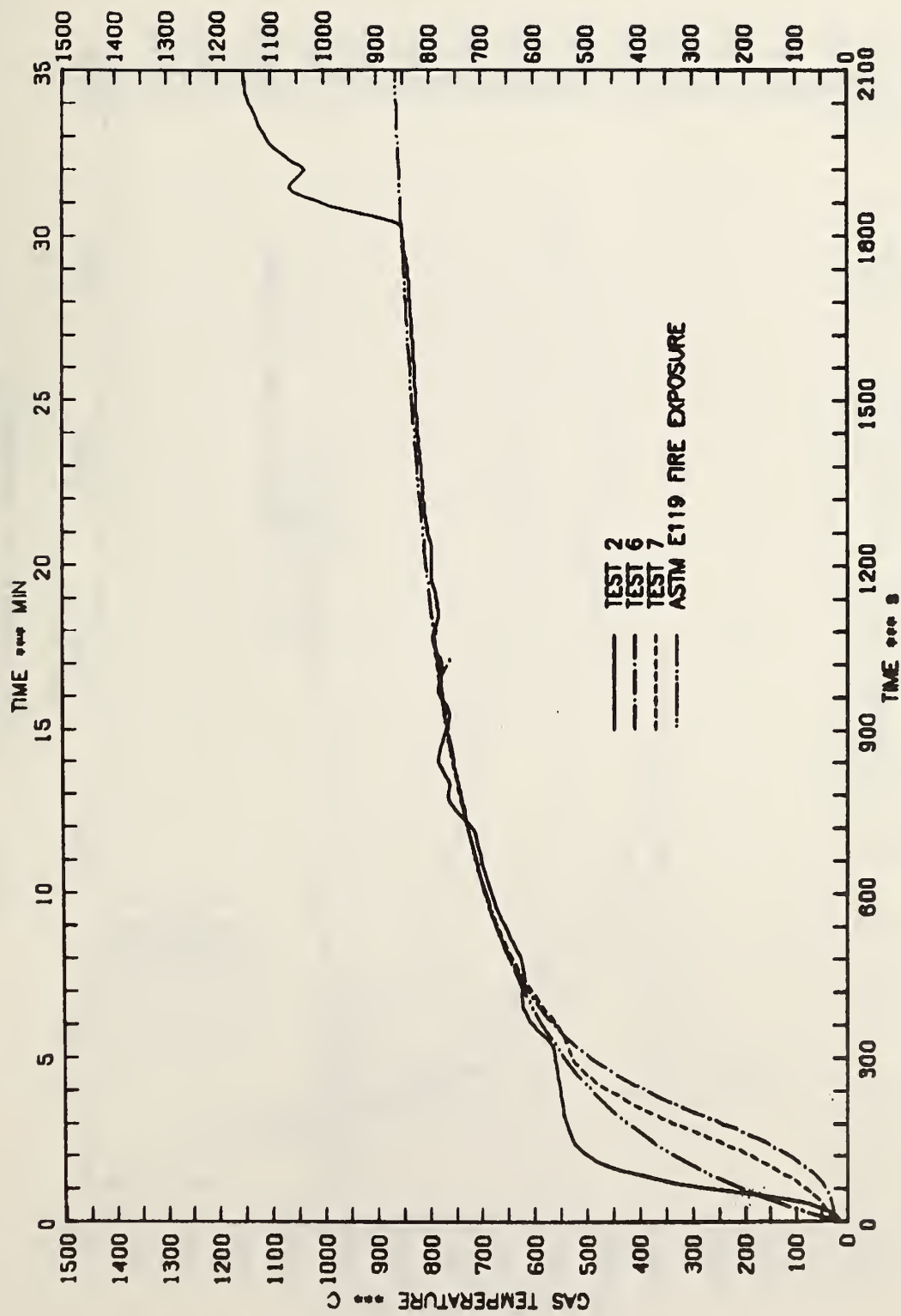
56

FIGURE 7.8 — AVERAGE FURNACE GAS TEMPERATURE
MEASURED WITH ASTM THERMOCOUPLES

57
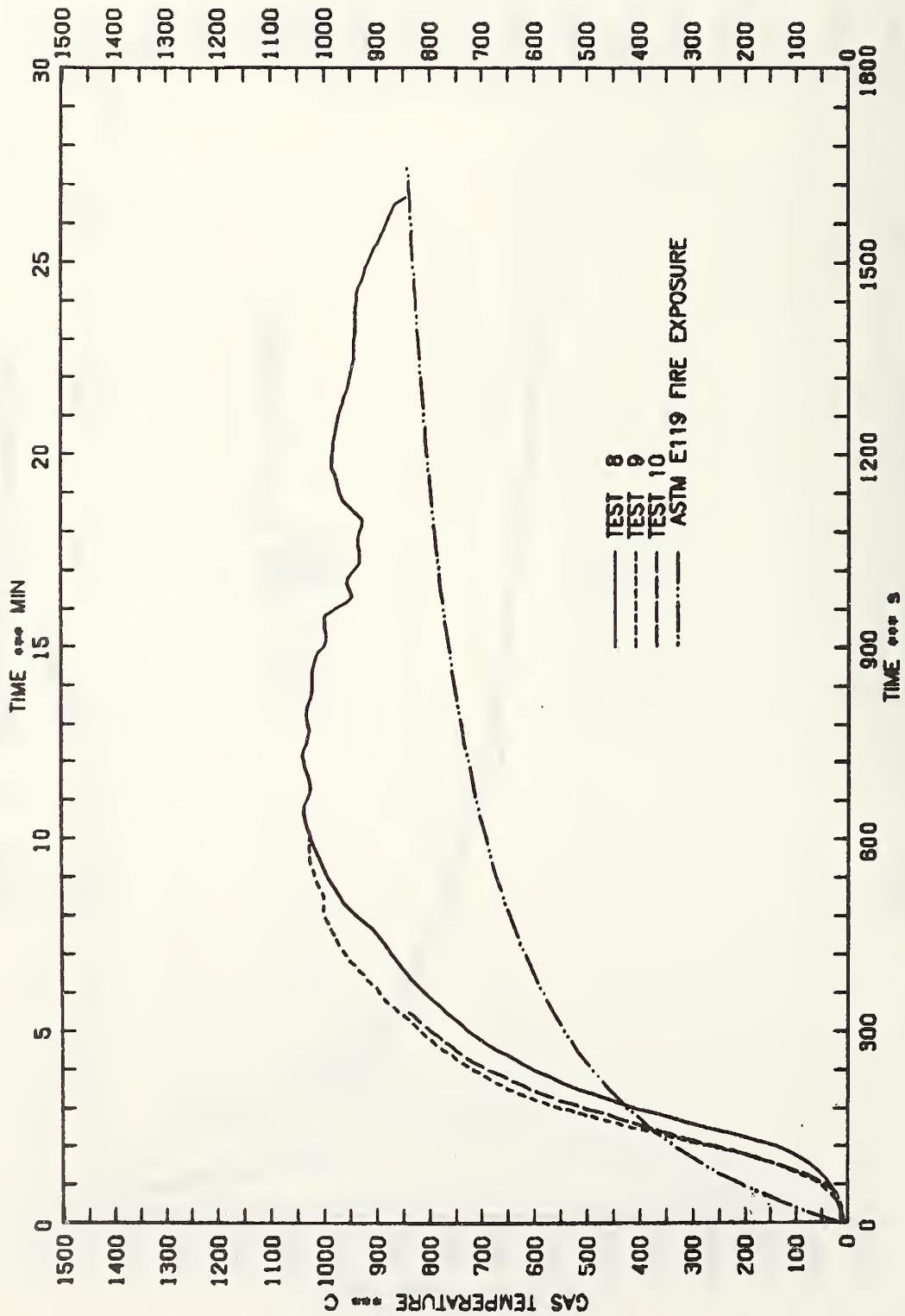
FIGURE 7.C – AVERAGE FURNACE GAS TEMPERATURE
MEASURED WITH ASTM THERMOCOUPLES

58
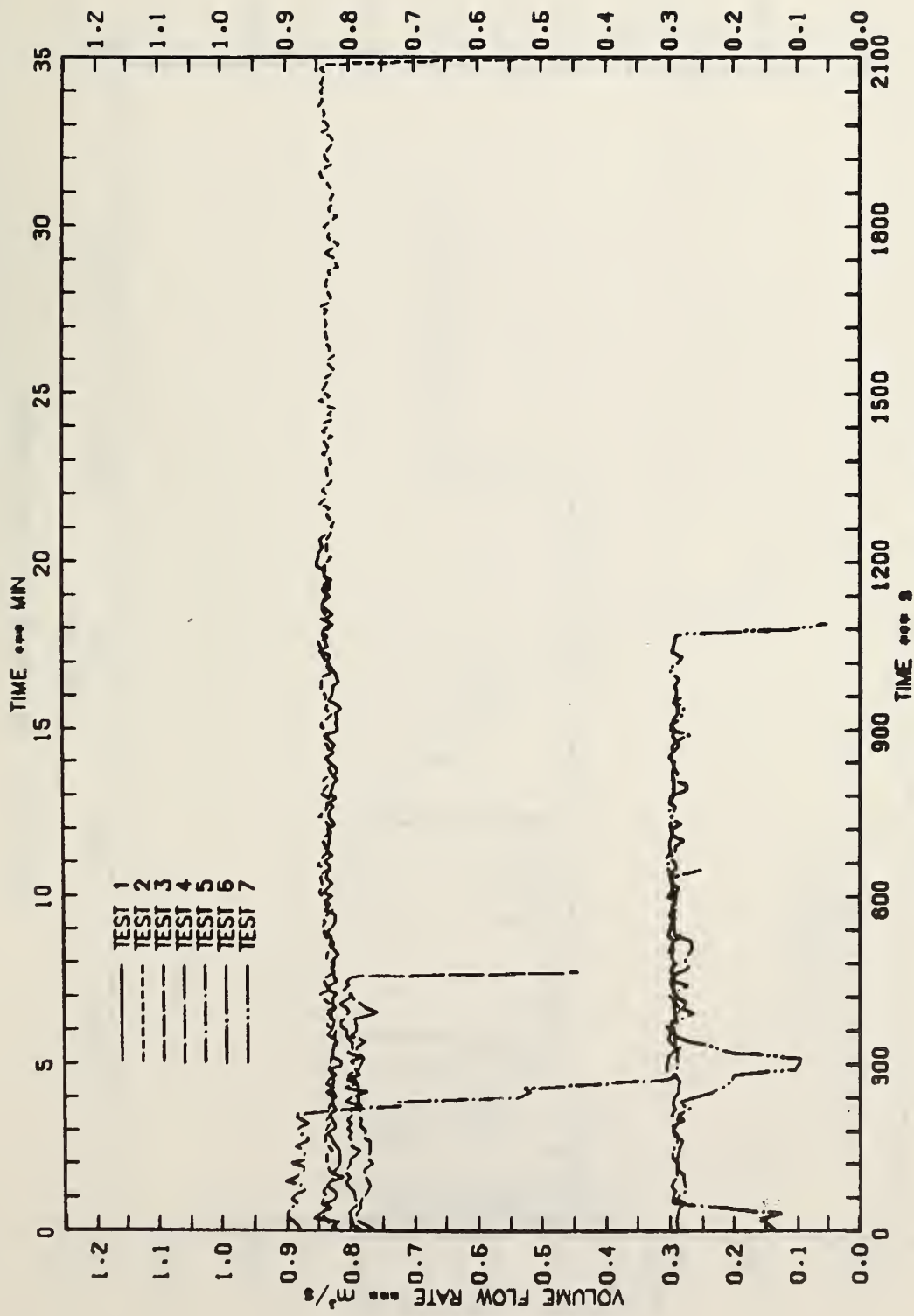
FIGURE 8A — AIR FLOW RATE TO THE FURNACE
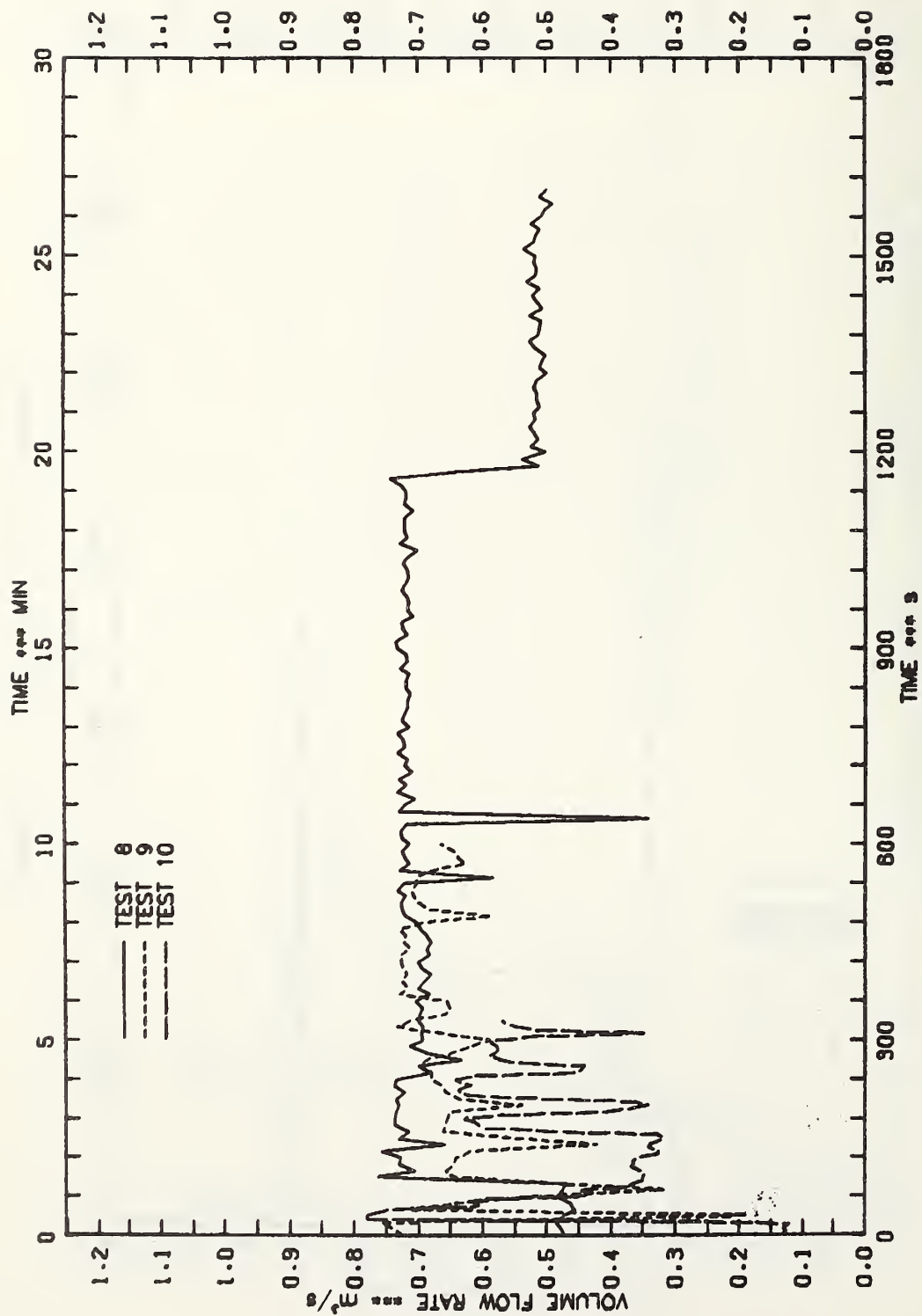
FIGURE 8.B — AIR FLOW RATE TO THE FURNACE
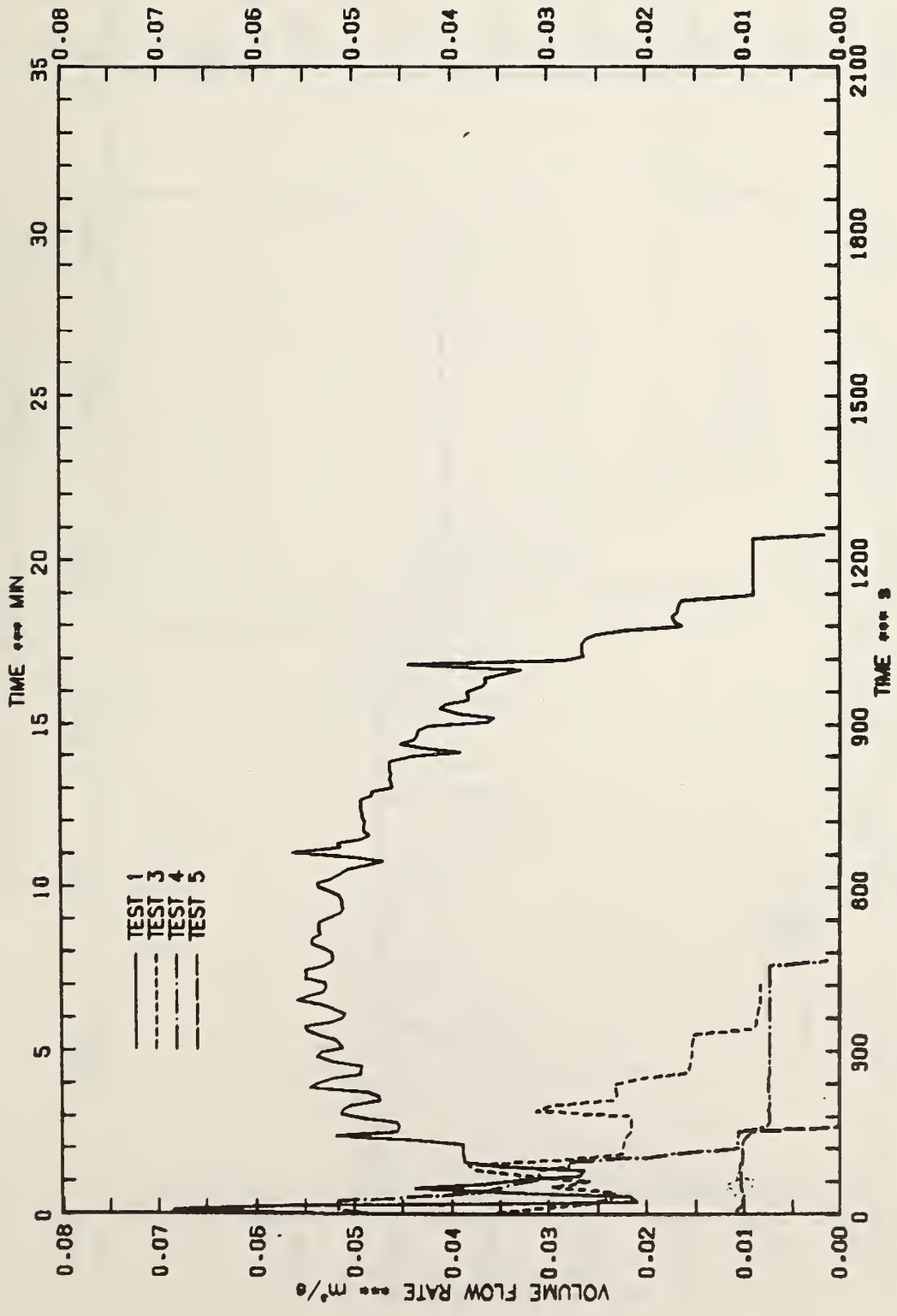
FIGURE 9A — FUEL FLOW RATE TO THE FURNACE

61
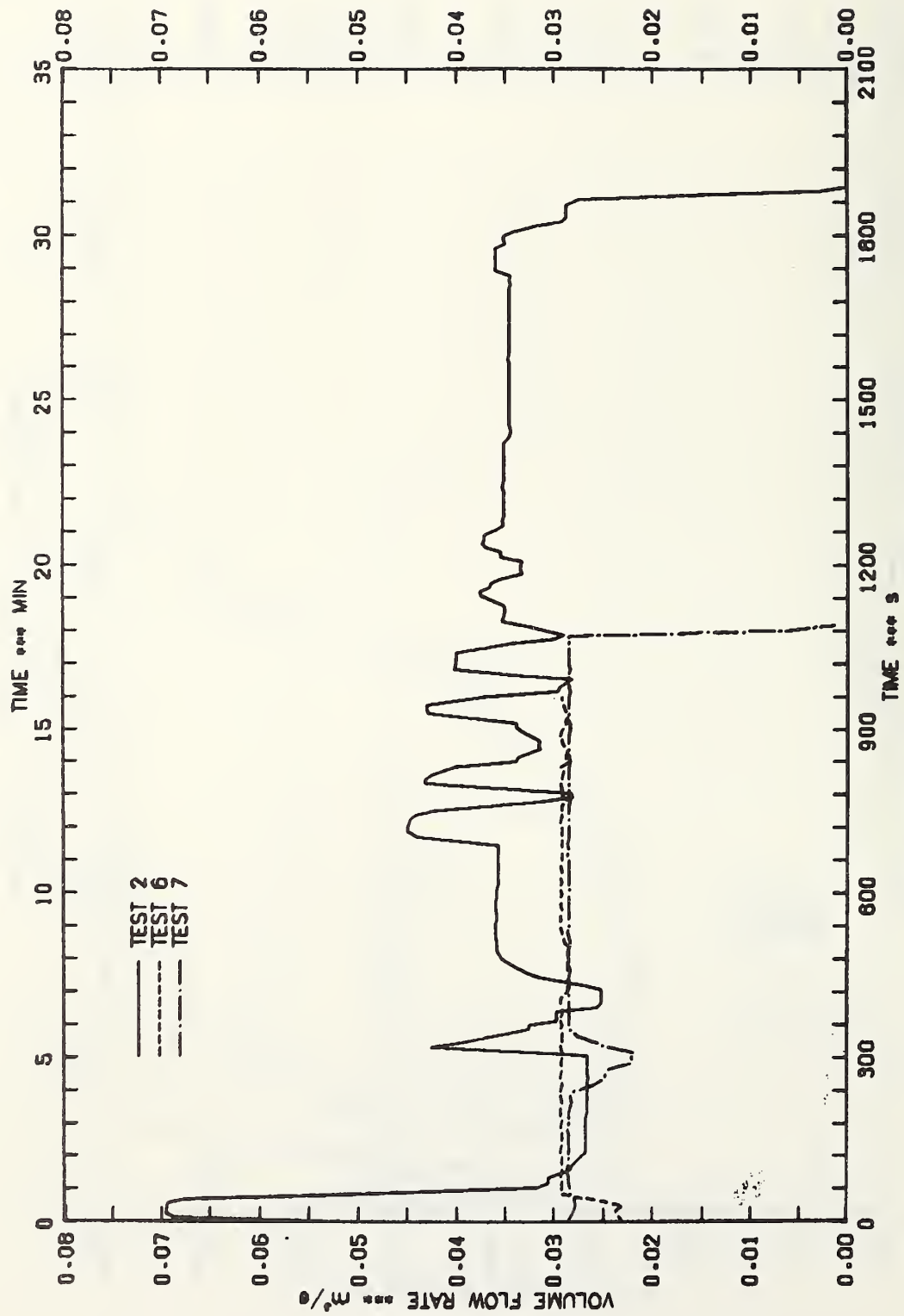
FIGURE 9.B - FUEL FLOW RATE TO THE FURNACE

62
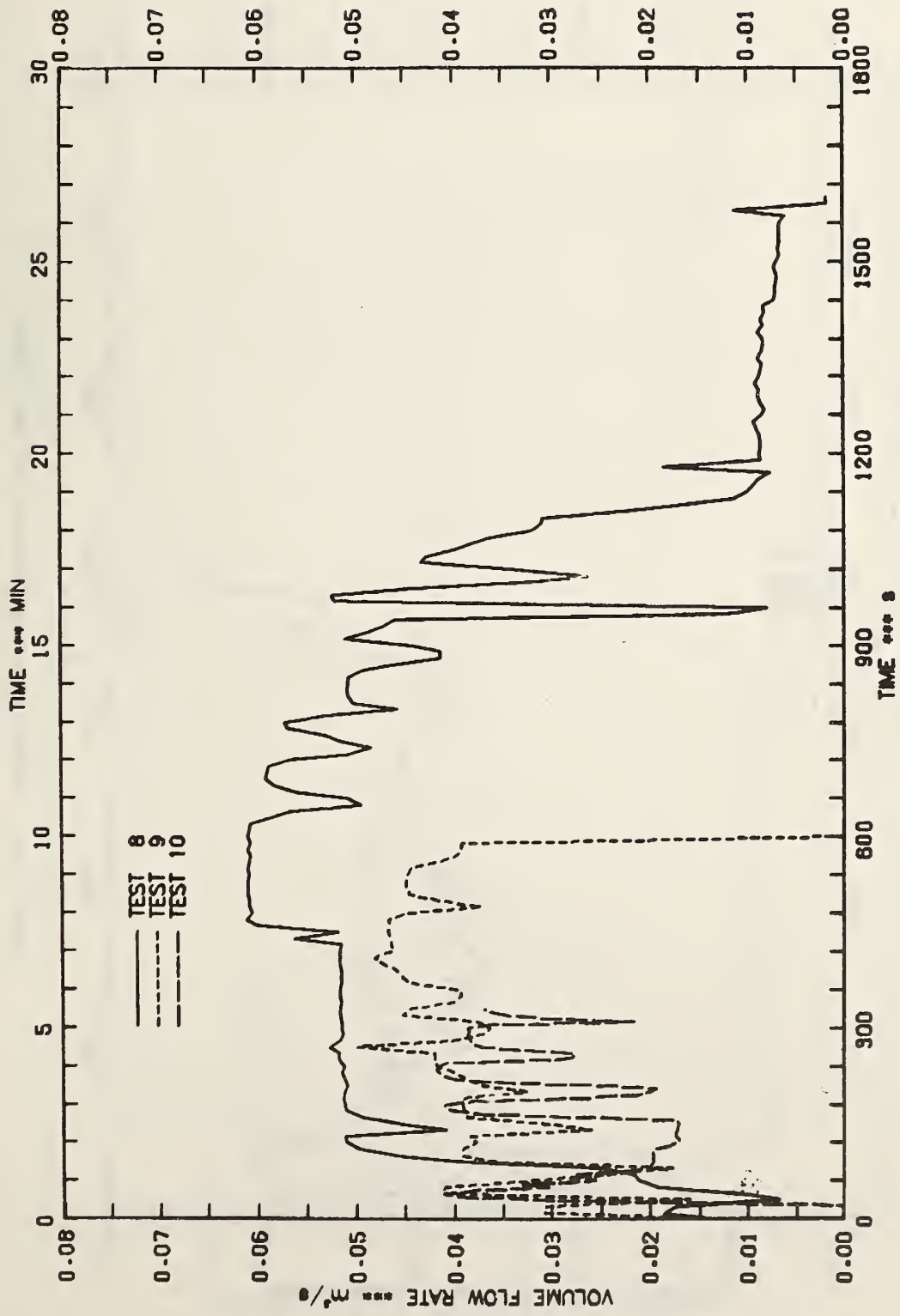
FIGURE 9.C - FUEL FLOW RATE TO THE FURNACE

63
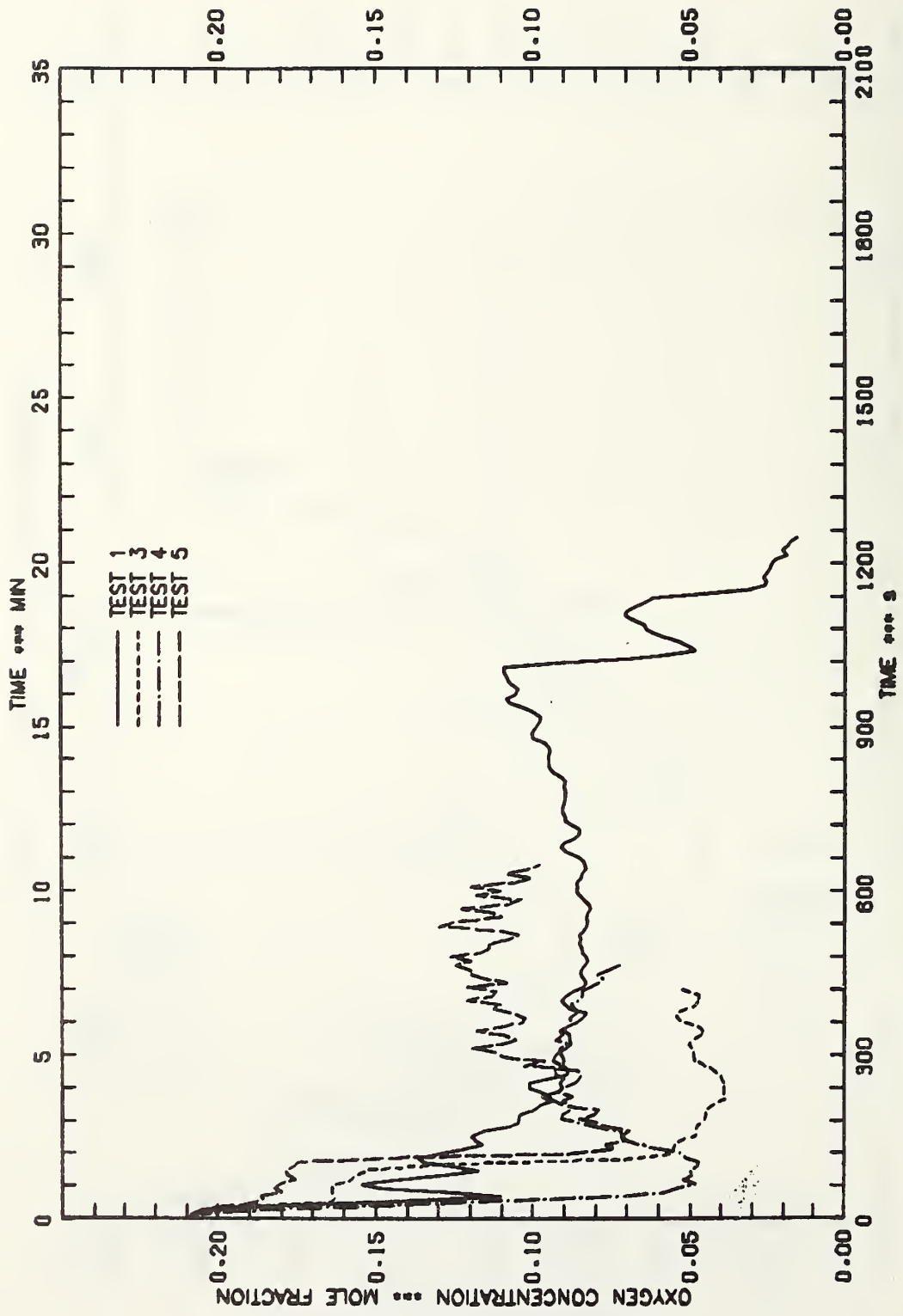
FIGURE 10.A – OXYGEN CONCENTRATION IN FLUE GAS STREAM

64
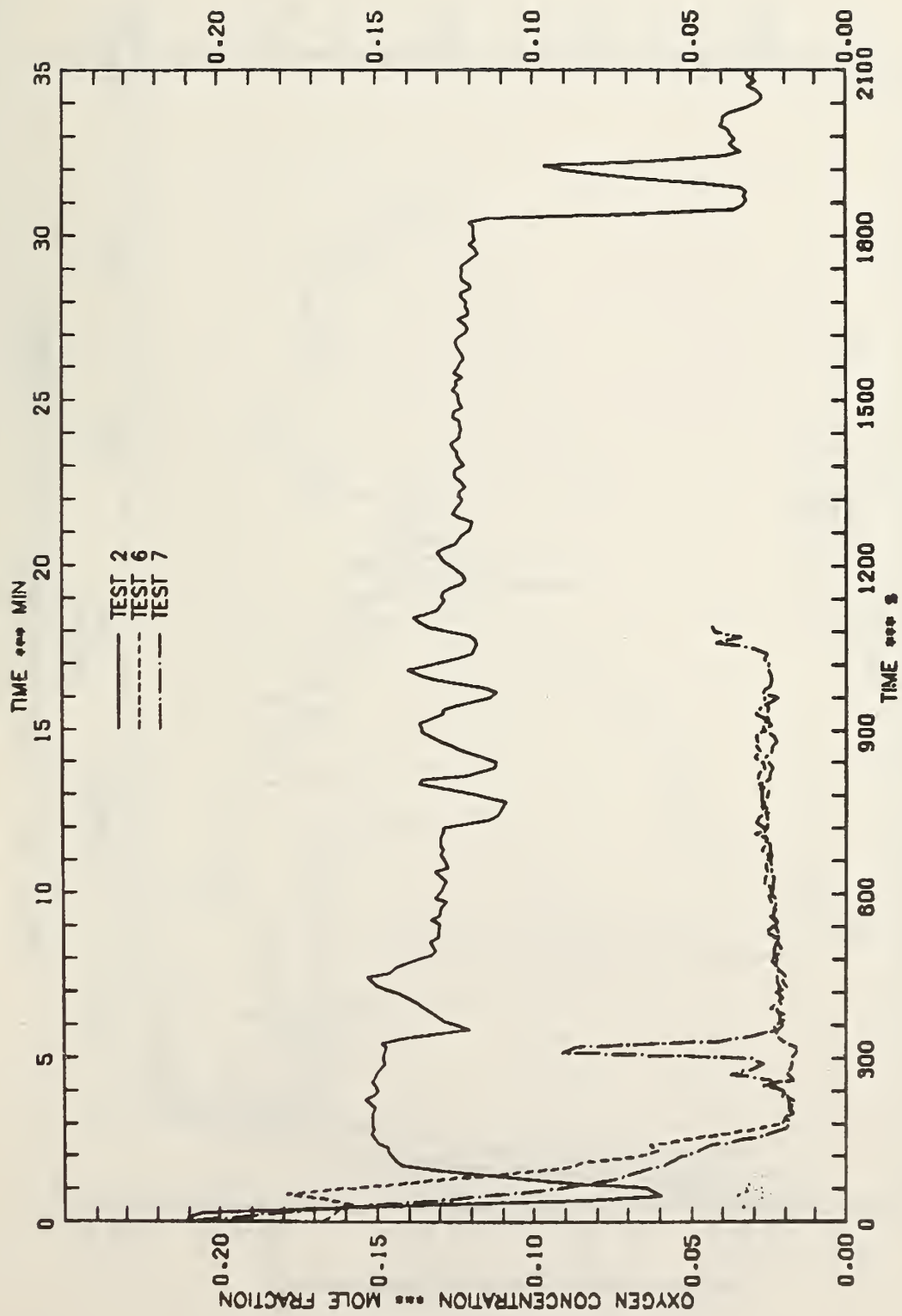
FIGURE 10.B - OXYGEN CONCENTRATION IN FLUE GAS STREAM
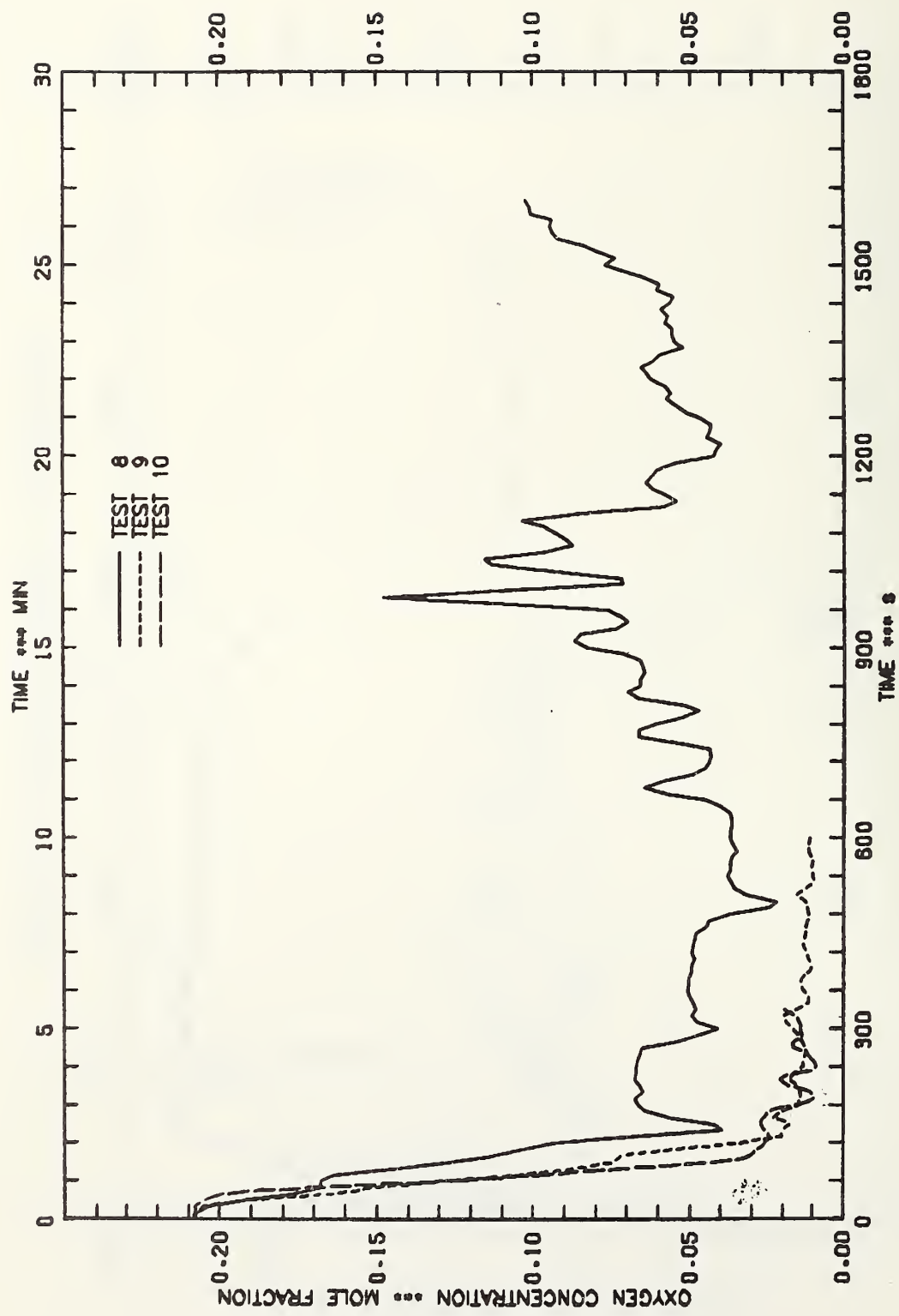
FIGURE 10.C - OXYGEN CONCENTRATION IN FLUE GAS STREAM
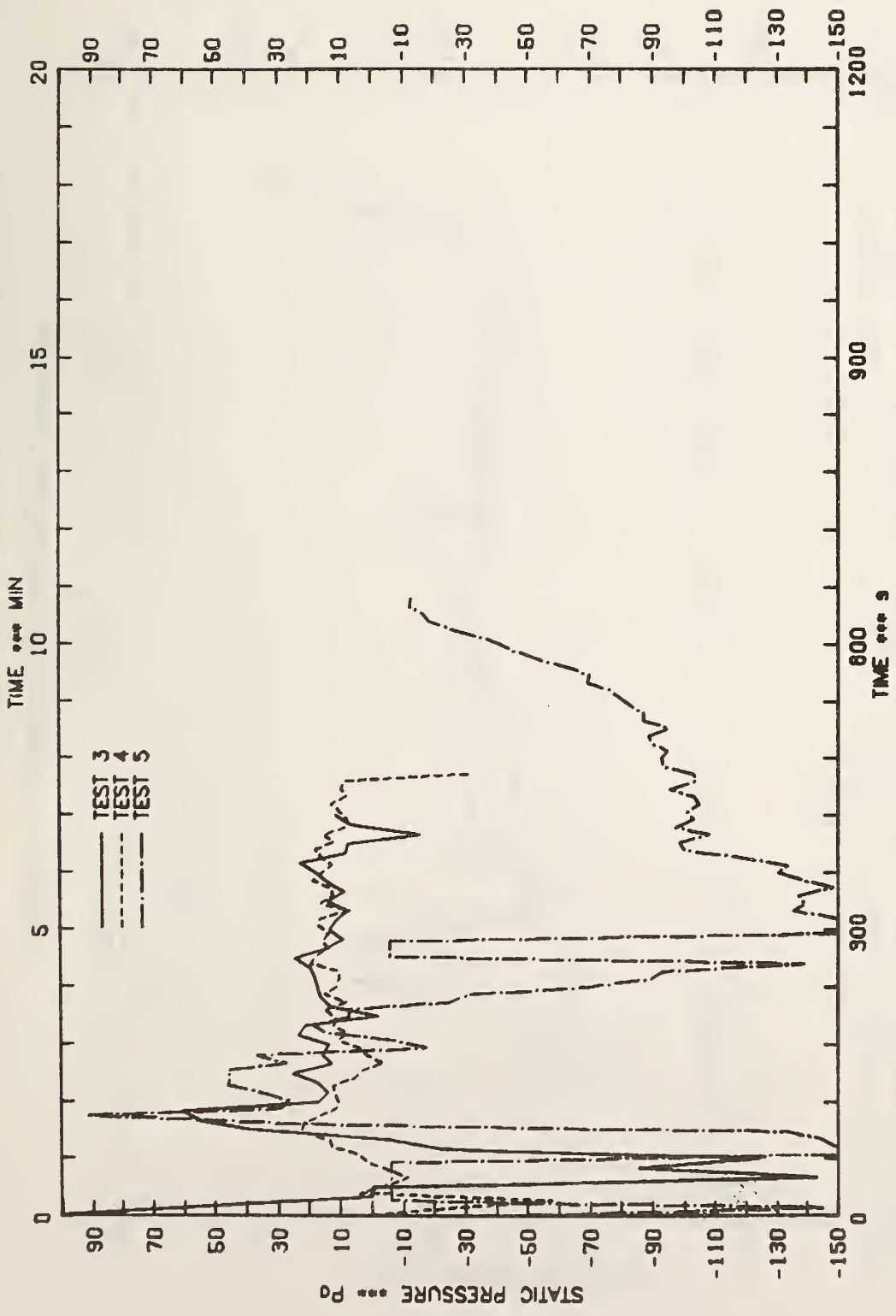
FIGURE 11.A – AVERAGE UPPER FURNACE STATIC PRESSURE

67

FIGURE 11.8 — AVERAGE UPPER FURNACE STATIC PRESSURE

68
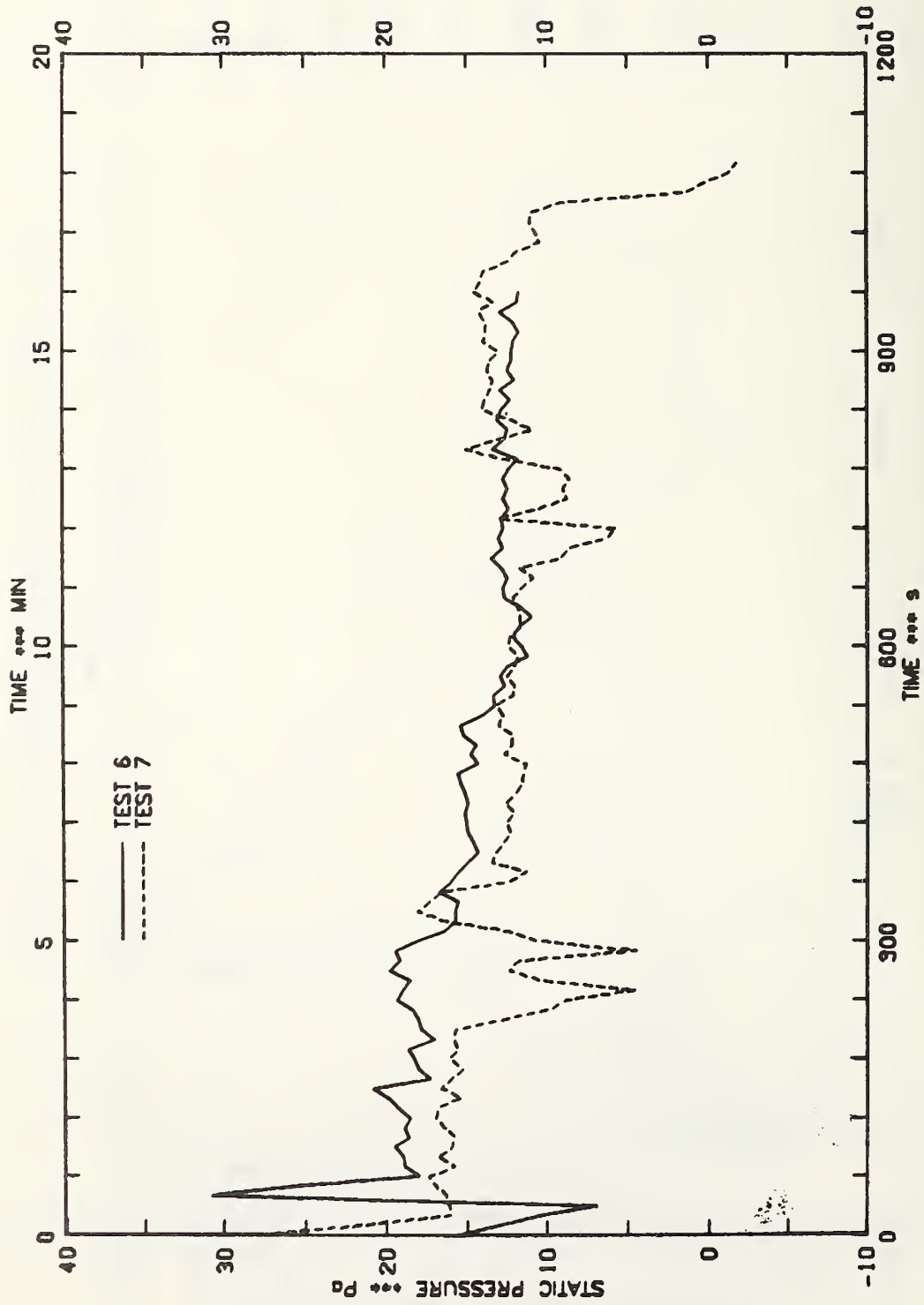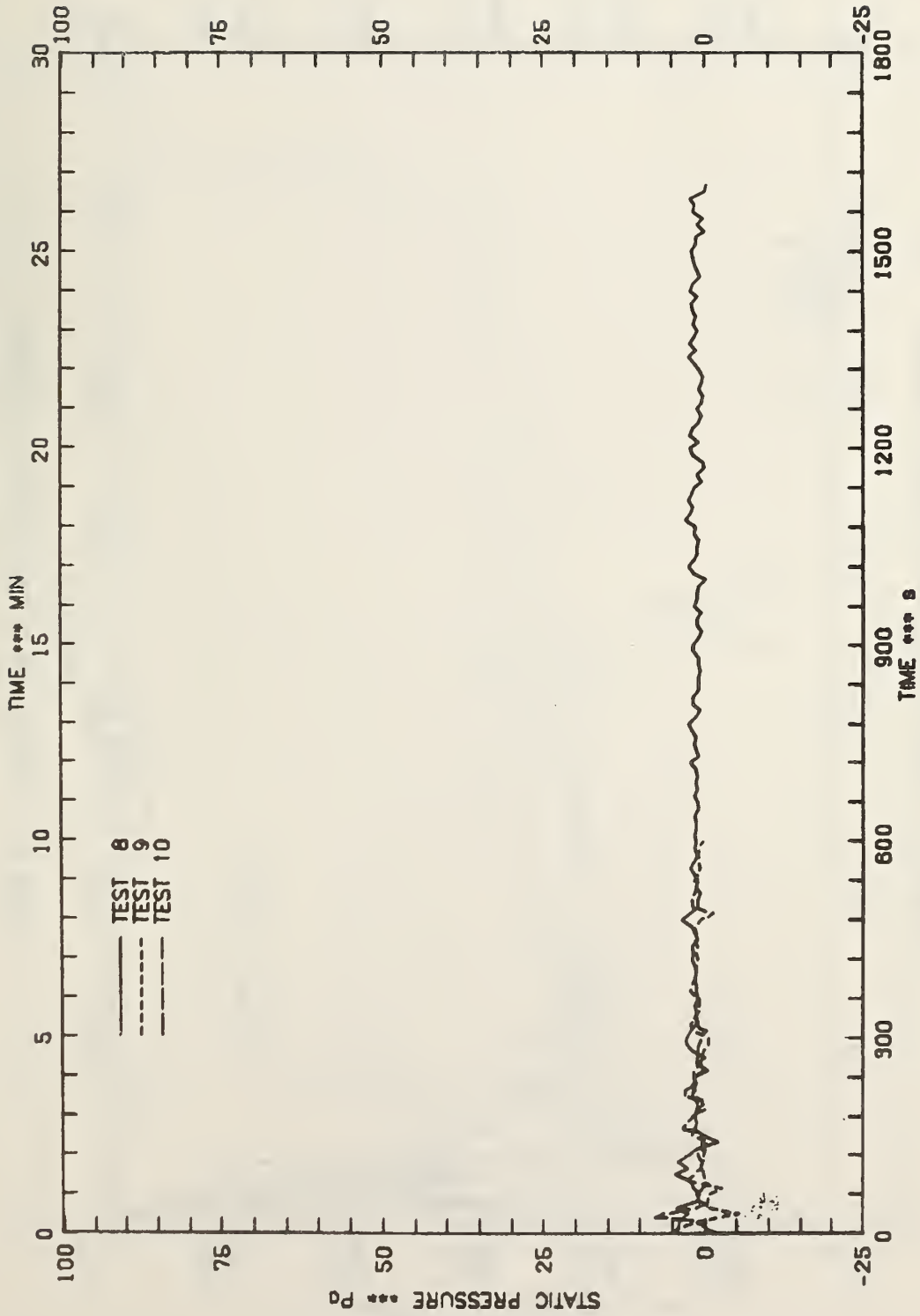
FIGURE 11.C - AVERAGE UPPER FURNACE STATIC PRESSURE

69
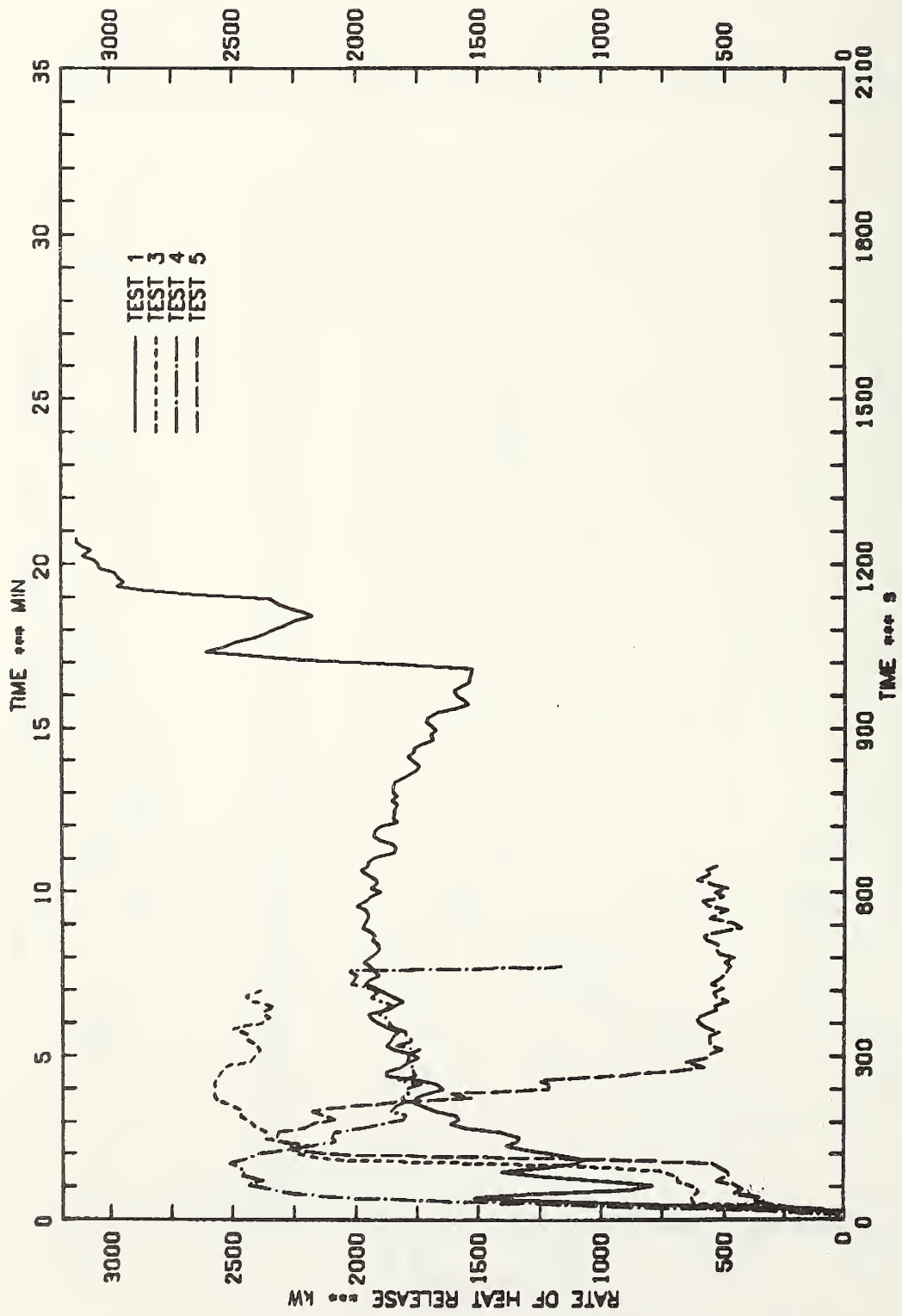
FIGURE 12.A - TOTAL RATE OF HEAT RELEASE IN FURNACE

70

FIGURE 12.B – TOTAL RATE OF HEAT RELEASE IN FURNACE

71
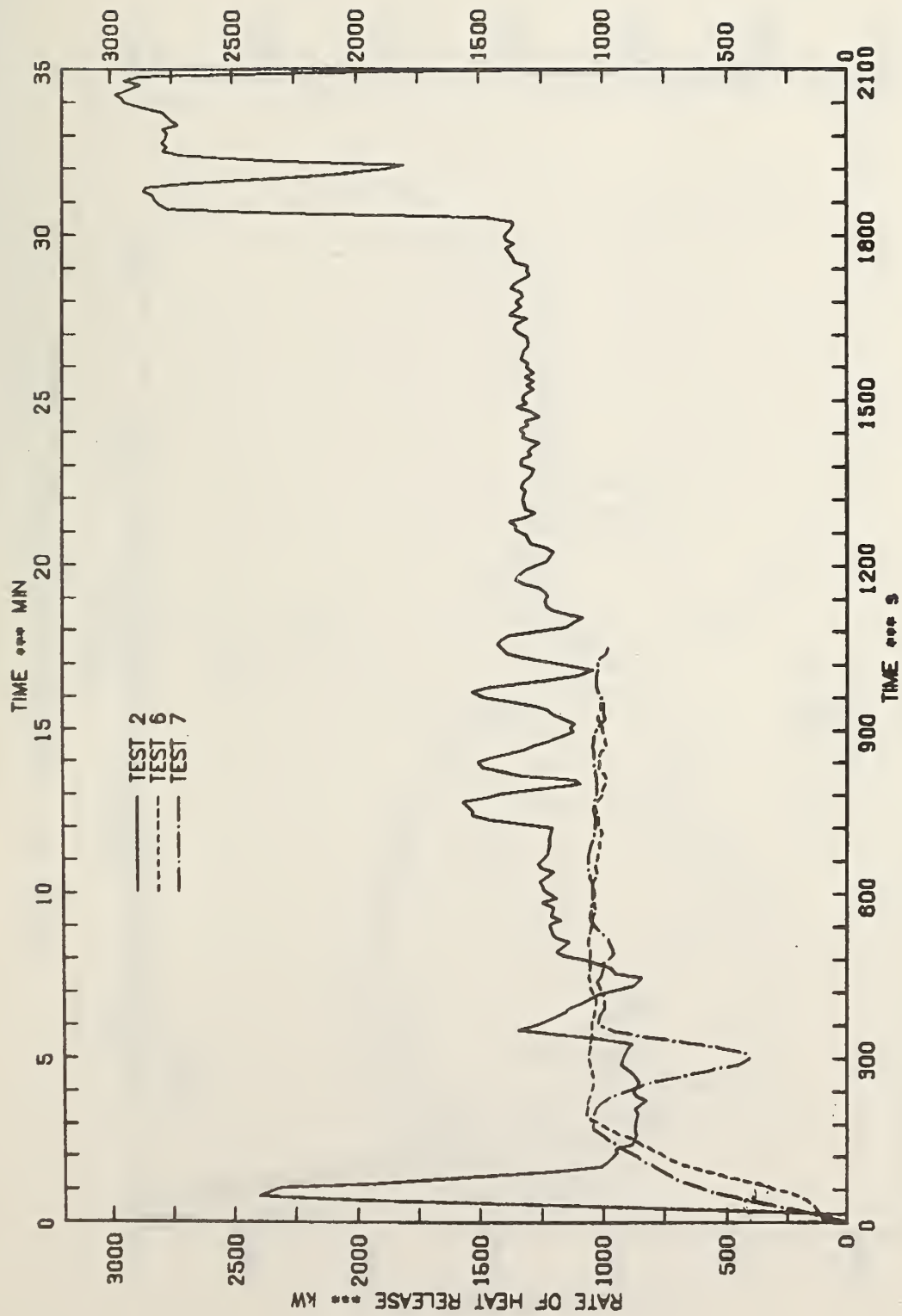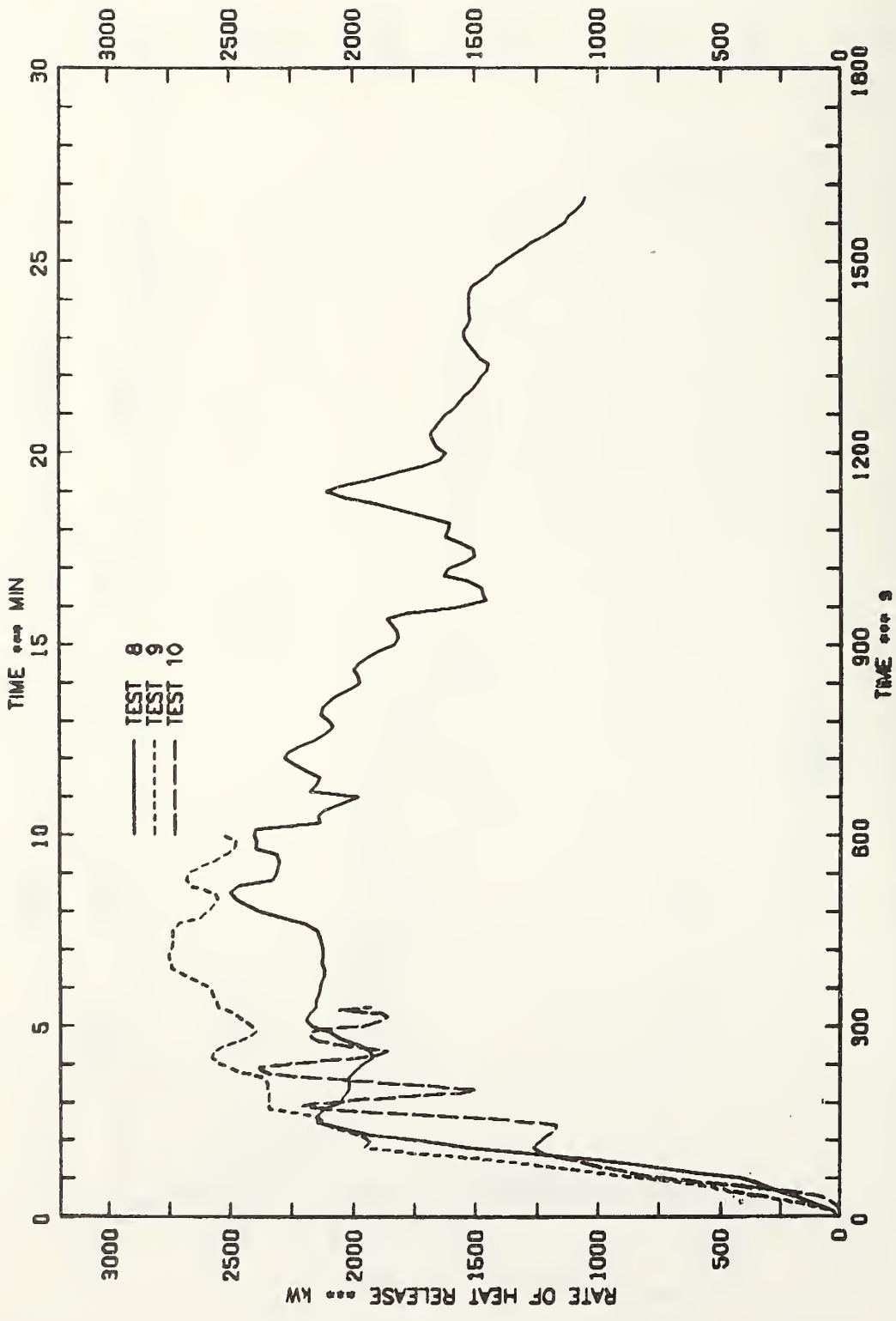
FIGURE 12.C – TOTAL RATE OF HEAT RELEASE IN FURNACE

72
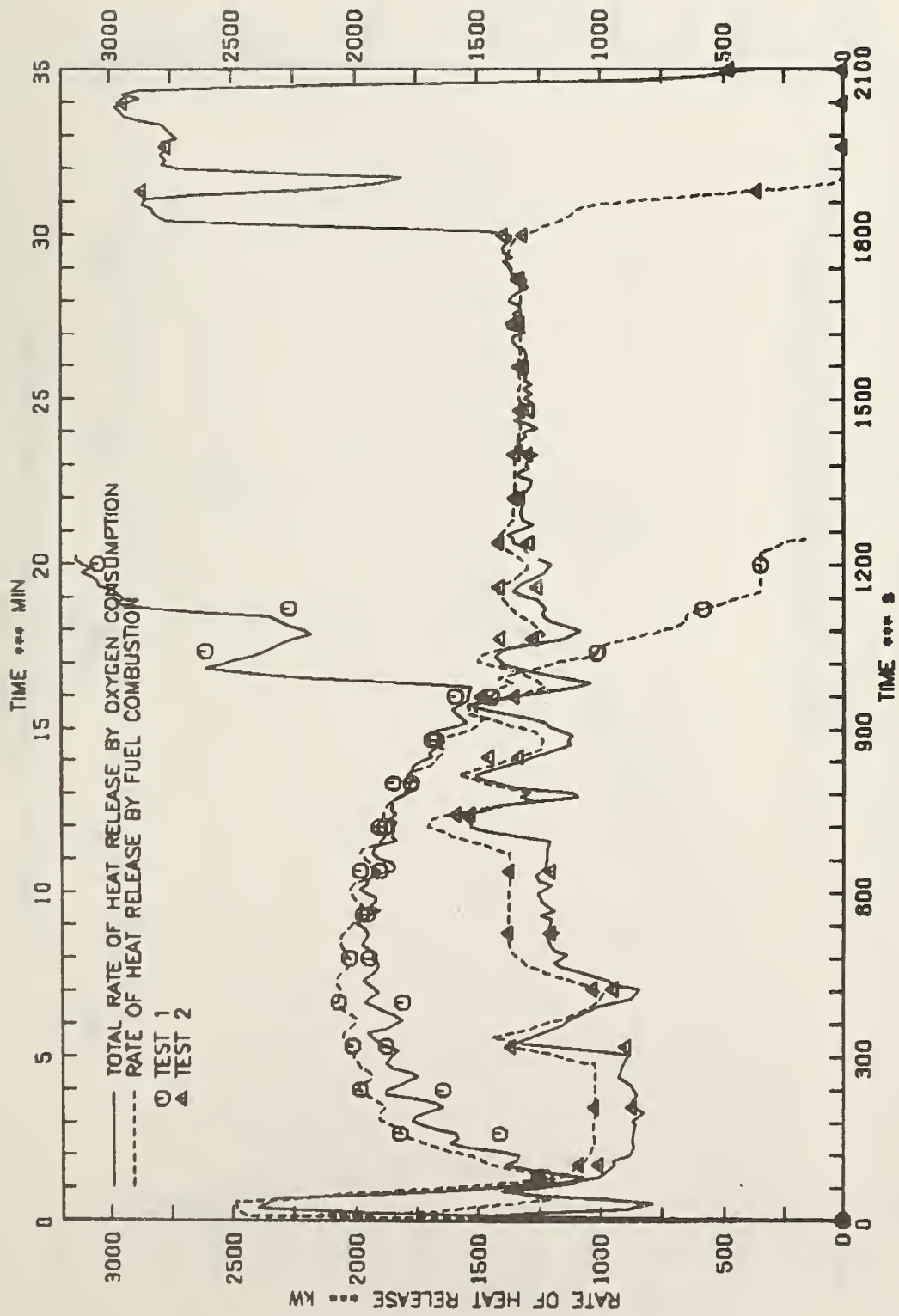
FIGURE 13.A — COMPARISON OF RATES OF HEAT RELEASE
IN FURNACE FOR TESTS 1 AND 2

73
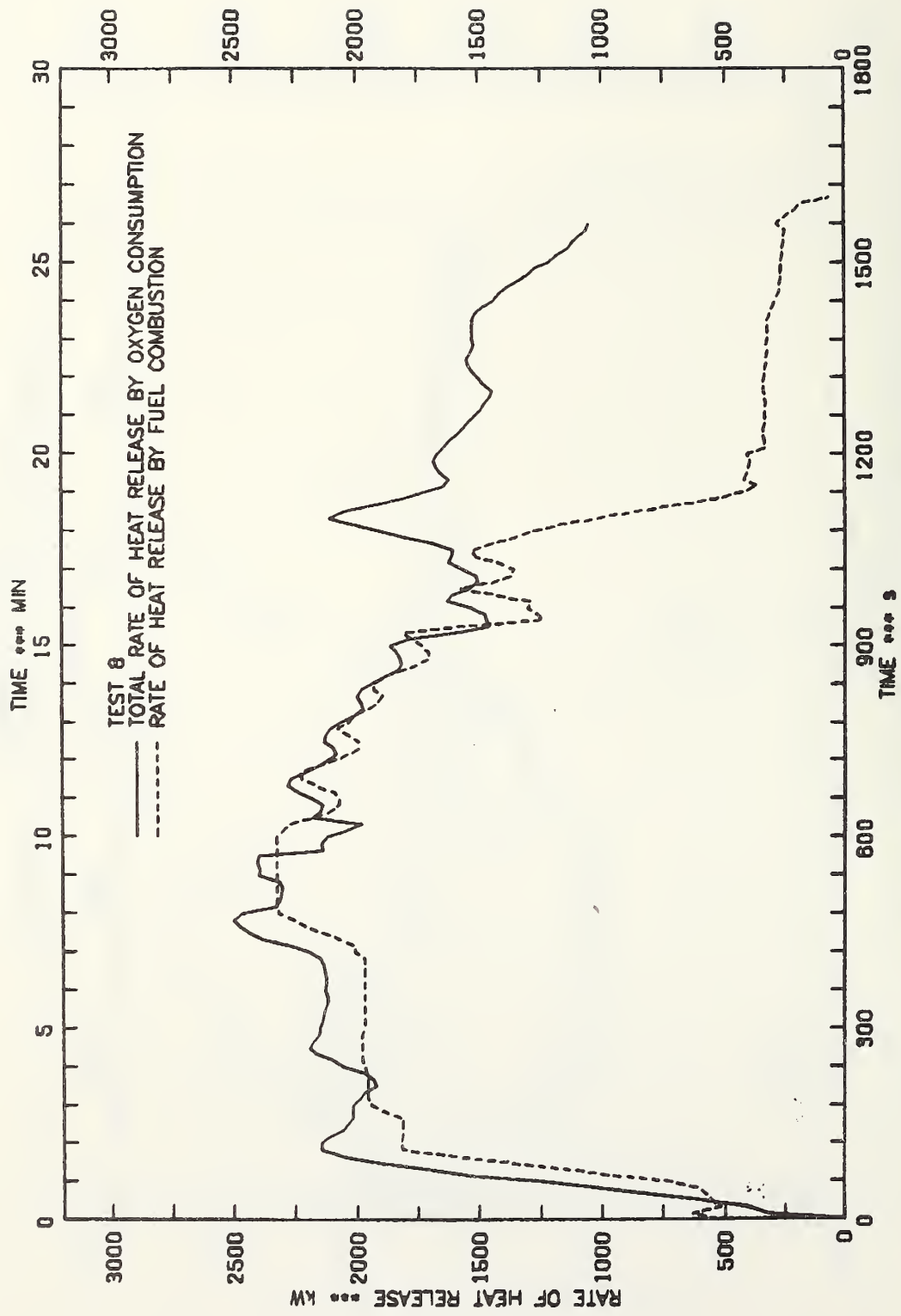
FIGURE 13.8 - COMPARISON OF RATES OF HEAT RELEASE
IN FURNACE FOR TEST 8

74
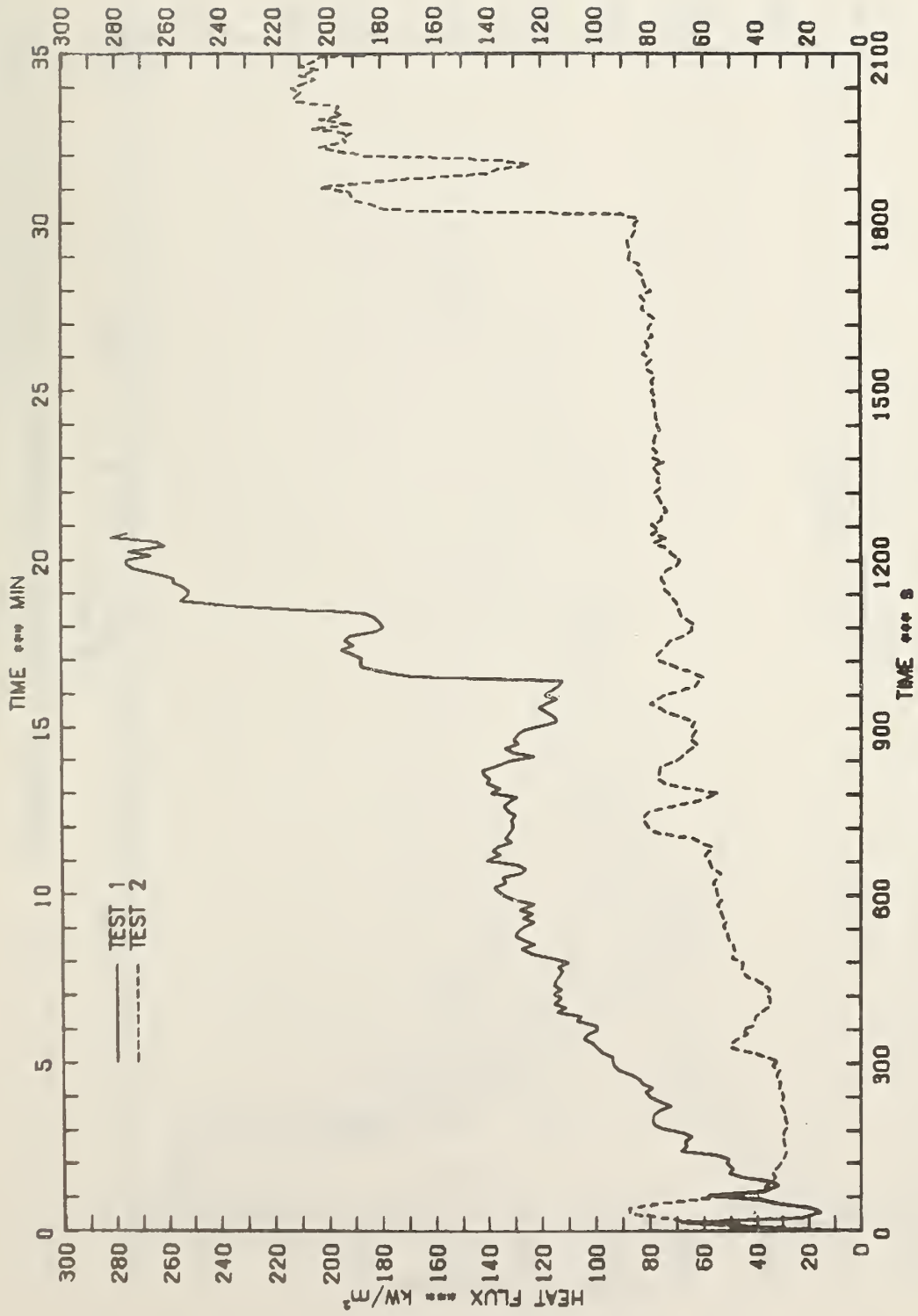
FIGURE 14-A — AVERAGE TOTAL HEAT FLUX
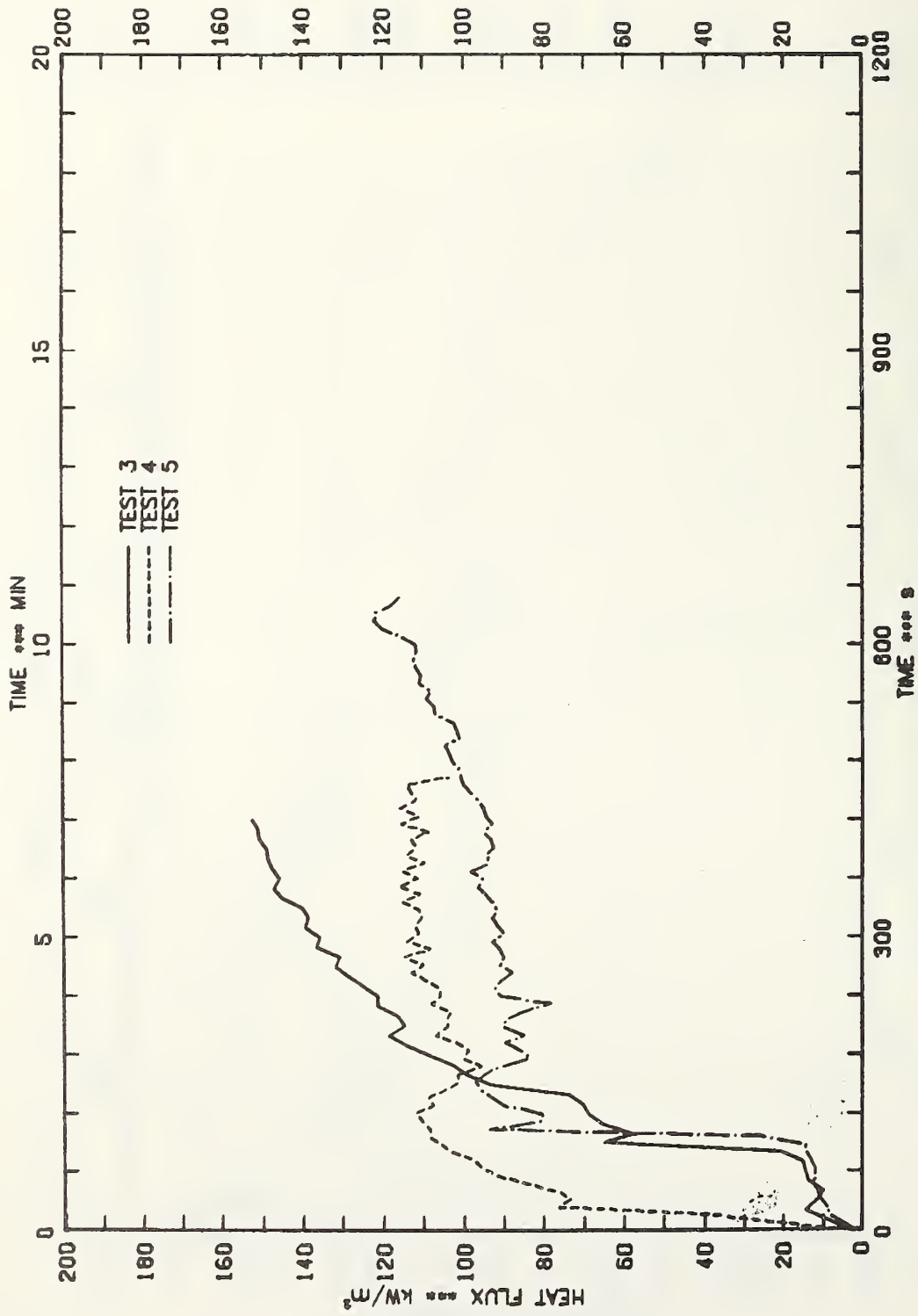
FIGURE 14.B — AVERAGE TOTAL HEAT FLUX
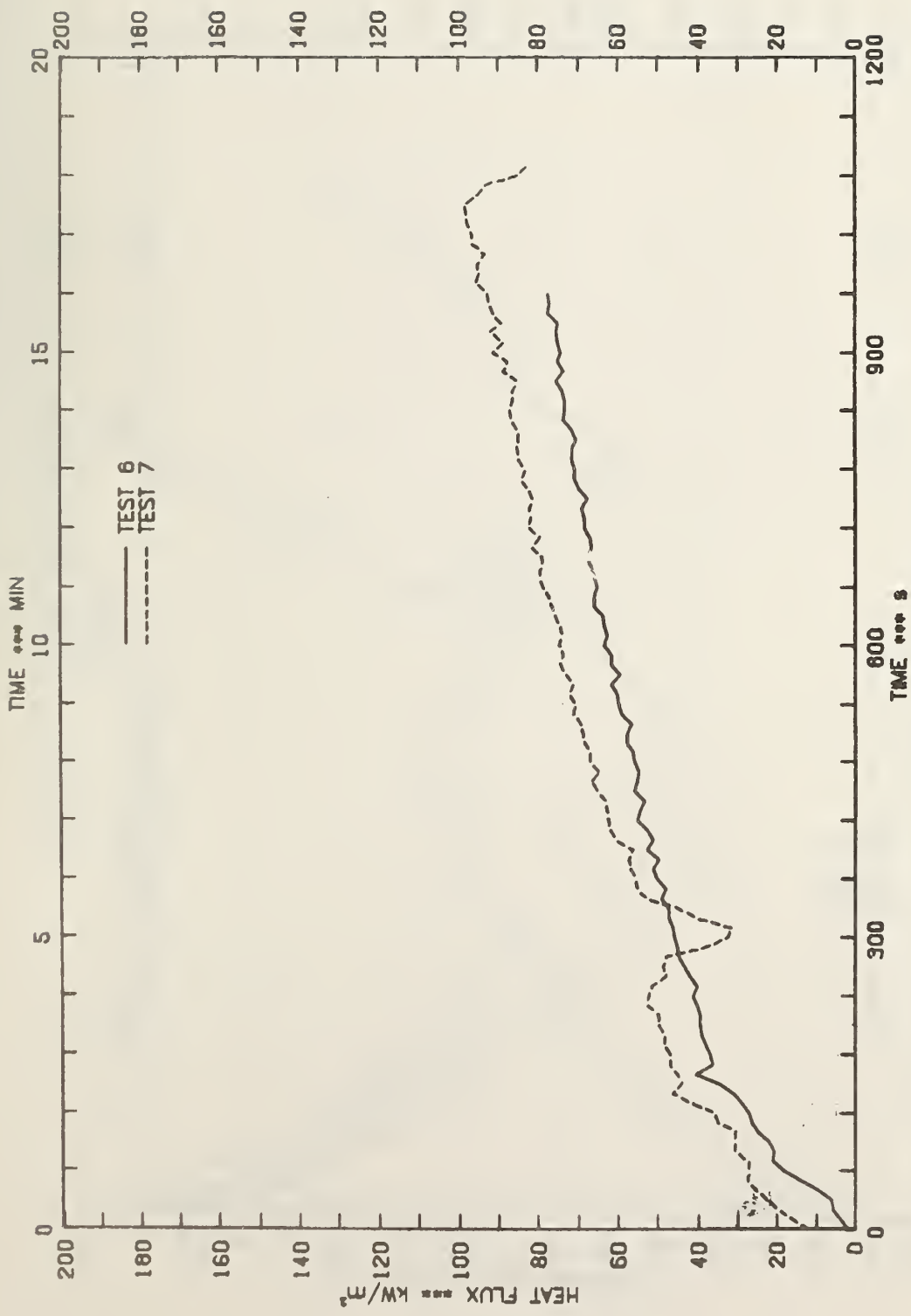
FIGURE 14.C — AVERAGE TOTAL HEAT FLUX
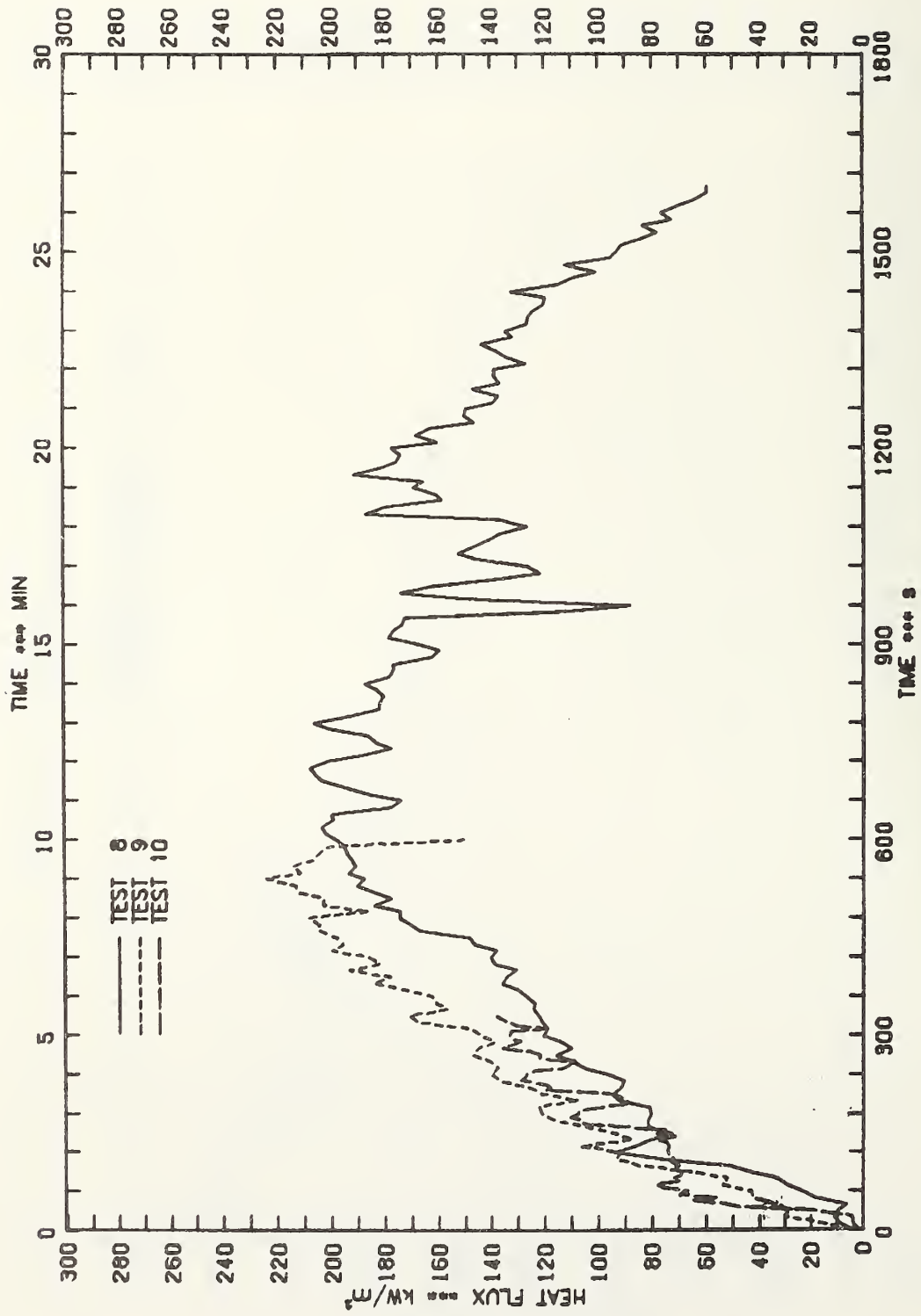
FIGURE 14.D — AVERAGE TOTAL HEAT FLUX

78
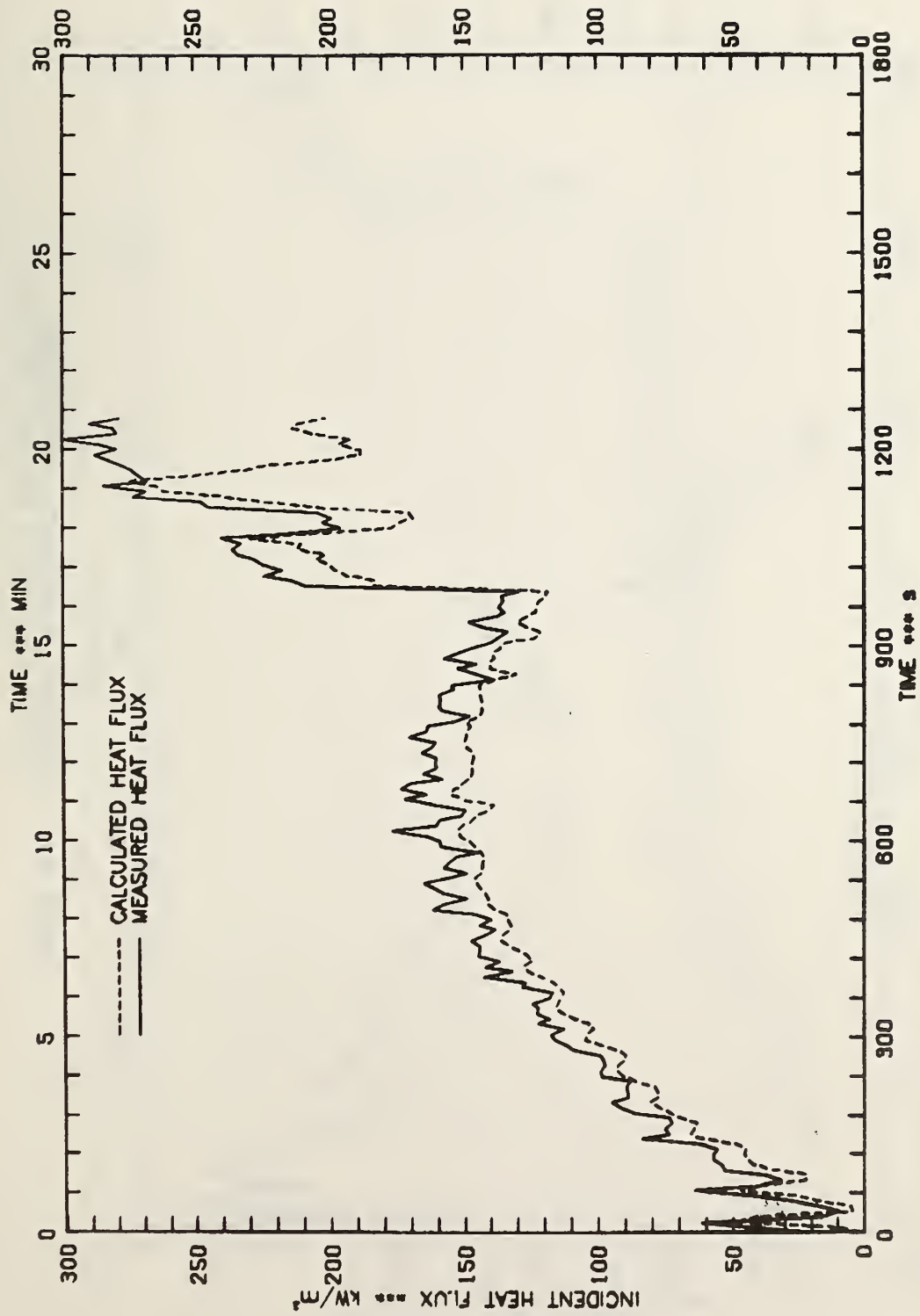
FIGURE 15.A – COMPARISON OF CALCULATED AND MEASURED HEAT FLUX
INCIDENT AT SOUTH WALL FOR TEST 1
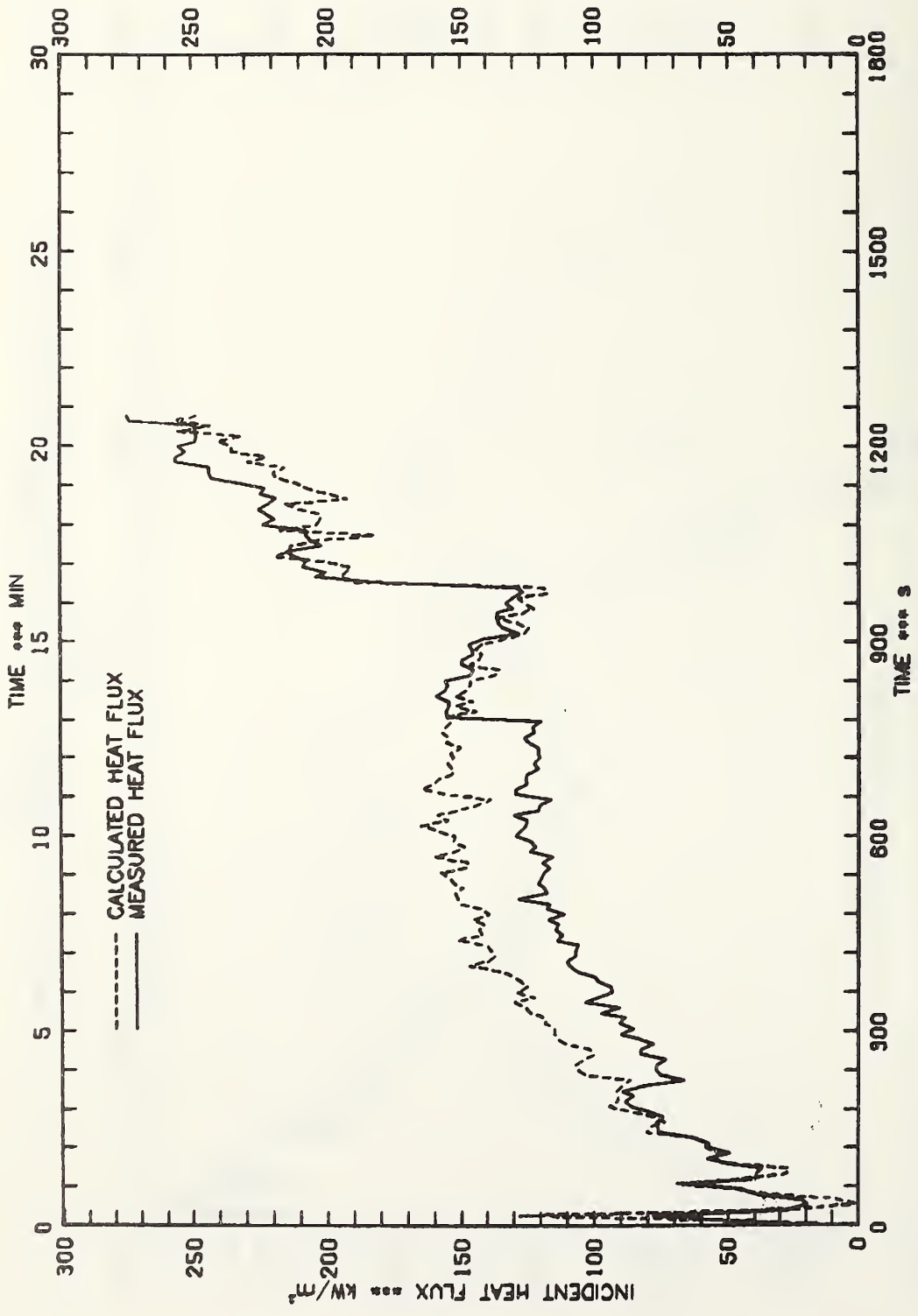
FIGURE 15.B — COMPARISON OF CALCULATED AND MEASURED HEAT FLUX INCIDENT AT EAST WALL FOR TEST 1

80
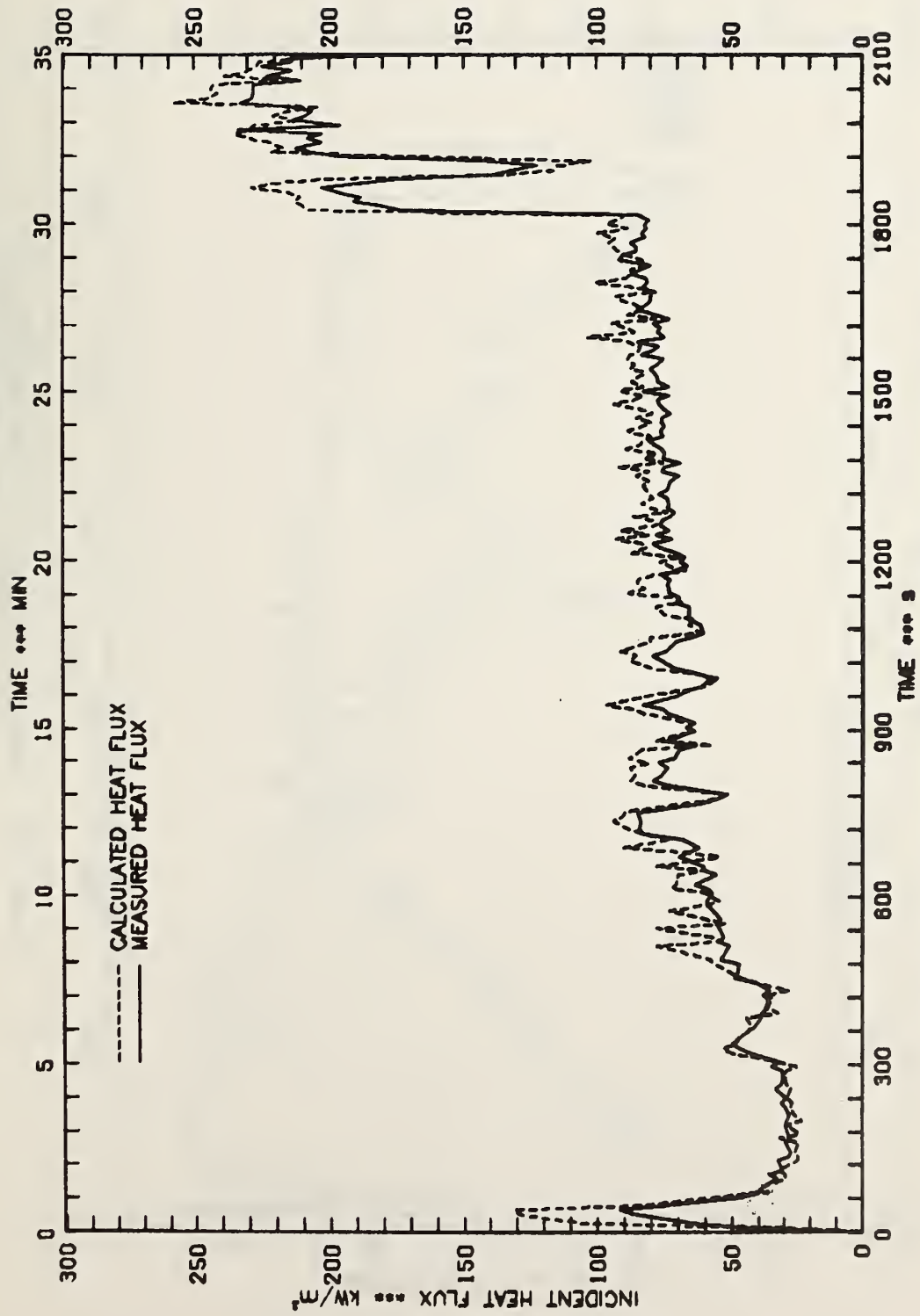
FIGURE 15.C — COMPARISON OF CALCULATED AND MEASURED HEAT FLUX
INCIDENT AT SOUTH WALL FOR TEST 2

81
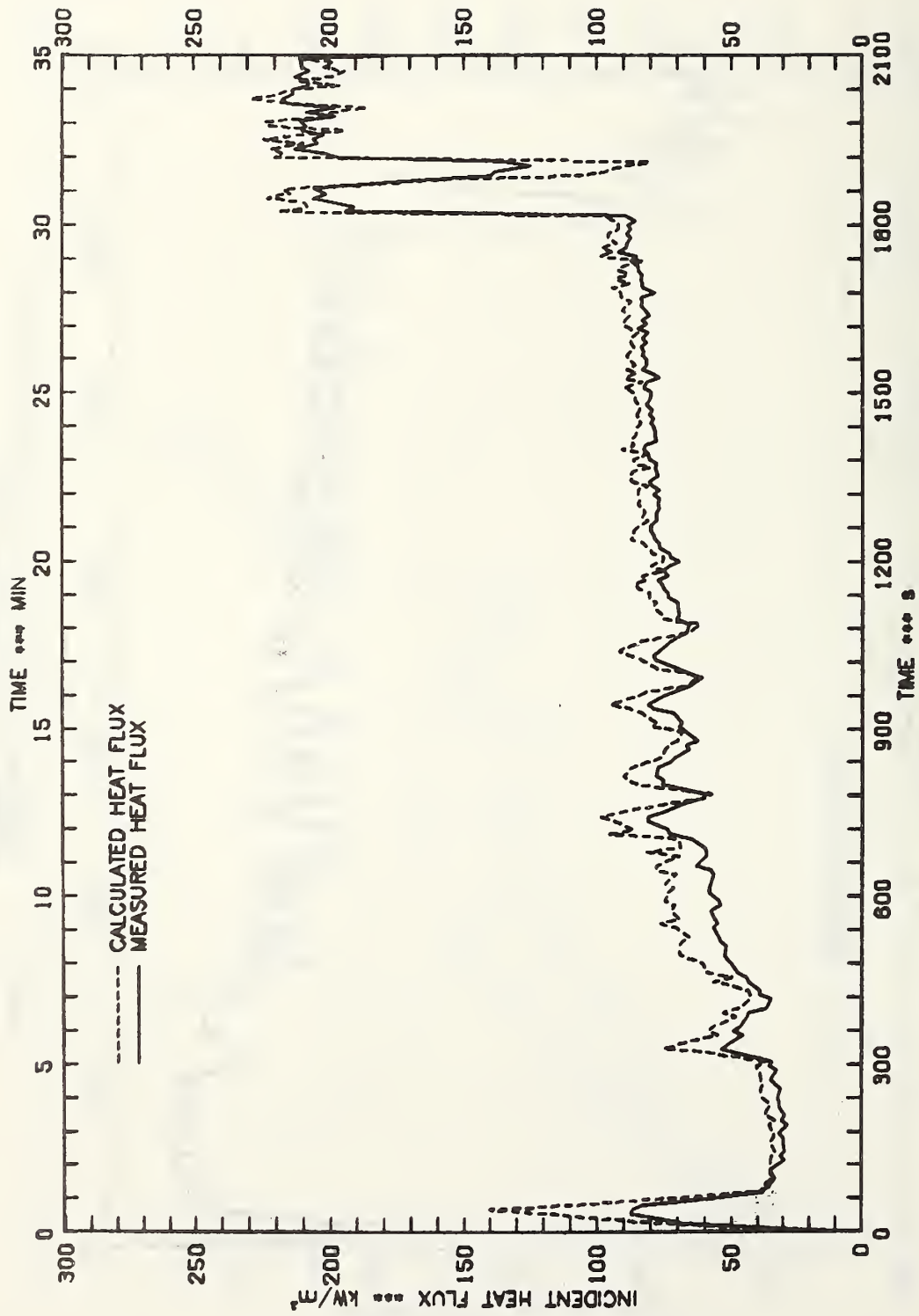
FIGURE 15.D — COMPARISON OF CALCULATED AND MEASURED
HEAT FLUX INCIDENT AT EAST WALL FOR TEST 2

82
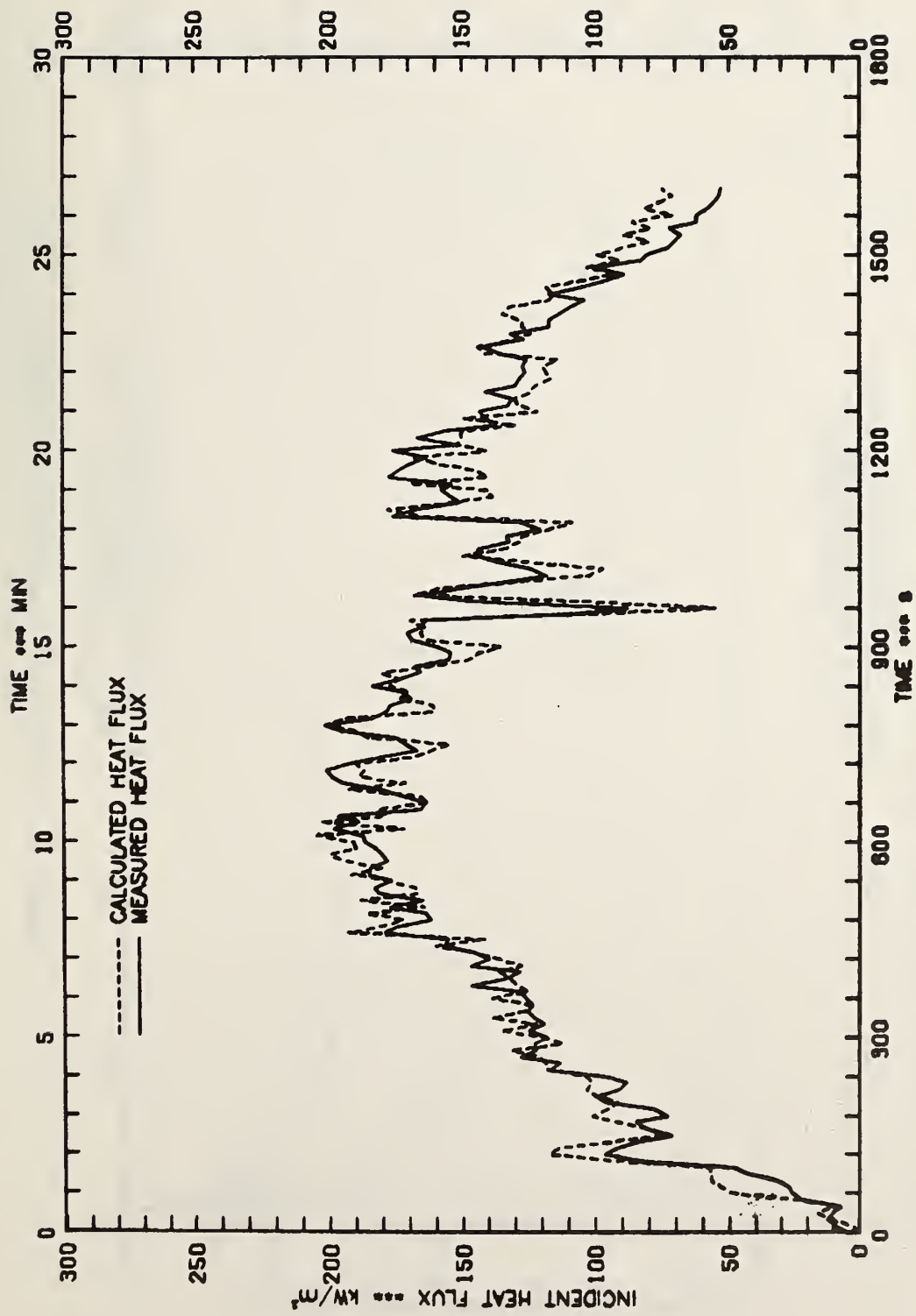
FIGURE 15.E - COMPARISON OF CALCULATED AND MEASURED HEAT FLUX
INCIDENT AT SOUTH WALL FOR TEST 8

83
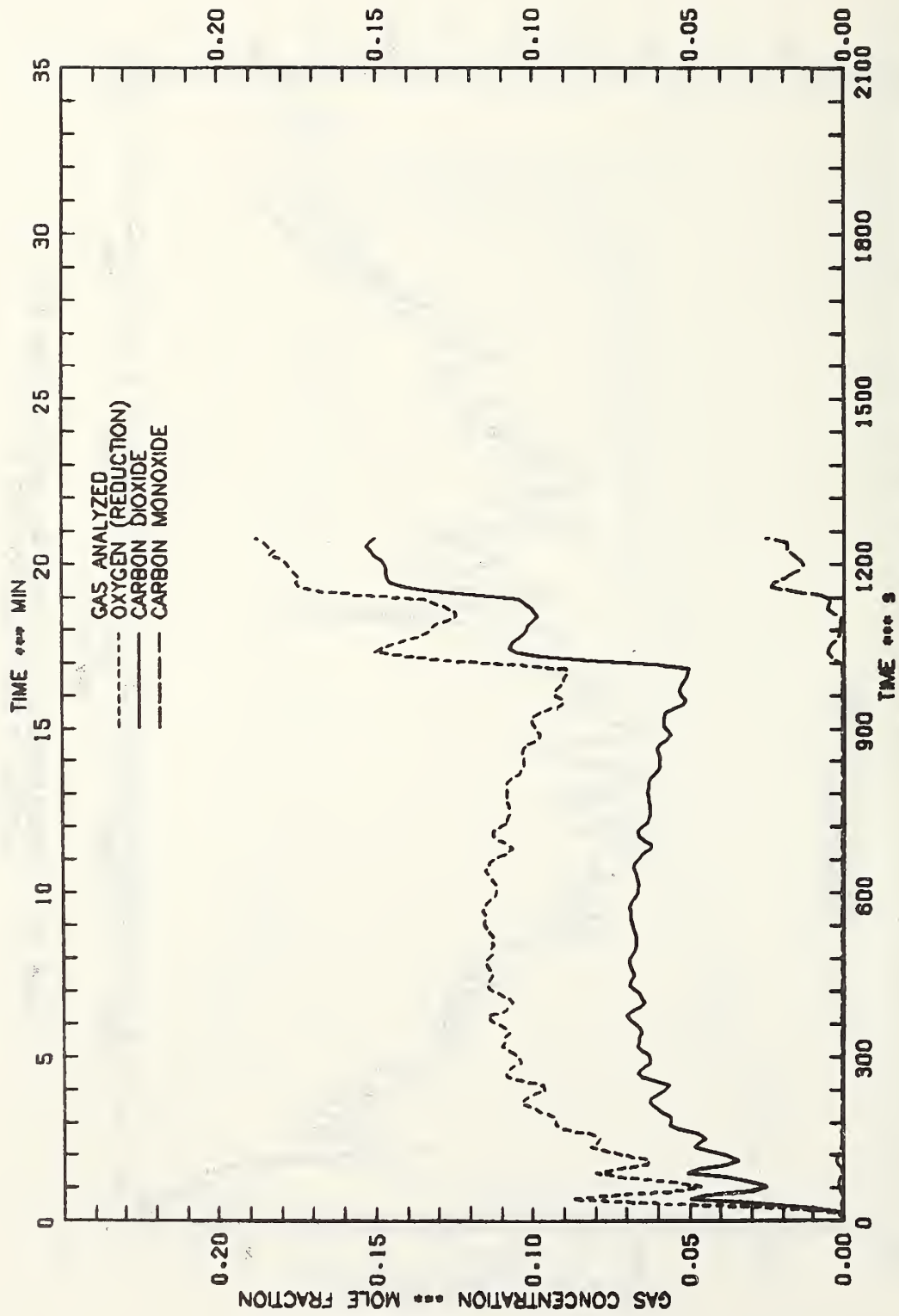
FIGURE 16.A - EXHAUST GAS CONCENTRATIONS FOR TEST 1
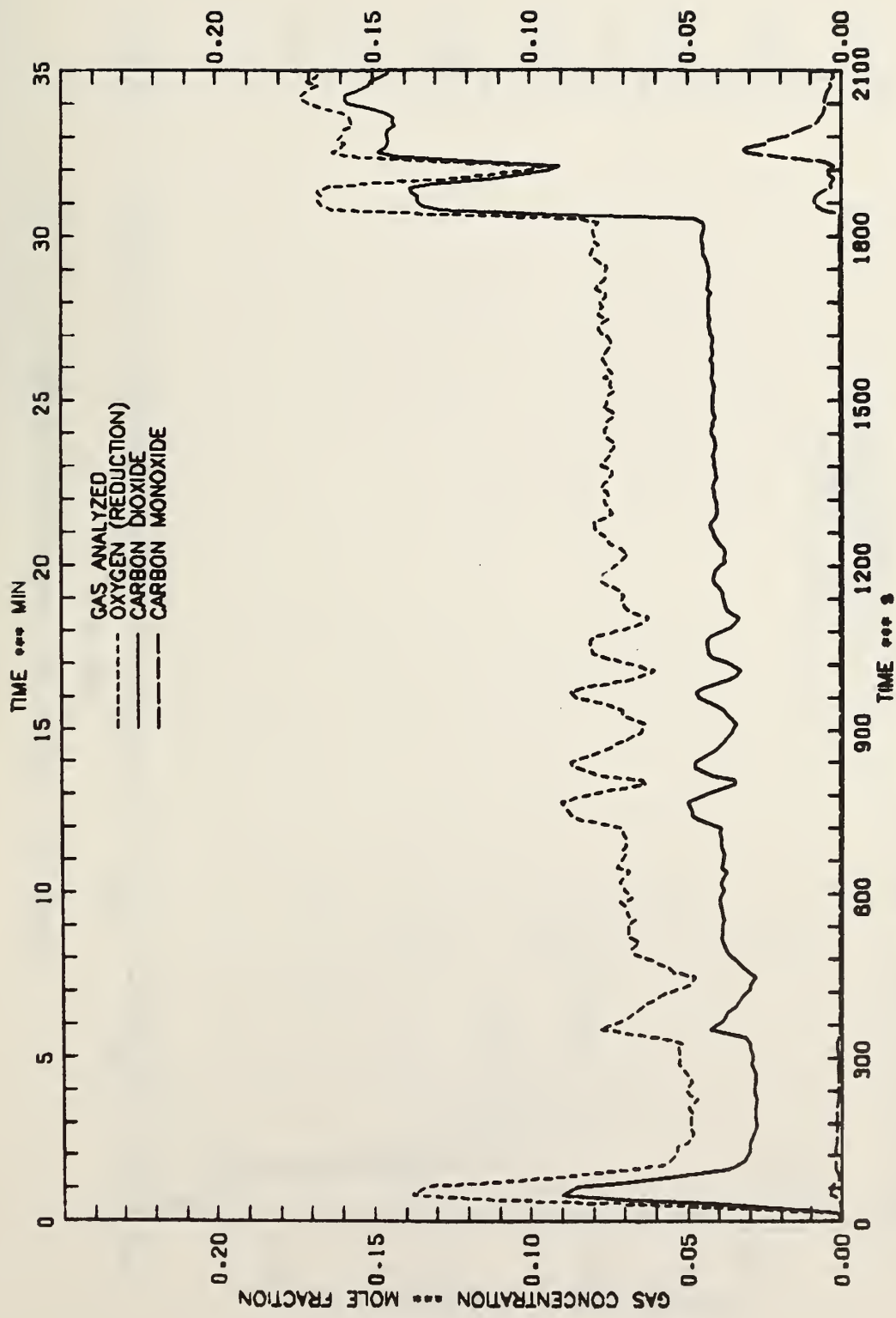
FIGURE 16.B - EXHAUST GAS CONCENTRATIONS FOR TEST 2
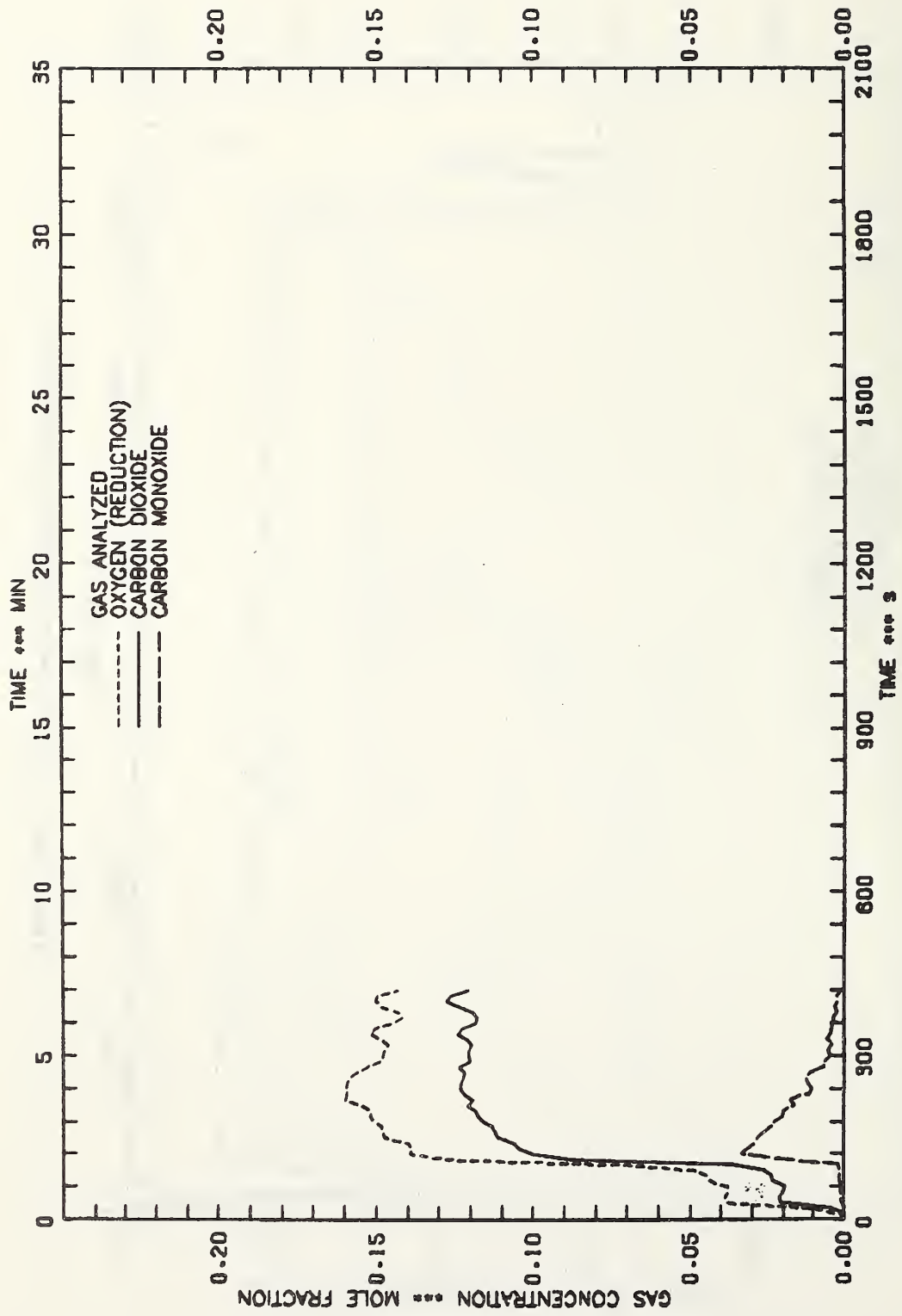
FIGURE 16.C — EXHAUST GAS CONCENTRATIONS FOR TEST 3
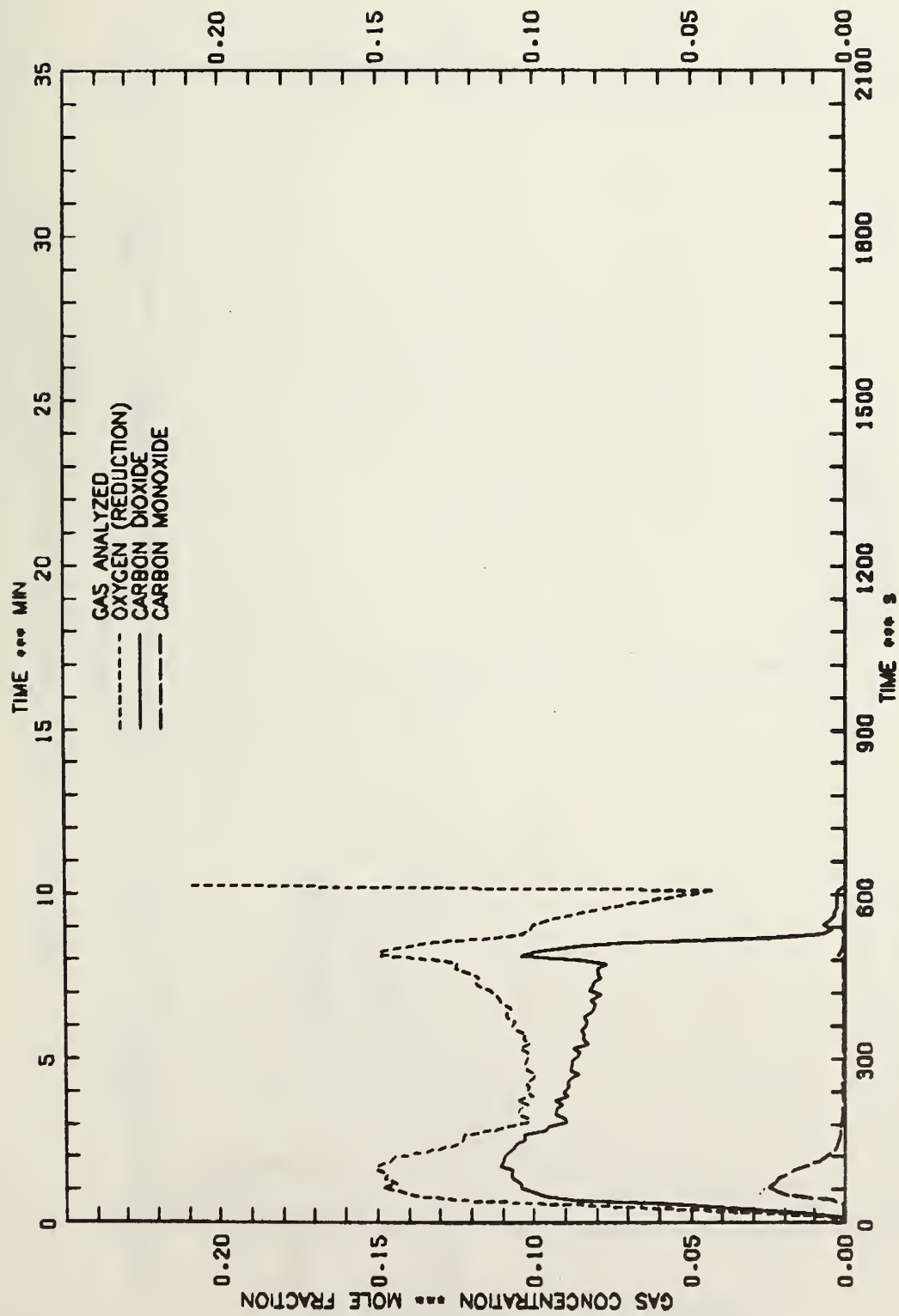
FIGURE 15.D - EXHAUST GAS CONCENTRATIONS FOR TEST 4

87
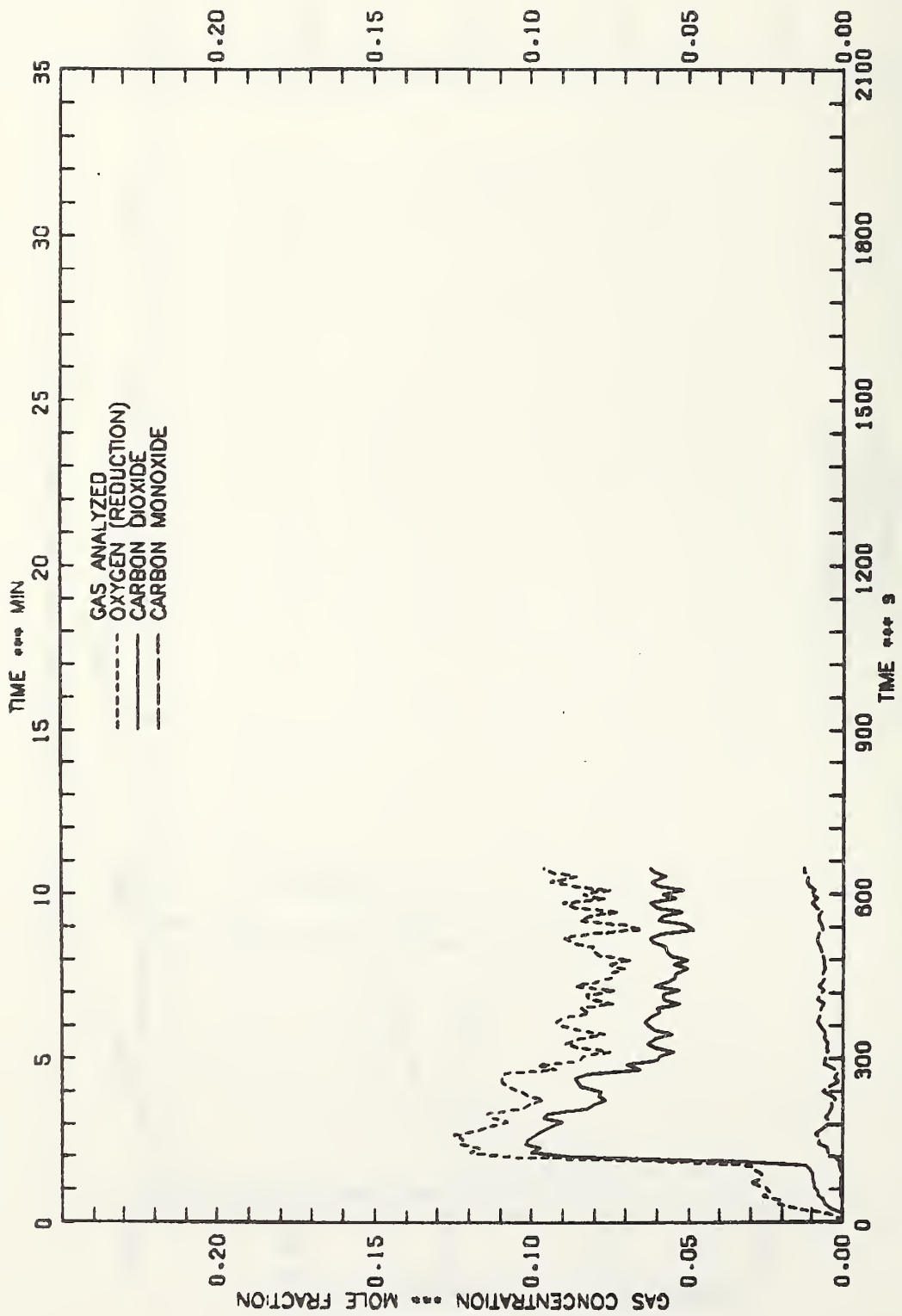
FIGURE 16.E — EXHAUST GAS CONCENTRATIONS FOR TEST 5
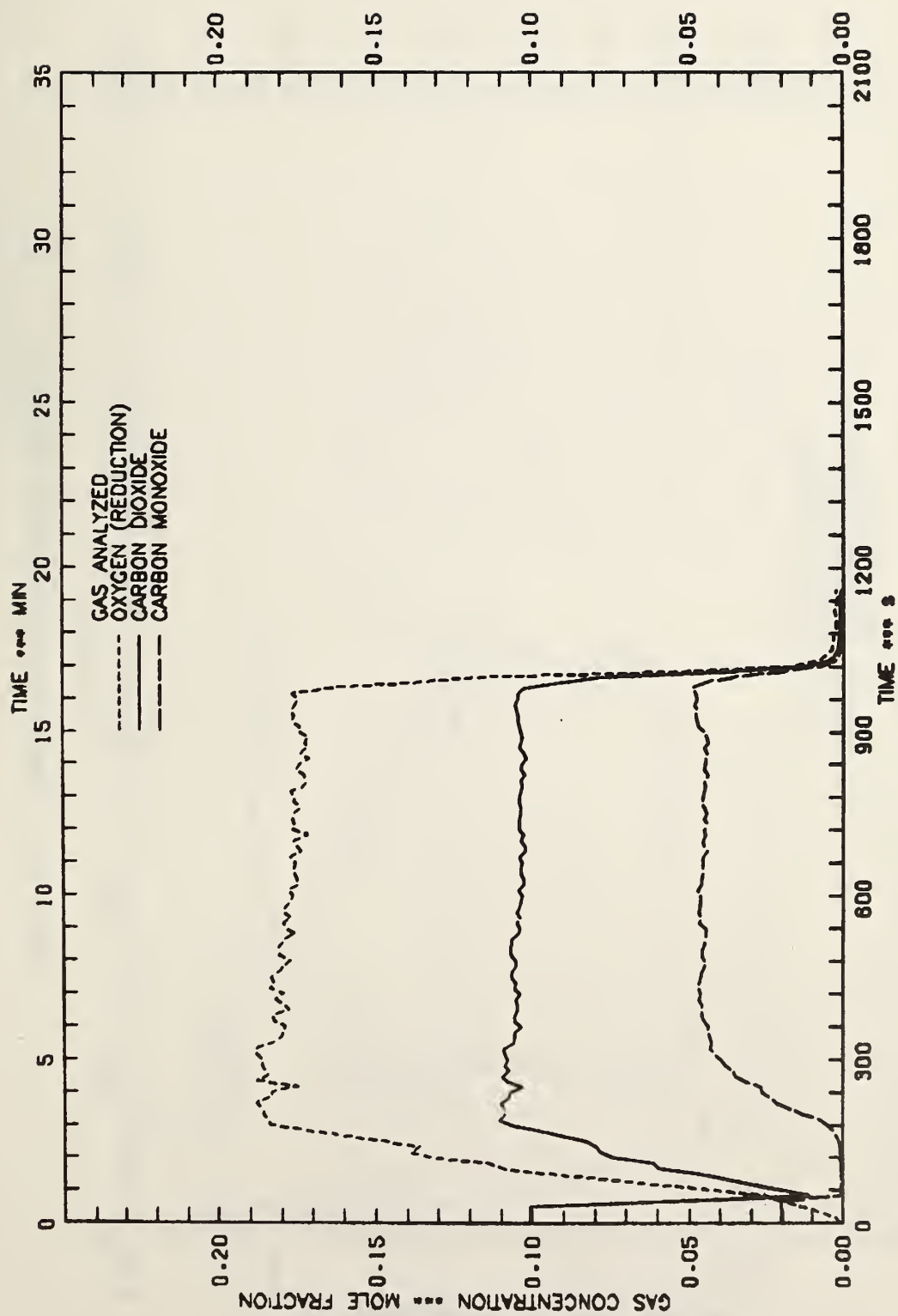
FIGURE 16.F – EXHAUST GAS CONCENTRATIONS FOR TEST 6
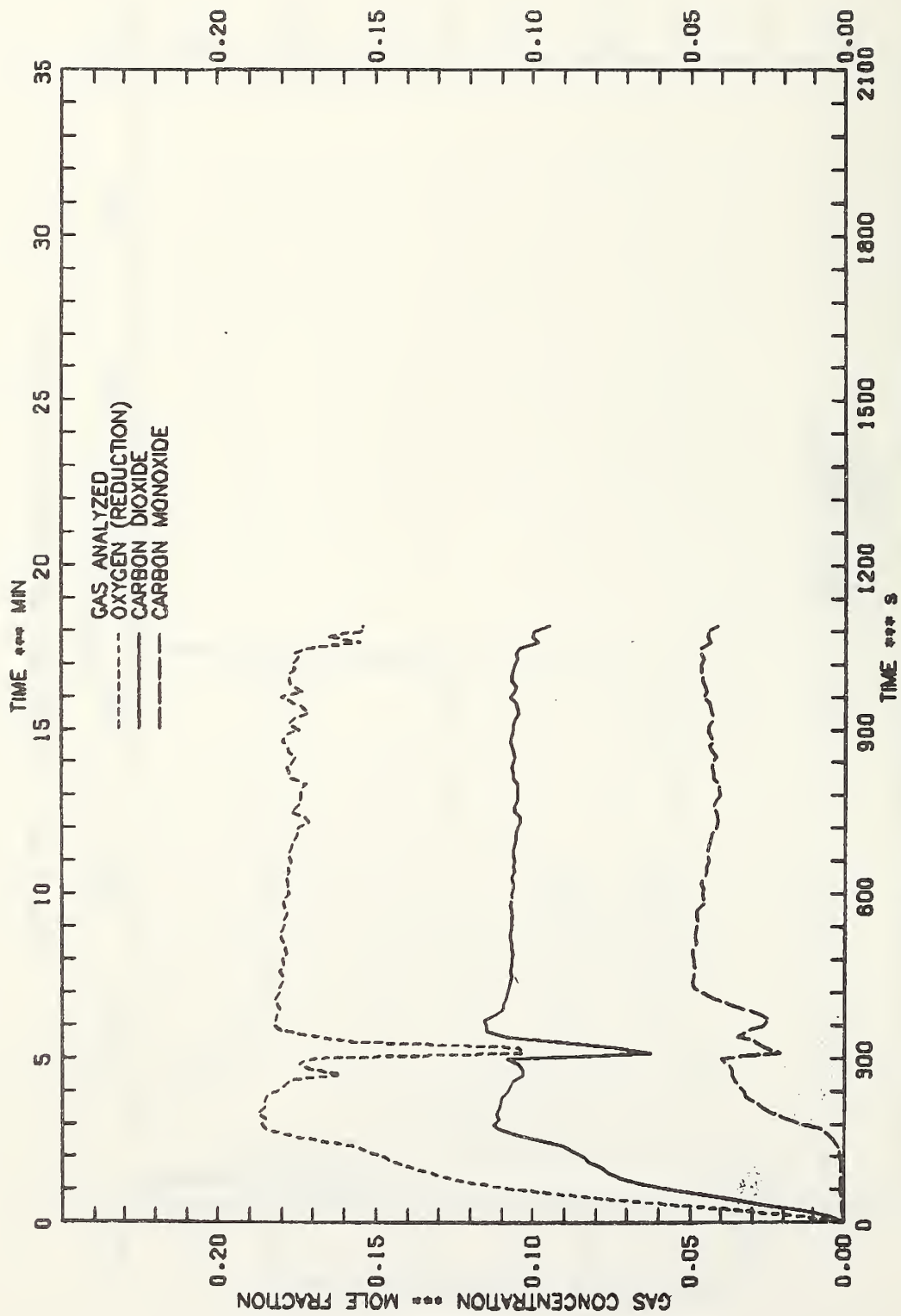
FIGURE 16.G — EXHAUST GAS CONCENTRATIONS FOR TEST 7
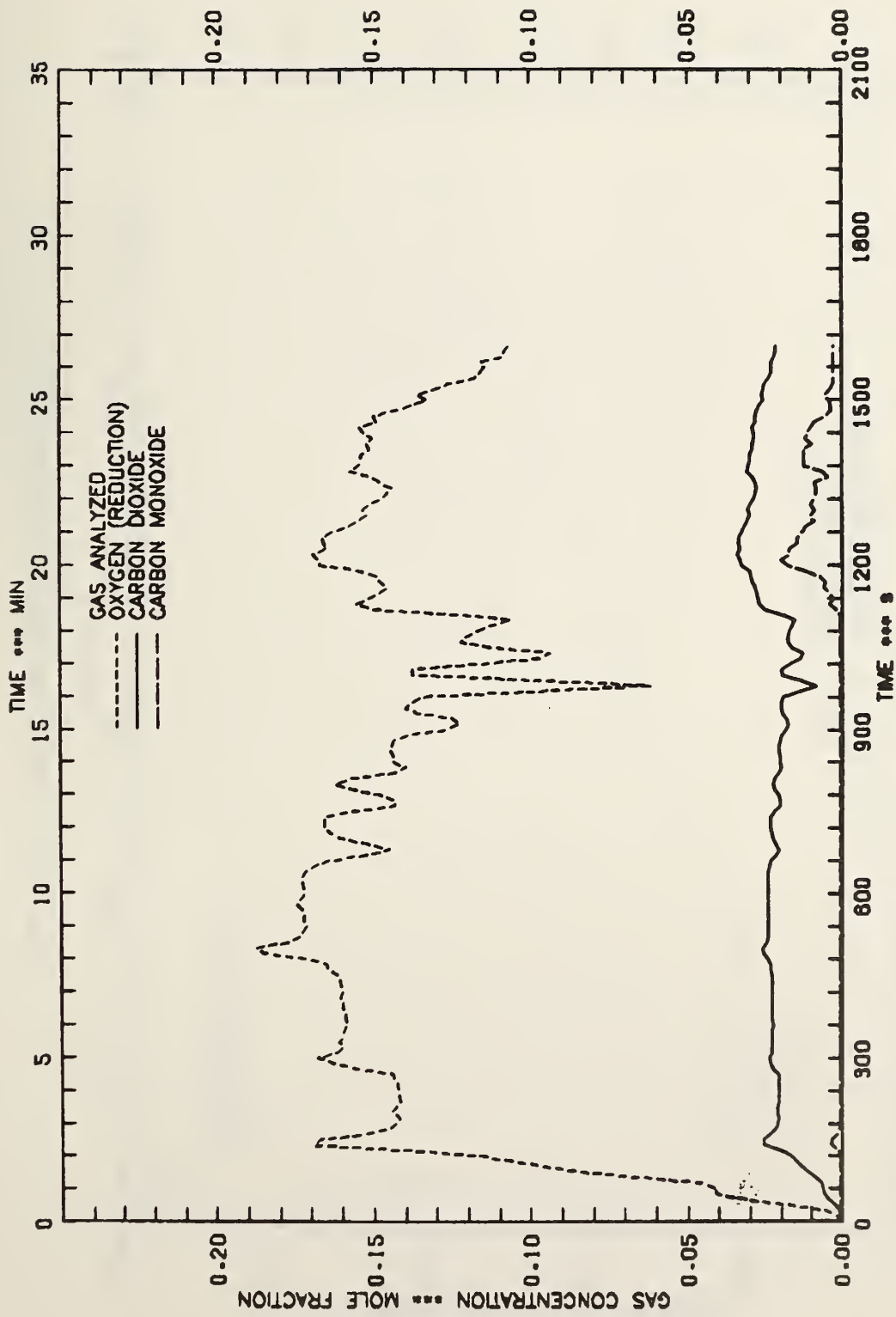
FIGURE 16.H – EXHAUST GAS CONCENTRATIONS FOR TEST 8
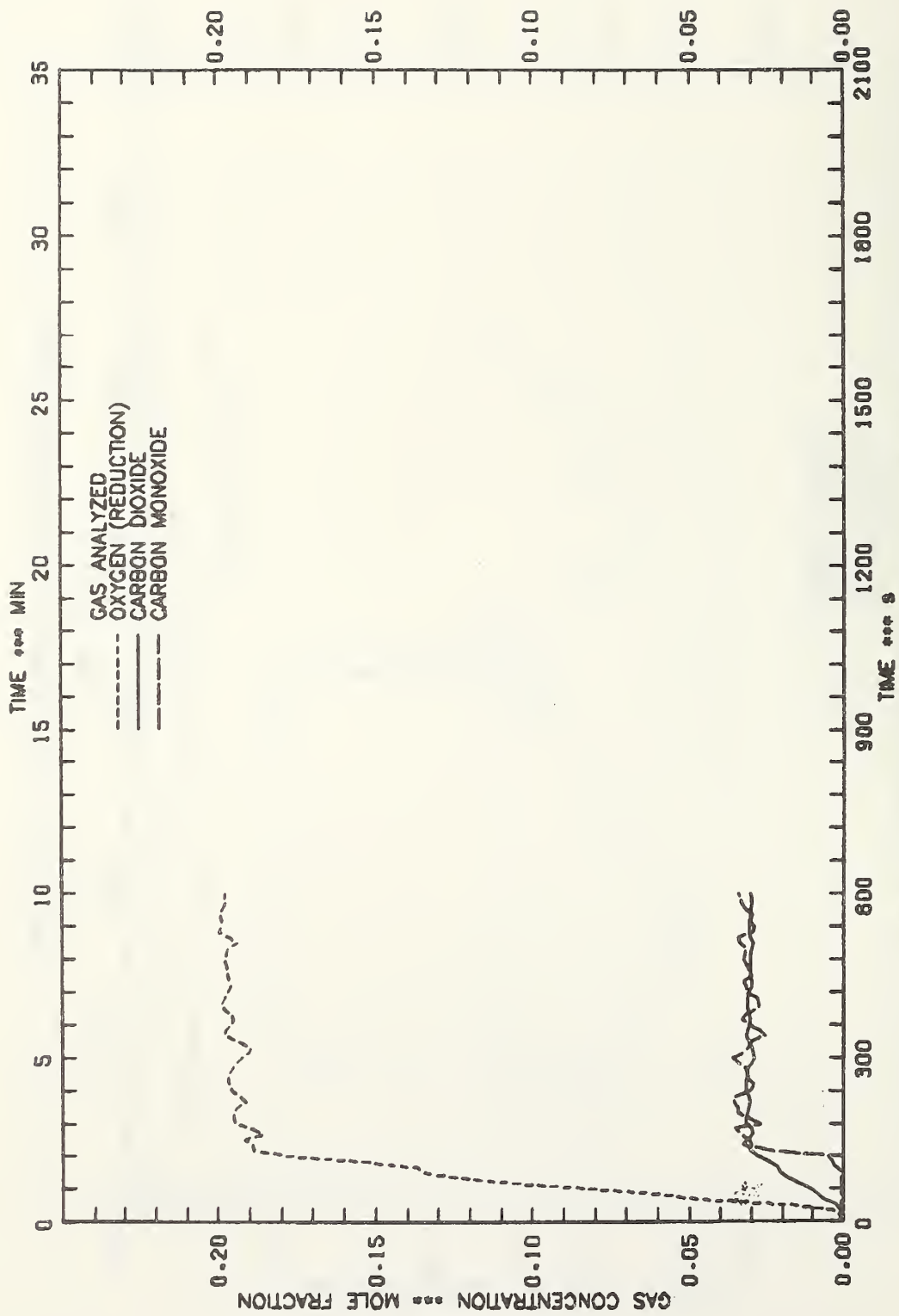
FIGURE 16.I - EXHAUST GAS CONCENTRATIONS FOR TEST 9

92
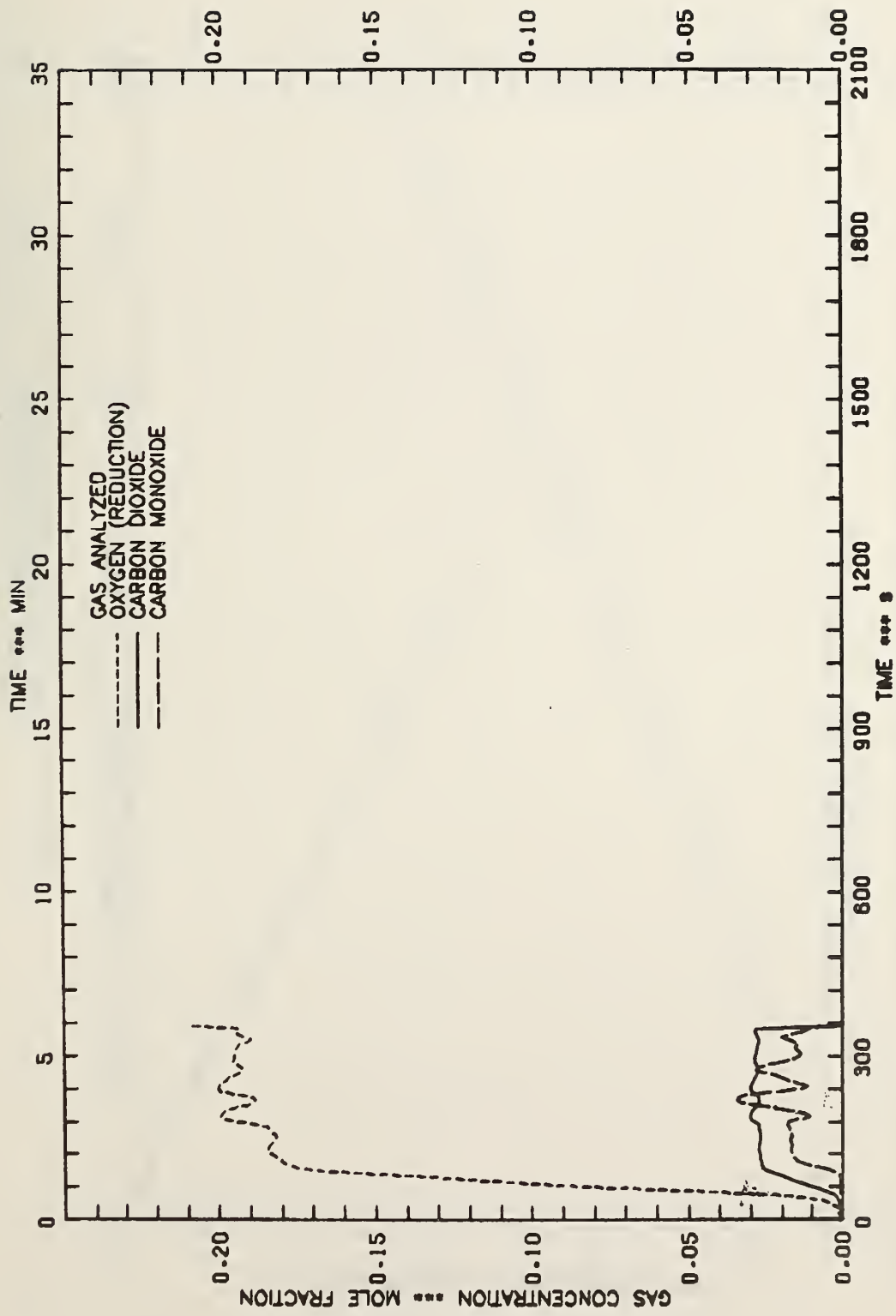
FIGURE 16J - EXHAUST GAS CONCENTRATIONS FOR TEST 10

93
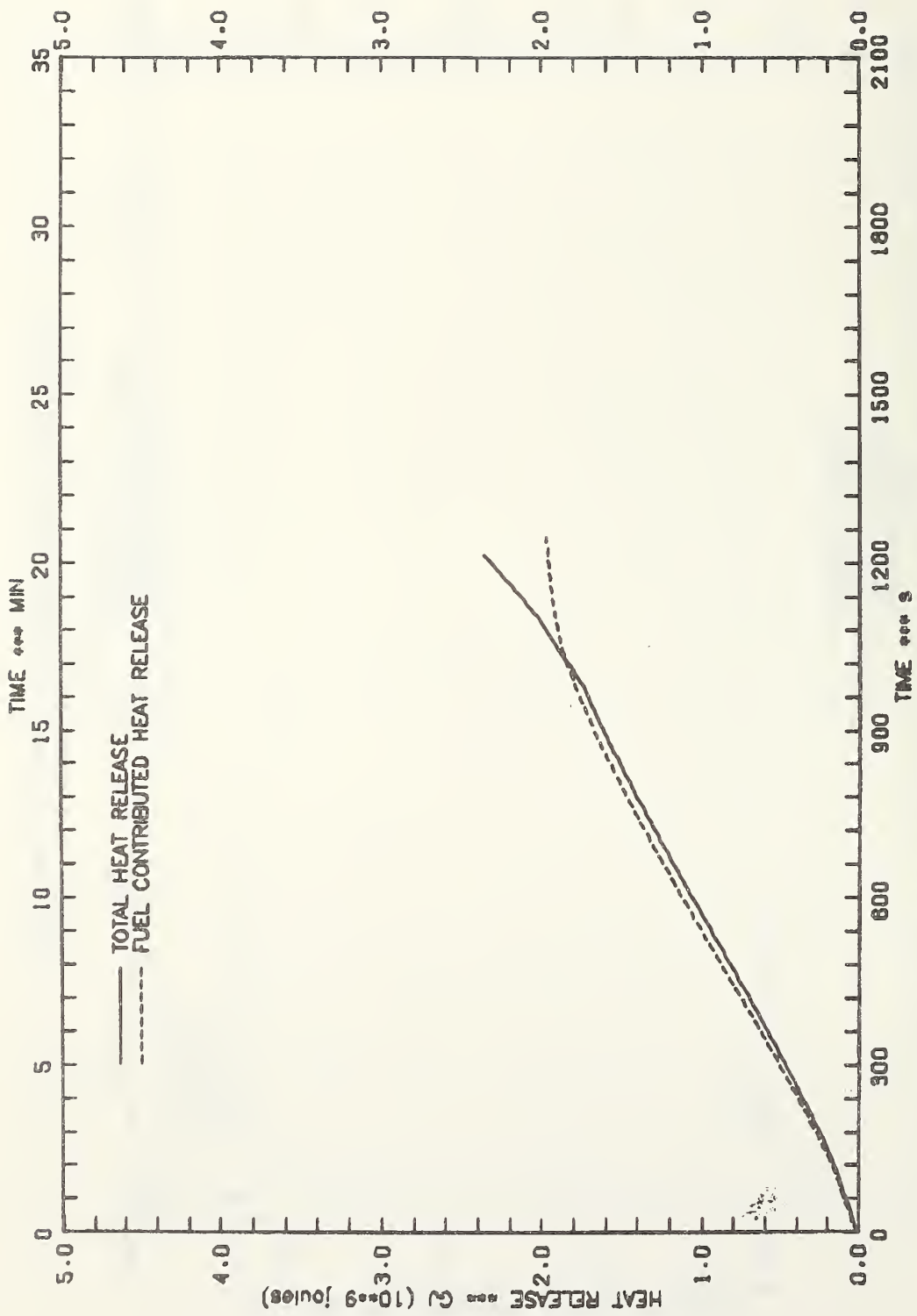
FIGURE 17-A — TOTAL HEAT RELEASE AND HEAT
RELEASE BY FUEL FOR TEST 1

TOTAL HEAT RELEASE
FUEL CONTRIBUTED HEAT RELEASE

TIME ••• MIN

TIME ••• S

HEAT RELEASE ••• GW (10**9 joules)
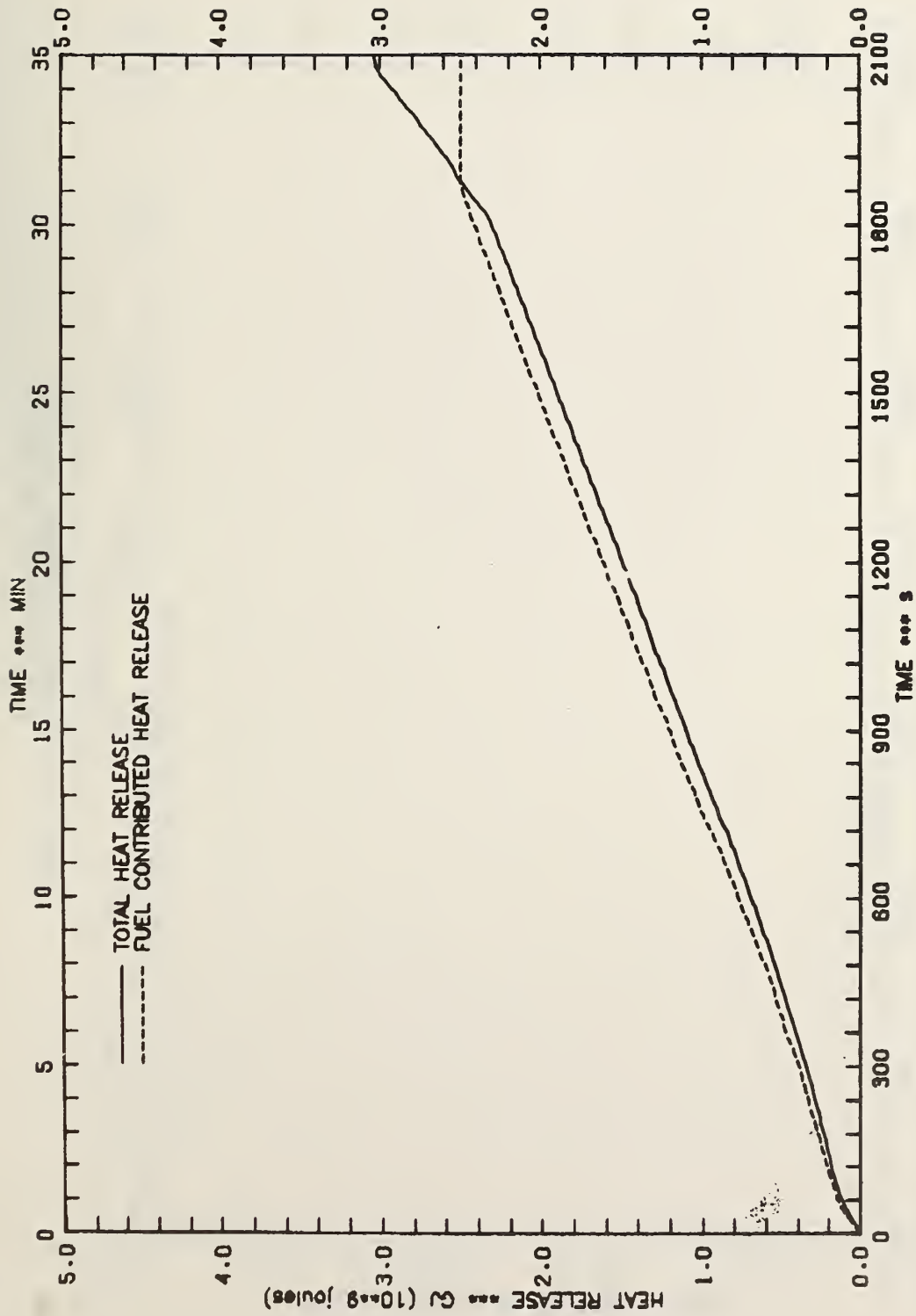
FIGURE 17.B — TOTAL HEAT RELEASE AND HEAT RELEASE BY FUEL FOR TEST 2

95
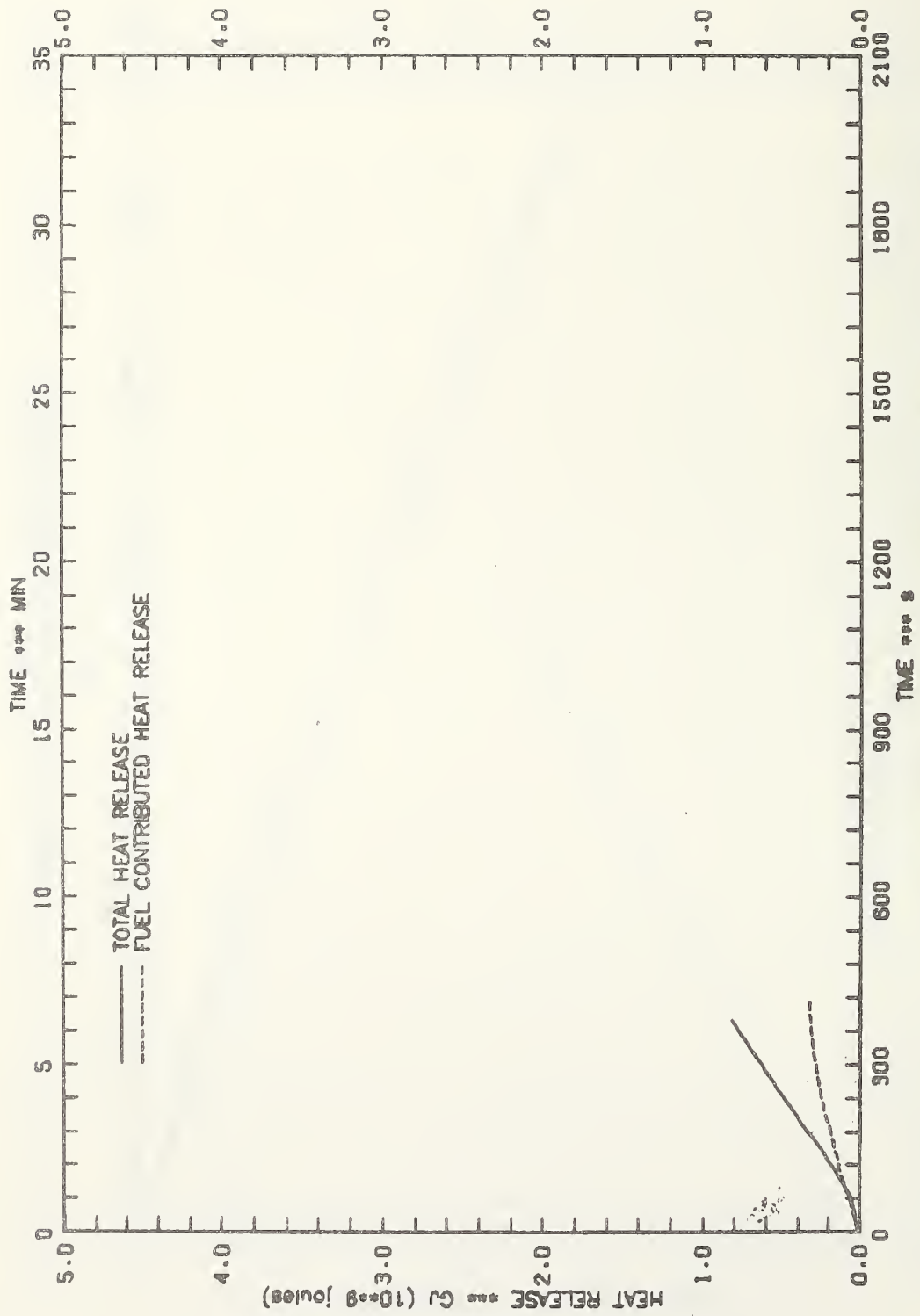
FIGURE 17.C — TOTAL HEAT RELEASE AND HEAT
RELEASE BY FUEL FOR TEST 3
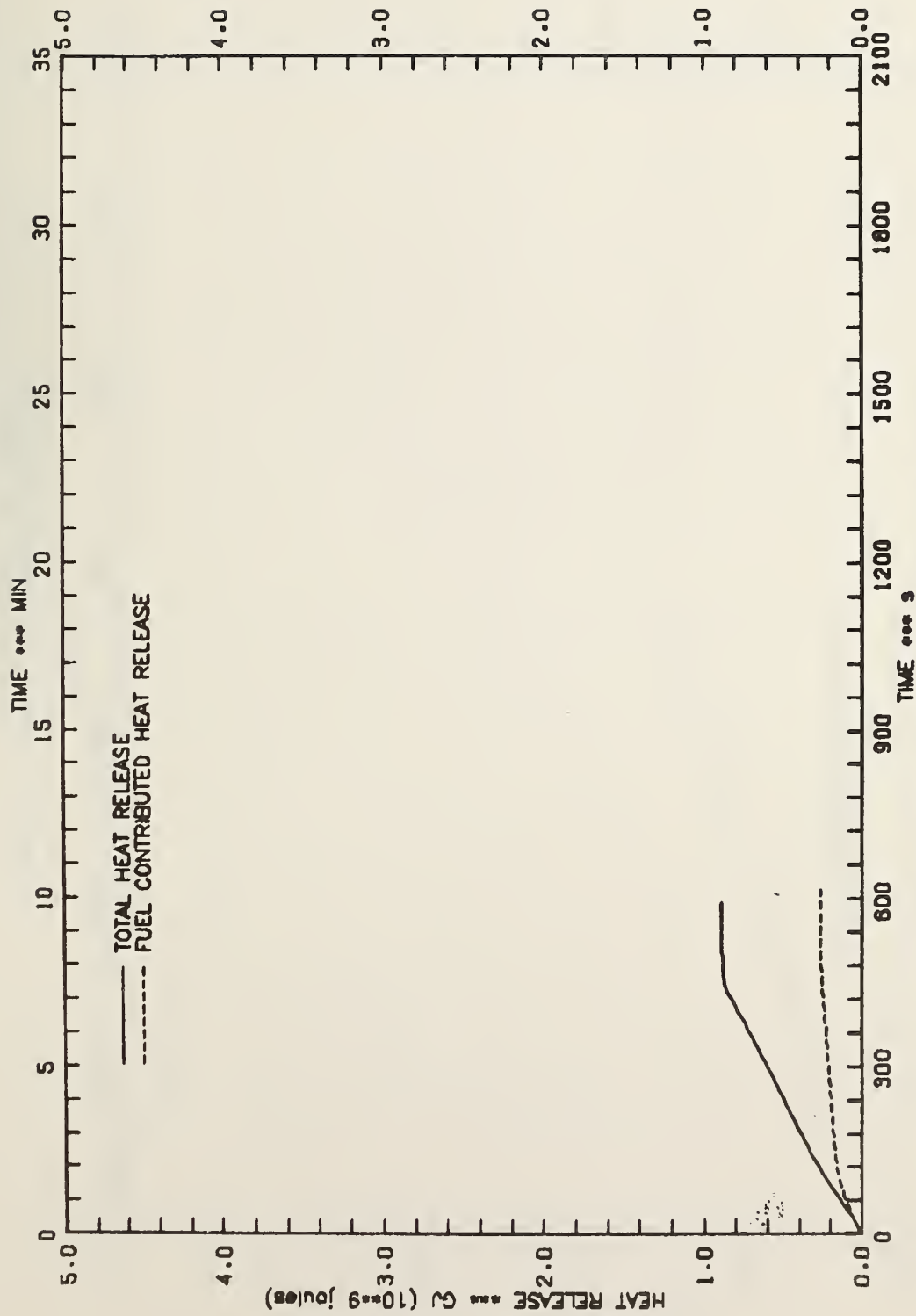
FIGURE 17.D — TOTAL HEAT RELEASE AND HEAT RELEASE BY FUEL FOR TEST 4
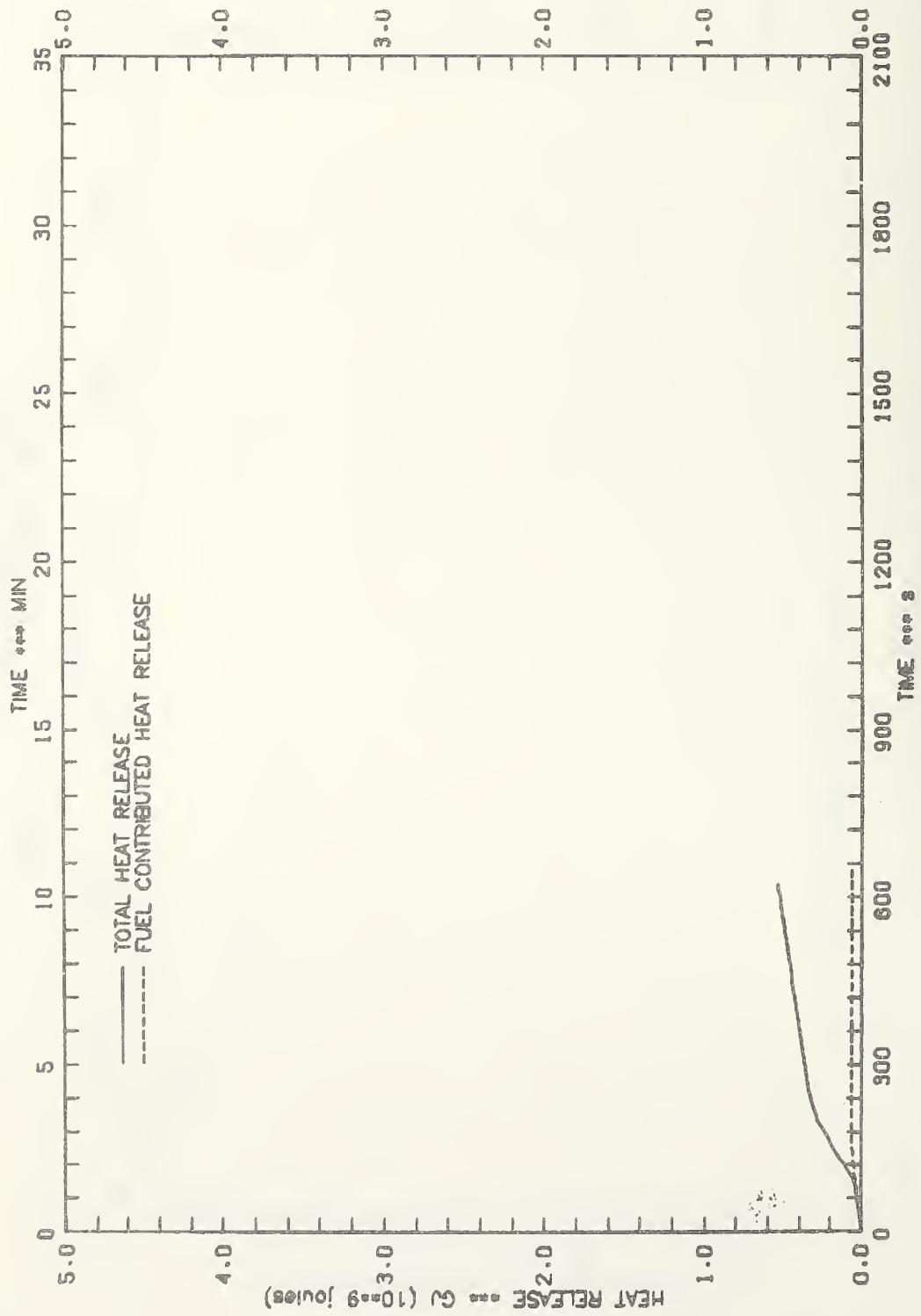
FIGURE 17.E – TOTAL HEAT RELEASE AND HEAT
RELEASE BY FUEL FOR TEST 5

98
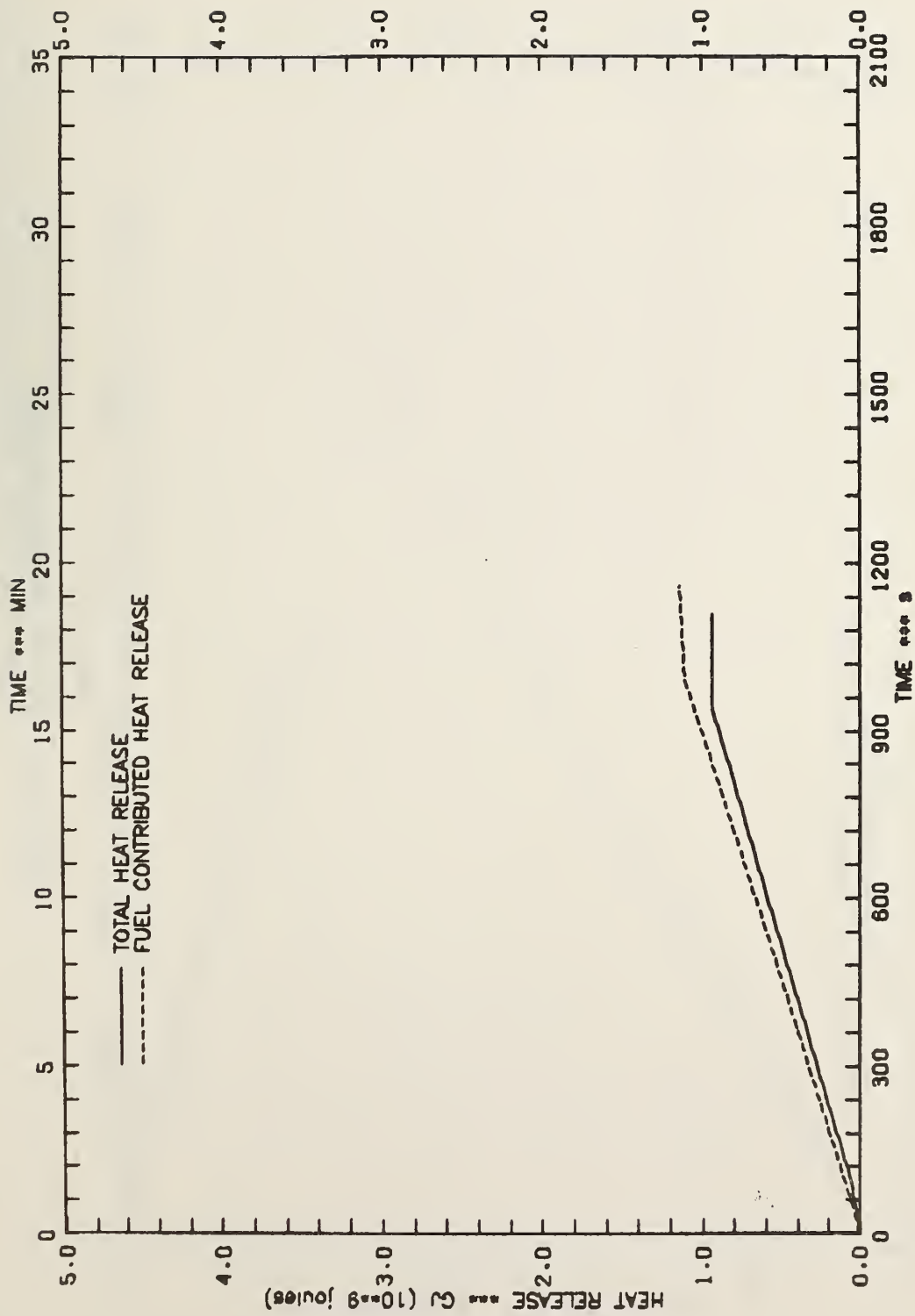
FIGURE 17.F – TOTAL HEAT RELEASE AND HEAT RELEASE BY FUEL FOR TEST 6
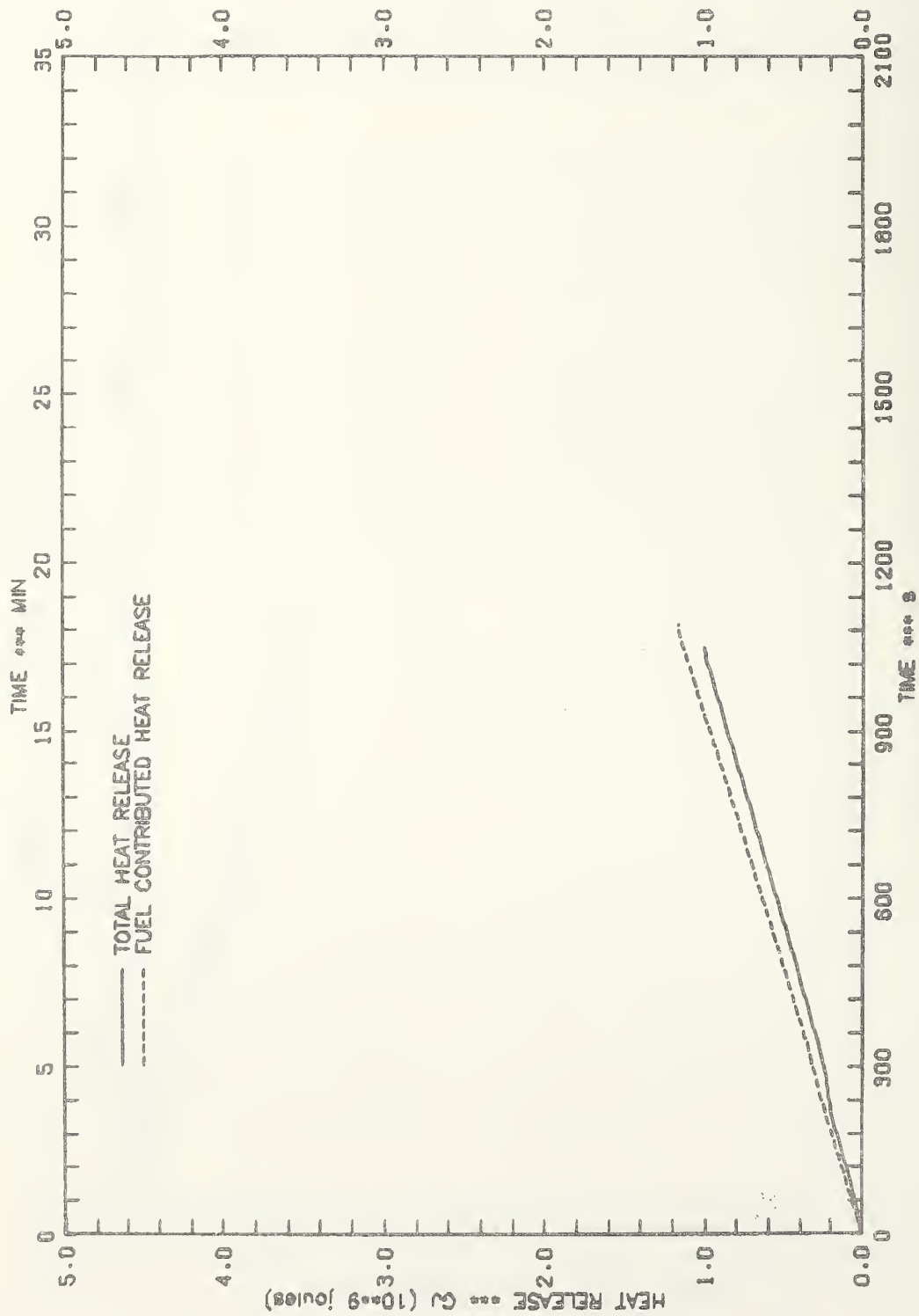
FIGURE 17.G — TOTAL HEAT RELEASE AND HEAT
RELEASE BY FUEL FOR TEST 7
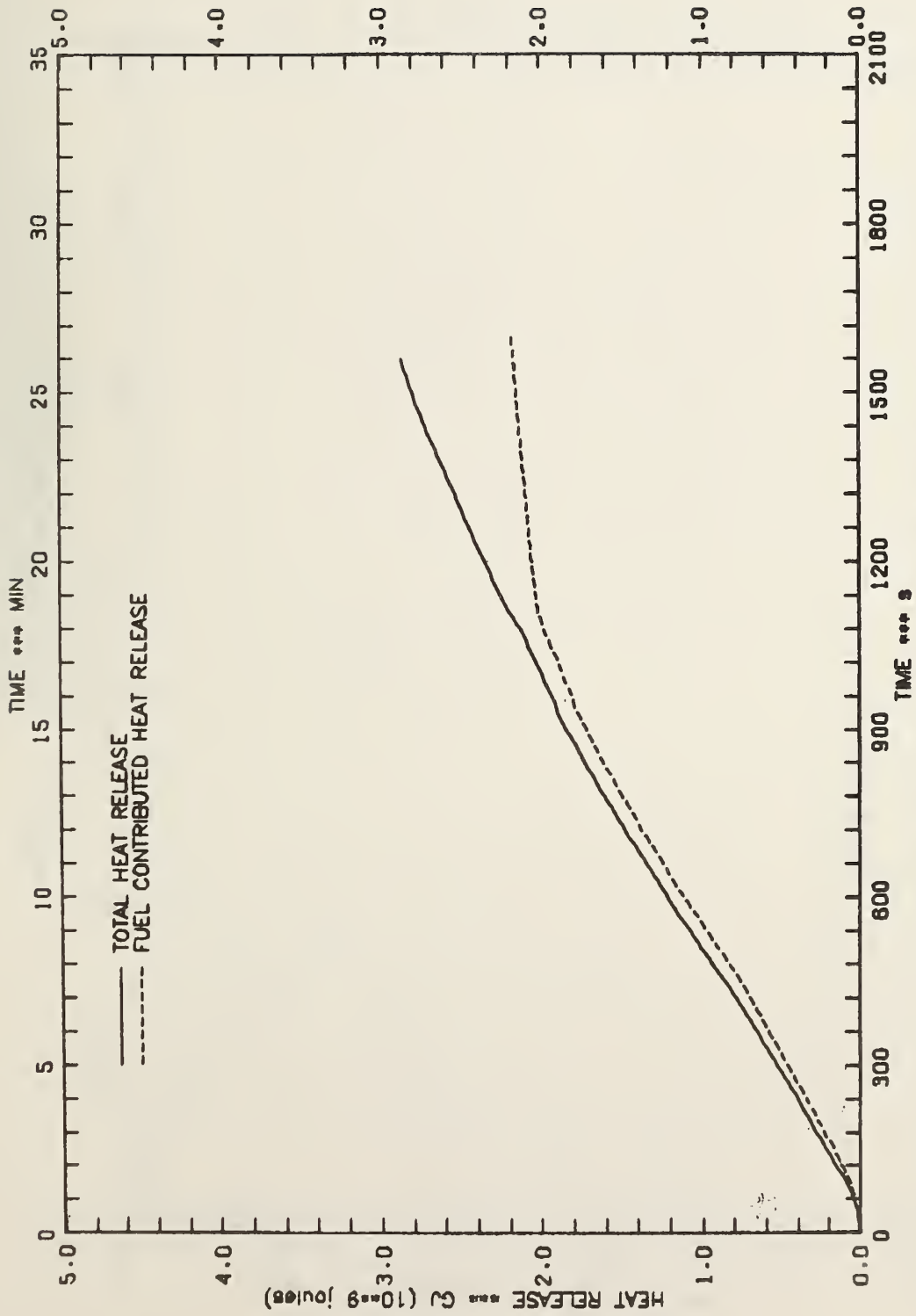
FIGURE 17.H — TOTAL HEAT RELEASE AND HEAT
RELEASE BY FUEL FOR TEST 8

101
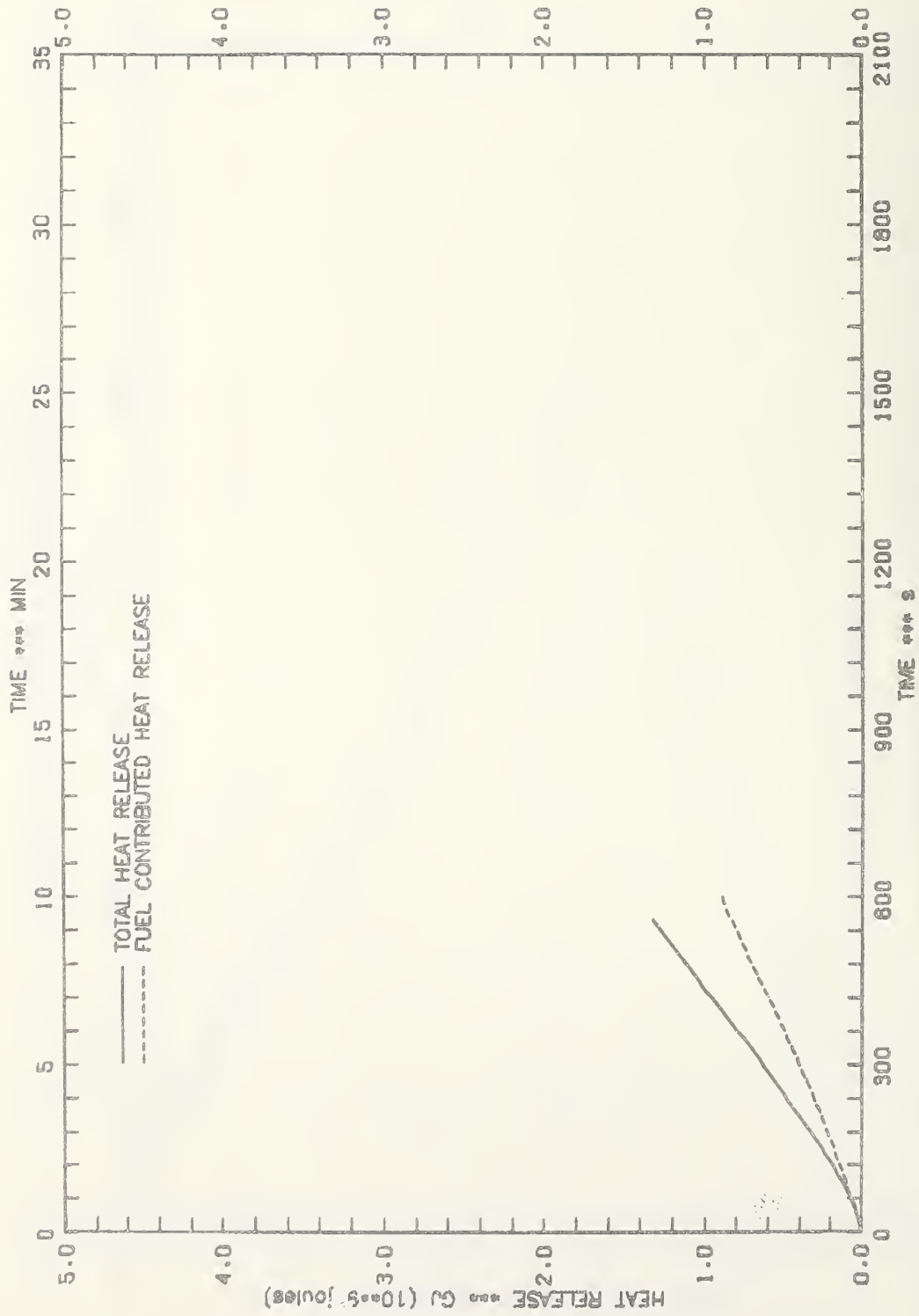
FIGURE 17.I – TOTAL HEAT RELEASE AND HEAT RELEASE BY FUEL FOR TEST 9
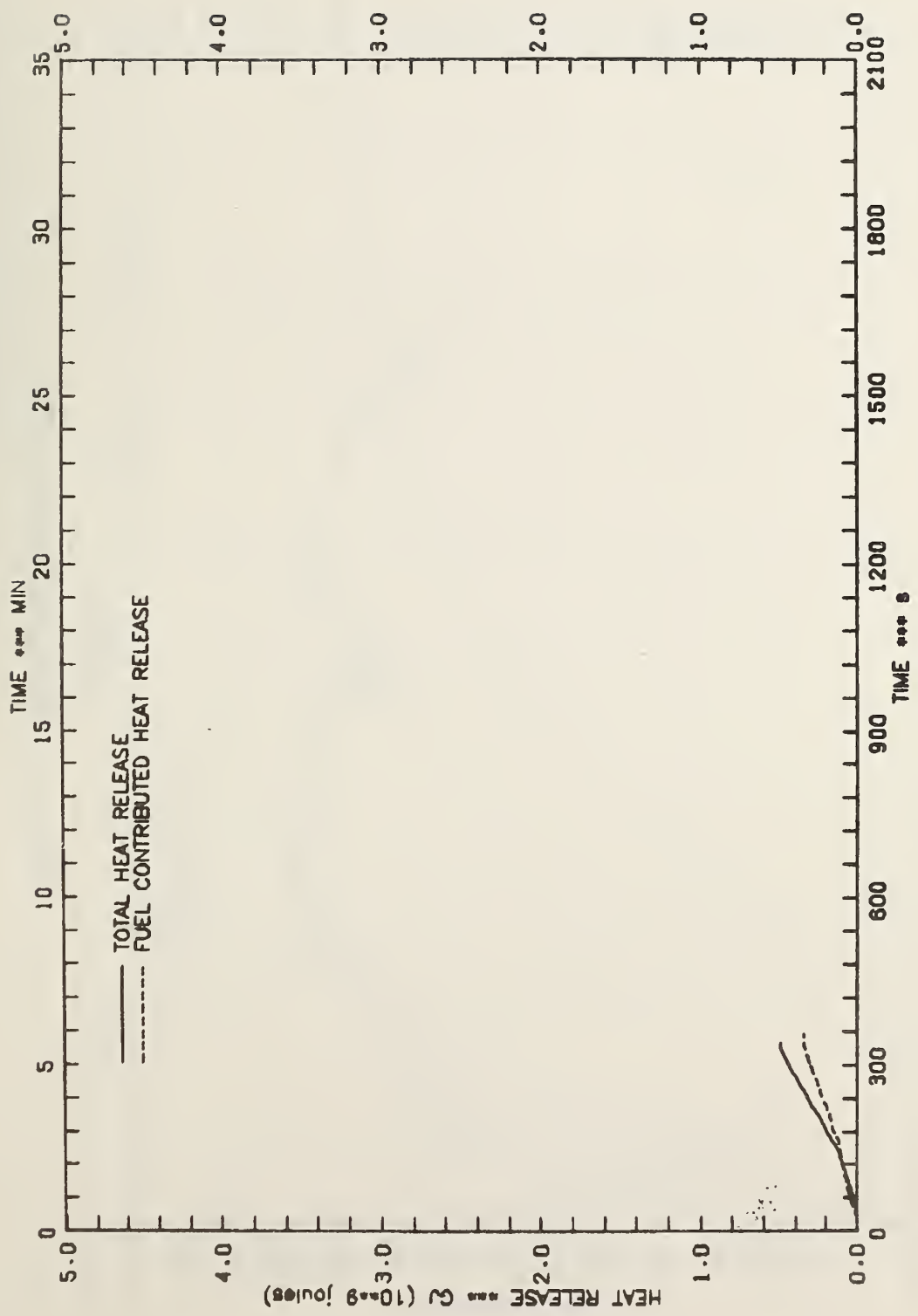
FIGURE 17J — TOTAL HEAT RELEASE AND HEAT
RELEASE BY FUEL FOR TEST 10

103

FIGURE 1B – PROPOSED FIRE EXPOSURE CURVE
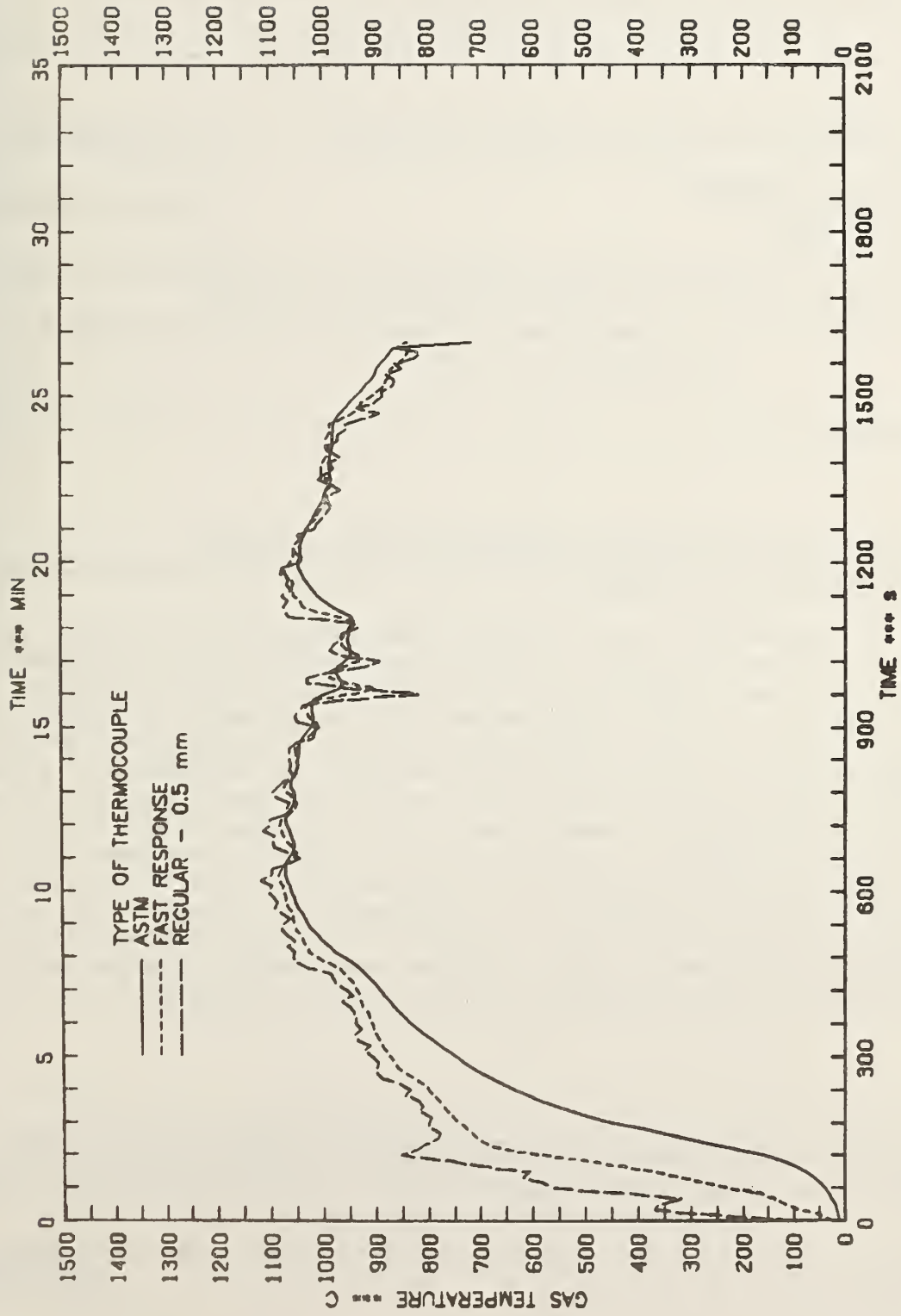
FIGURE 19 — COMPARISON OF THERMOCOUPLE TYPES
AT CENTER OF FURNACE FOR TEST 8

4. TITLE AND SUBTITLE

Fire Endurance Tests of Selected Residential Floor Constructions

5. AUTHOR(S)

Jin B. Fang

11. ABSTRACT (A 200-word or less factual summary of most significant information. If document includes a significant bibliography or literature survey, mention it here)

A series of 10 load-bearing, wood- and steel-framed residential floors was evaluated for structural fire resistance in a fire endurance furnace. Nine wood-frame and one light gauge steel-frame, protected and unprotected floor/ceiling assemblies, each measuring 3.05 x 2.44 m in size, were exposed from the underside to either the newly developed high-intensity, short-duration fire exposure or the standard ASTM E 119 time-temperature curve. The fire endurance time based on the passage of flames to the unexposed face of the floor with unprotected wood joists varied from 6 to 9 minutes under the newly developed fire exposure and 16 to 18 minutes subject to the standard ASTM fire. Under the identical fire exposure, the exposed steel-framed floor failed in approximately 4.5 minutes compared to 9 minutes for the unprotected wood-frame floor. The wood floors evaluated in the test furnace had a shorter fire resistance period in comparison with those tested previously under room fire conditions probably due to faster charring rates and additional heat contribution from the burning of combustible materials in the structure with the excess air present in the furnace.

12. KEY WORDS (Six to twelve entries; alphabetical order; capitalize only proper names; and separate key words by semicolons)

Fire endurance; fire tests; flame through; floors; furnace tests; joists; steel; wood